

HEAT TRANSFER IN HELICALLY COILED  
TUBES WITH LAMINAR FLOW

By

MOHAMMAD A. ABUL-HAMAYEL

Bachelor of Science in Engineering  
Arizona State University  
Tempe, Arizona  
1970

Master of Science  
University of California at Santa Barbara  
Santa Barbara, California  
1973

Submitted to the Faculty of the Graduate College  
of the Oklahoma State University  
in partial fulfillment of the requirements  
for the Degree of  
DOCTOR OF PHILOSOPHY  
May, 1979

Thesis  
1979D  
A166h  
cop. 3



HEAT TRANSFER IN HELICALLY COILED  
TUBES WITH LAMINAR FLOW

Thesis Approved:

*Kenneth H. Bell*  
\_\_\_\_\_  
Thesis Adviser

*John F. Euba*  
\_\_\_\_\_

*Gerald W. Parker*  
\_\_\_\_\_

*Robert H. Robinson, Jr.*  
\_\_\_\_\_

*Leslie S. Fiedler*  
\_\_\_\_\_

*Norman N. Hurkum*  
\_\_\_\_\_  
Dean of the Graduate College

## PREFACE

Experimental measurements of the heat transfer coefficient for laminar flow inside a helical coil were made. Three fluids, ethylene glycol, distilled water and normal butyl alcohol, were studied using a helical coil with a  $D_c/d_i$  ratio of 20.2. The tube was heated by passing DC current through the tube wall. All the experimental runs were conducted under approximately constant wall heat flux. Local outer surface temperatures were measured circumferentially and axially along the length of the coil. The study covered the fluid flow range extending from a Reynolds number of 30 to 5500 and a Prandtl number of 2.24 to 113.1.

I am gratefully indebted to my adviser, Dr. K. J. Bell, for his expert guidance during the course of my doctoral program. I am also thankful to the members of my Advisory Committee, Dr. J. H. Erbar, Dr. R. L. Robinson, Jr., Dr. J. D. Parker, and Dr. L. S. Fishler, for their constructive criticisms and suggestions. I would like to thank Dr. C. B. Panchal for helpful suggestions made from time to time. The help provided by all faculty and staff of the School of Chemical Engineering is also acknowledged.

I thank the Saudi Arabian government and the University of Petroleum and Minerals for providing me with the financial support throughout the course of my study.

I am grateful to Mr. E. E. McCroskey, the Storeroom Manager, for his assistance in the fabrication of the equipment.

I shall always be indebted to my parents, my brothers and sisters for their abundant love and encouragement. I also thank my wife, Mervet, for her patience, devotion, understanding, and support during the years of my graduate study.

## TABLE OF CONTENTS

Chapter	Page
I. INTRODUCTION. . . . .	1
II. LITERATURE REVIEW . . . . .	6
III. EXPERIMENTAL EQUIPMENT. . . . .	16
Description of Individual Units. . . . .	16
Helical Coil. . . . .	16
Fluid Bath. . . . .	19
Pump. . . . .	19
DC Power Source . . . . .	20
Heat Exchanger. . . . .	21
Measuring Devices. . . . .	21
Insulated Wire Thermocouples. . . . .	21
Manometer . . . . .	24
Rotameter . . . . .	24
DC Ammeter and Voltmeter. . . . .	24
Mercury-in-glass Thermometers . . . . .	25
Digital Thermocouple Indicator. . . . .	25
Auxiliary Equipment. . . . .	25
Rotameter Calibration and Fluid Flow Rate Measurement Equipment . . . . .	26
Digital Thermocouple Indicator Calibration Equipment . . . . .	27
VI. EXPERIMENTAL PROCEDURE. . . . .	28
Calibration Procedure. . . . .	28
Thermocouple Calibration. . . . .	28
Manometer Calibration . . . . .	30
Rotameter Calibration . . . . .	30
Digital Thermocouple Indicator Calibration. . . . .	31
Start-up Procedure . . . . .	32
Data Gathering Procedure . . . . .	33
V. DATA REDUCTION. . . . .	36
Calculation of the Error Percentage in Heat Balance . . . . .	37

Chapter	Page
Calculation of the Local Inside Wall Temperature and the Inside Wall Radial Heat Flux . . . . .	38
Calculation of the Local Heat Transfer Coefficient. . . . .	39
Calculation of the Dimensionless Axial Distance and the Dimensionless Inside Wall Temperature . . . . .	39
Calculation of the Relevant Dimensionless Numbers. . . . .	40
VI. RESULTS AND DISCUSSION. . . . .	43
General Discussion . . . . .	43
Comparison with a Straight Tube Under Similar Flow Conditions . . . . .	45
Axial Temperature Profiles. . . . .	48
Testing of Literature Correlations. . . . .	61
Development of Correlation. . . . .	66
VII. CONCLUSIONS AND RECOMMENDATIONS . . . . .	78
BIBLIOGRAPHY . . . . .	81
APPENDIX A -- EQUIPMENT DATA . . . . .	85
APPENDIX B -- CALIBRATION DATA . . . . .	88
APPENDIX C -- EXPERIMENTAL DATA. . . . .	93
APPENDIX D -- PHYSICAL PROPERTIES. . . . .	101
APPENDIX E -- SAMPLE CALCULATIONS. . . . .	108
APPENDIX F -- CALCULATED RESULTS . . . . .	128
APPENDIX G -- COMPUTER PROGRAM LISTINGS. . . . .	148
APPENDIX H -- ERROR ANALYSIS . . . . .	178

## LIST OF TABLES

Table	Page
I. Physical Dimensions of the Helical Coil. . . . .	18
II. Definition of the Dimensionless Numbers Evaluated. . . . .	41
III. Comparison of Literature Correlations to the Present Experimental Data. . . . .	61
IV. Comparison of Literature Correlations to the Present Experimental Data within the Applicable Range of the Correlations. . . . .	64
V. Measured Outside Tube Diameter After Formation of Helical Coil. . . . .	86
VI. Rotameter Specifications . . . . .	87
VII. Calibration Data for the Rotameter for Distilled Water. . . . .	89
VIII. Calibration Data for Inlet and Outlet Thermocouples During In-Situ Calibration of Surface Thermo- couples on the Helical Coil. . . . .	90
IX. Calibration Data for Surface Thermocouples . . . . .	91
X. Calibration Data for Heat Loss from Test Section . . . . .	92
XI. Heat Balance for Ethylene Glycol . . . . .	112
XII. Heat Balance for Distilled Water . . . . .	114
XIII. Heat Balance for N-Butyl Alcohol . . . . .	115
XIV. Uncorrected Outside Surface Temperatures for Run 108 . . . .	117
XV. Corrected Outside Surface Temperatures for Run 108 . . . .	118
XVI. Calculated Inside Wall Temperatures for Run 108. . . . .	119
XVII. Radial Heat Flux for Inside Surface for Run 108. . . . .	120
XVIII. Dimensionless Axial Distance and Inside Wall Temperatures for Run 108 . . . . .	123



## LIST OF FIGURES

Figure	Page
1. Idealized Diagram of the Secondary Flow Pattern in a Curved Tube . . . . .	3
2. Idealized Diagram for Fluid Flow in a Helically Coiled Tube for Natural Convection Heat Transfer at Low Reynolds Number (Heated Wall) . . . . .	4
3. Schematic Diagram of Experimental Set-Up. . . . .	17
4. Layout of the Thermocouples on the Tube Cross-Section of the Helical Coil . . . . .	22
5. Sketch of the Experimental Set-Up for Thermocouple Calibration . . . . .	29
6. Heat Transfer Coefficient Profile . . . . .	47
7. Comparison of the Variation of Wall Temperature for Ethylene Glycol . . . . .	49
8. Comparison of the Variation of Wall Temperature for Distilled Water . . . . .	50
9. Comparison of the Variation of Wall Temperature for N-Butyl Alcohol . . . . .	51
10. Axial Wall Temperature Profiles for Distilled Water . . . . .	53
11. Axial Wall Temperature Profiles for Ethylene Glycol . . . . .	54
12. Axial Wall Temperature Profiles for N-Butyl Alcohol . . . . .	55
13. Variation of Wall Temperature at $\phi = 90^\circ$ with Axial Distance for Ethylene Glycol. . . . .	57
14. Variation of Wall Temperature at $\phi = 90^\circ$ with Axial Distance for Distilled Water. . . . .	58
15. Variation of Wall Temperature at $\phi = 90^\circ$ with Axial Distance for N-Butyl Alcohol. . . . .	59

Figure	Page
16. Schematic Diagram of the Interaction Between Secondary Flow and Thermal Boundary Layer . . . . .	60
17. Variation of the Peripheral Average Nusselt Number with Graetz Number for Ethylene Glycol. . . . .	69
18. Variation of the Peripheral Average Nusselt Number with Graetz Number for Distilled Water . . . . .	70
19. Variation of the Peripheral Average Nusselt Number with Graetz Number for N-Butyl Alcohol . . . . .	71
20. Local Heat Transfer Coefficient Ratio Versus $Gr/(De^2)$ . . .	74
21. Error Ratio Versus Dean Number for Thermocouple Station 15. . . . .	77

## NOMENCLATURE

A	- heat transfer surface area
AAPD	- average absolute percent deviation
$C_p$	- specific heat of the fluid
$D_c$	- helical coil diameter
De	- Dean number, $Re\sqrt{d_i/D_c}$ , defined by Equation (2.1)
$d_i$	- inside diameter of the tube
$d_i/D_c$	- helical coil curvature ratio
$d_o$	- straight tube outside diameter
e	- fluid element
emf	- electromotive force
f	- Fanning friction factor, $16/Re$
g	- gravitational acceleration
G	- mass velocity of the fluid
Gr	- Grashof number, $d_i^3 \rho^2 g \beta \Delta t / \mu^2$
Gz	- Graetz number, $WC_p / kL$
$h_i$	- local heat transfer coefficient based on the tube inside diameter
h	- peripheral average heat transfer coefficient, defined by Equation (6.2)
$h'$	- peripheral average heat transfer coefficient, defined by Equation (6.4)
I	- current in the test section

$k$	- thermal conductivity
$l$	- length of the heated portion of the test section
$L$	- total length of heat transfer loop
$Nu$	- Nusselt number, $hd_1/k$
$Pr$	- Prandtl number, $C_p \mu/k$
$Q$	- heat flow rate
$q$	- heat flow rate
$Q/A$	- heat flux
$Ra$	- Rayleigh number, $Gr \cdot Pr$
$Re$	- Reynolds number, $d_1 G/\mu$
$T$	- fluid temperature
$T_w$	- dimensionless inside wall temperature
$t$	- tube wall thickness
$t_b$	- bulk fluid temperature
$t_w$	- inside wall temperature
$\bar{t}_w$	- circumferential average wall temperature
$v$	- fluid velocity
$W$	- mass flow rate of fluid
$z$	- dimensionless axial distance, defined by Equation (5.6)

#### Greek Letters

$\beta$	- coefficient of volume expansion of the fluid
$\mu$	- fluid viscosity
$\rho$	- fluid density
$\epsilon$	- electrical resistivity
$\phi$	- angular position

### Subscripts

avg	- average
b	- bulk fluid
c	- helical coil
cr	- critical
f	- evaluated at fluid film temperature, $(\bar{t}_w + t_b)/2$
i	- inside of tube
in	- coil inlet
o	- outside of tube
out	- coil exit
s	- straight tube
w	- wall

## CHAPTER I

### INTRODUCTION

Heat transfer in a curved tube is of fundamental importance in various heat exchangers having heating or cooling coils. Curved tubes are also used for heat transfer in heat engines and industrial equipment. Some of the specific applications are:

1. Helical coils are used for transferring heat in mixing operations, chemical reactors and agitated vessels as well as in process heat exchangers.

2. Helical coils have been used in rocket engines and in jacketed vessels.

3. Helical coils have been studied for possible applications in the design of a "daily dialyzer", to be used as an artificial kidney. Weissman and Mockros (42) recently studied the use of helical coils to improve mass transfer rates in membrane blood oxygenators.

4. Due to the fact that helical coils have a compact configuration, more heat transfer can be provided per unit of space than by the use of straight tubes. Helically-coiled tubes are used extensively in the cryogenic industry for the liquefaction of gases. Coiled tube heat exchangers can economically satisfy the severe size and operating conditions required by the Single Pressure Mixed Refrigerant Process which is used for the liquefaction of natural gas.

Heat transfer in laminar flow can be considerably higher in coiled

tubes than it is in straight tubes. The reason for this is the existence of a so-called secondary flow resulting from the tube curvature. When a fluid moves through a straight tube, the fluid velocity near the center line is higher than that near the wall. However, in the case of a coiled tube, each fluid element experiences a centrifugal force acting away from the center of curvature of the coil tube and in the plane of cross-section of the tube. Therefore, this force causes the motion of the fluid element from the inside of the curvature to the outside. The fluid at the outer wall returns to the inside along the tube wall to replace the fluid forced outwards. This results in the formation of two vortices symmetrical about a horizontal plane through the tube center. A highly idealized diagram of the secondary flow pattern is shown in Figure 1.

It is possible, under some conditions, that natural convection becomes an important factor in the heat transfer process. At low Reynolds numbers, the natural convection effect will often predominate, depending upon the temperature difference. The gravity force due to the difference in density causes the motion of fluid element in the vertical direction. If the fluid near the wall is heated, the heavier fluid at the center of the pipe moves towards the bottom and the fluid at the bottom will return to the top along the tube wall to replace the fluid flowing downwards. Figure 2 gives an idealized flow pattern for the natural convection fluid motion at low Reynolds numbers when the fluid is being heated.

The objectives of the research program were to study the various heat transfer mechanisms that occur with laminar flow in a helically

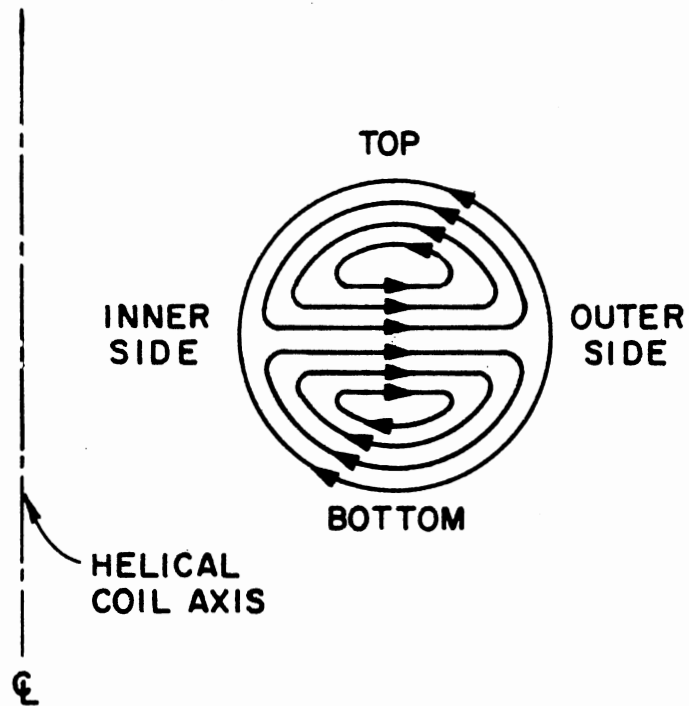


Figure 1. Idealized Diagram of the Secondary Flow Pattern in a Curved Tube



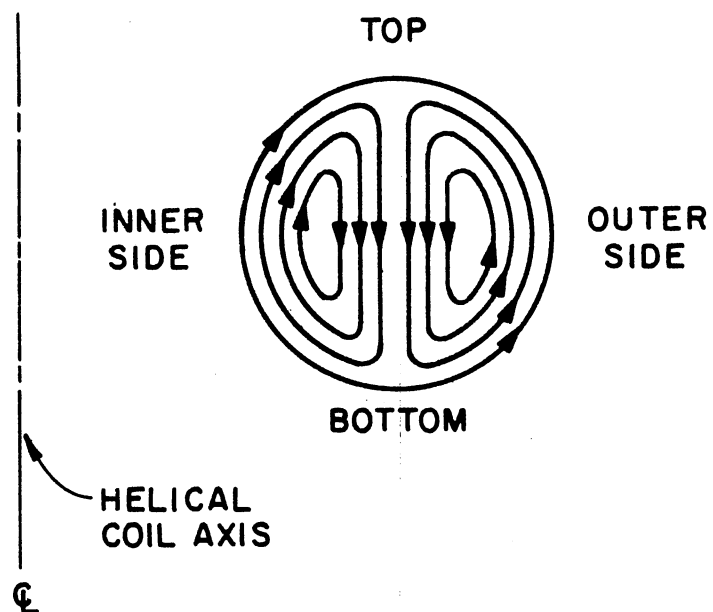


Figure 2. Idealized Diagram for Fluid Flow in a Helically Coiled Tube for Natural Convection Heat Transfer at Low Reynolds Number (Heated Wall)

coiled tube. However, the principal objective of this work was to investigate heat transfer mechanisms in the entrance region of the helical coil, where oscillatory behavior is expected.

Experimental data were gathered for the helical coil using ethylene glycol, distilled water and n-butyl alcohol. A total of 60 runs was made; 26 runs with ethylene glycol, 14 runs with distilled water and 20 runs with n-butyl alcohol as the working fluid. The study covered the fluid flow range extending from a Reynolds number of 30 to 5500 and a Prandtl number of 2.24 to 113.1.

## CHAPTER II

### LITERATURE REVIEW

The literature describing fluid flow in curved tubes dates back almost 100 years. A chronological bibliography of important papers on fluid flow in helical coils was compiled by Koutsky and Adler (20). Srinivasan et al. (38) critically examined the various published correlations for determining the pressure drop and heat transfer coefficient in helical and spiral coils. Singh (37) gives a complete literature survey of the work done on fluid mechanics of flow in helical coils up to 1970. This survey will be limited to the work done on heat transfer in the helically coiled tubes with laminar flow.

The first theoretical study in curved pipes was made by Dean (8,9). Dean first showed that the parameter

$$De = Re \sqrt{d_i/D_c} \quad , \quad (2.1)$$

now known as the Dean number, is the unique dynamic similarity parameter governing fluid motion in curved tubes. Using a perturbation technique, he analyzed the secondary flow field as a deviation from Poiseuille flow.

Berg and Bonilla (5) were the first to make a reasonably comprehensive experimental study in the laminar flow regime. They studied three coils with  $D_c/d_i$  ratios of 5.3, 6.08 and 17.21. Air, water and Essoluble 30 lubricating oil were heated in the coil by condensing

steam on the outside of the coil. They could not fit all their data to a single generalized correlation. They tried to incorporate the natural convection effect in their correlation but did not obtain a worthwhile correlation. The length-average heat transfer coefficient in a coil was correlated within an average deviation of some 20 per cent with each of the following empirical equations:

$$\frac{h_i d_i}{C_p \mu} = \text{Re}^{1.26} [0.0000355 + 0.0009 \left(\frac{d_i}{D_c}\right)] \quad (2.2)$$

where all properties are evaluated at the mean bulk temperature, and

$$\frac{h_i d_i}{C_p \mu} = \text{Re}^{1.29} [0.0000229 + 0.000636 \left(\frac{d_i}{D_c}\right)] \quad (2.3)$$

where all properties are evaluated at the mean film temperature.

Berg and Bonilla proposed the following equation for the heating of air in laminar flow with an average deviation of less than 10 per cent.

$$\frac{h d_i}{k} = 0.000468 \left( \frac{W C_p}{k \sqrt{d_i D_c}} \right)^{1.33} \quad (2.4)$$

The heat capacity,  $C_p$ , is evaluated at the fluid average temperature and  $k$  is evaluated at the average tube wall temperature.

Berg and Bonilla (5) found higher inside film heat transfer coefficients for oil and lower inside film heat transfer coefficients for air for flow in coils when compared with those in straight tubes under similar flow conditions. This casts some doubt on the consistency of their work.

Seban and McLaughlin (34) measured local heat transfer coefficients in electrically heated coils. They tested two coils having  $D_c/d_i$  ratios

of 17 and 104 for Reynolds numbers ranging from 12 to 65,000. They used a medium heavy Freezene oil to study the laminar flow regime and water for the turbulent flow regime. They experimentally measured the circumferential variation of heat transfer coefficients in the fully developed temperature field and also measured the axial variation of the heat transfer coefficients on the inside and outside of curvature in the thermal entrance region.

Seban and McLaughlin (34) reported that in some of the runs, the coefficients varied abnormally with increasing down-stream distance. The abnormality consisted of either a cyclic rise and fall in the coefficients with increasing downstream distance, or an increase in the coefficient at the last thermocouple station. They observed that the thermal entrance length was much shorter for helical coils than that for straight tubes at comparable Reynolds numbers.

They proposed the following empirical equation for the peripheral average heat transfer coefficient for laminar flow in helical coils:

$$Nu = (0.13) \left[ \frac{f_c}{8} (Re)^2 \right]^{1/3} \quad (2.5)$$

where  $f_c$  is calculated from White's equation (43); namely:

$$\frac{f_c}{f_s} = \left[ 1 - \left\{ 1 - \left[ \frac{11.6}{Re \sqrt{d_i/D_c}} \right]^{0.45} \right\}^{1/0.45} \right]^{-1}$$

and  $f_s = \frac{16}{Re}$ .

The applicable range for Equation (2.5) is  $12 < Re < 5600$  and  $100 < Pr < 657$ . Fluid properties were evaluated at a film temperature which was the average of the mixed mean fluid and the tube inner wall temperatures.

Kubair and Kuloor (21) studied heat transfer to aqueous solutions of glycerol flowing through helical coils heated with steam. They studied Reynolds numbers between 80 and 6000. They tested six helical coils having  $d_i/D_c$  ratios of 0.037, 0.056, 0.074, 0.097, 0.022 and 0.031. The peripheral and axial average Nusselt number was correlated within a maximum deviation of  $\pm 10$  percent and average deviation less than 5 percent. They proposed the following correlation:

$$Nu = [1.98 + 1.8(\frac{d_i}{D_c})^{0.7}]Gz \quad (2.6)$$

for  $80 < Re < 6,000$ ;  $20 < Pr < 100$ ; and  $10 < Gz < 1,000$ .

Mori and Nakayama (25) numerically solved the continuity and Navier-Stokes equations for helical coils by integral methods, subdividing the flow pattern into a core and a boundary-layer region. They proposed the following equation to predict the Nusselt number in the fully developed region in the laminar flow regime:

$$Nu = \frac{0.864}{\zeta}(2.35 + \sqrt{De}) \quad (2.7)$$

where

$$\zeta = \frac{2}{11} \left[ 1 + \left\{ 1 + \frac{77}{4(Pr)^2} \right\}^{0.5} \right] \quad (2.8)$$

The range for Equation (2.7) is stated to be applicable for  $De > 30$  as  $Pr \rightarrow \infty$ , and for  $De > 60$  as  $Pr \approx 1$ .

To support their theoretically obtained equation, Mori and Nakayama (24) measured the velocity and temperature distributions for air flowing through a curved pipe having one complete turn with a  $D_c/d_i$  ratio of 40. The pipe was electrically heated by nichrom wire wound around it. From the observed distributions, the peripheral average Nussult nubmers were

calculated. They reported that the Nusselt numbers calculated from experimental data were in good agreement with the results of their theoretical analysis.

It was shown by Dravid et al. (13), however, that Mori and Nakayama's Prandtl number dependence is incorrect. For  $Pr > 1$ , Mori and Nakayama (24,25) integrated the energy integrals of the thermal boundary layer over the hydrodynamic boundary layer rather than over the thermal boundary layer. Dravid et al. (13) and Akiyama and Cheng (2) have shown that the theoretical results from the integral methods are valid near  $Pr = 1.0$  only, and the result for  $Pr \rightarrow \infty$  is invalid. In Equation (2.8),  $\zeta$  is the ratio of the thermal to hydrodynamic boundary layer thickness. It can be argued that  $\zeta$  should have an asymptotic value of zero at infinite Prandtl number instead of  $4/11$ , because while the hydrodynamic boundary layer thickness is independent of the Prandtl number, the thermal boundary layer thickness decreases monotonically with increasing Prandtl number to zero at infinite Prandtl number.

Schmidt (33) experimentally evaluated the heat transfer and the pressure drop for fluid flow in helical coils. He tested five coils having  $d_i/D_c$  ratios of 0.2035, 0.0983, 0.0493, 0.0244, and 0.0123. The test fluids were air, water, and Shell Voluta oil 919.

Schmidt reported the following correlation for determining the peripheral and axial average Nusselt number for heat transfer in helically coiled tubes:

$$Nu = 3.65 + 0.08 \left[ 1 + (0.80) \left( \frac{d_i}{D_c} \right)^{0.9} \right] (Re)^{\alpha} Pr^{1/3} \quad (2.9)$$

where

$$\alpha = 0.5 + (0.2903) \left( \frac{d_i}{D_c} \right)^{0.194}$$

Equation (2.9) is applicable for  $100 < Re < Re_{cr}$ .

It has been demonstrated by Kalb and Seader (18) and Tarbell and Samuels (39) that the  $D_c/d_i$  ratio, in the range of 10-100, has a negligible effect on the average Nusselt number and should not appear explicitly in the mean values of heat transfer results. However, the  $D_c/d_i$  ratio has a definite effect on the peripheral variation of the fully developed local Nusselt number.

Özsisik and Topakoglu (28) evaluated the heat transfer for fully developed flow by solving the governing differential equation using the perturbation method. They reported that the Nusselt number in curved pipes depends on the Reynolds number, Prandtl number and the curvature of pipe. Later it was found by Akiyama and Cheng (2) that the method used by Özsisik and Topakoglu is applicable only for the very low Dean number flow regime.

Shchukin (35) studied heat transfer to water flowing through helical coils. The results of the experimental study were correlated by the following formula:

$$Nu = 0.0575 (Re)^{0.33} (De)^{0.42} (Pr)^{0.43} \left( \frac{Pr}{Pr_w} \right)^{0.25} \quad (2.10)$$

with  $26 < De < 7000$  and  $6.2 < D_c/d_i < 62.5$ .

Dravid et al. (13) have obtained numerical solutions of the relevant equations for entrance region heat transfer in curved tubes using the fully developed velocity profiles obtained by Mori and Nakayama (24). Dravid et al. showed that the Nusselt number behaves in an



oscillatory manner. These oscillations, caused by the interaction of the secondary flow with the developing thermal boundary layer, damp out as the region of the fully developed temperature field is approached. Dravid et al. also made measurements of the axially local peripheral-average Nusselt number using an electrically heated coil of  $d_i/D_c$  ratio of 0.0537. The boundary condition of axially uniform wall heat flux with peripherally uniform wall temperature was used. They tested five fluids covering a Prandtl number range from 5 to 175. Although the oscillations had not decayed at the end of the tube, Dravid et al. confirmed the early convergence of the fully developed region first reported by Seban and McLaughlin (34). Experimental work by Dravid et al. gave the following equation for the fully developed Nusselt number;

$$Nu = (0.76 + 0.65 \sqrt{De}) Pr^{0.175} \quad (2.11)$$

provided that

$$50 < De < 2000;$$

and

$$5 < Pr < 175.$$

Akiyama and Cheng (2) predicted the fully developed flow and heat transfer characteristics by solving the governing differential equation using a combination of line iterative method and boundary vorticity method. They found that the perturbation method (8,28) is applicable only for the very low Dean number flow regime. They also pointed out that the approximate method (1,24) based on the boundary layer concept near the pipe wall is valid only for high Dean number flow regime. The following equation was developed using the new parameter,  $De^2 Pr$ , to

account for the Prandtl number effect on heat transfer in curved pipes.

$$\frac{Nu}{(Nu)_o} = 0.181 (De^2 Pr)^{1/4} \left[ 1 - \frac{0.839}{(De^2 Pr)^{1/4}} + \frac{35.4}{(De^2 Pr)^{1/2}} - \frac{207}{(De^2 Pr)^{3/4}} + \frac{419}{(De^2 Pr)} \right] \quad (2.12)$$

The applicable range for Equation (2.12) is stated to be for Dean number  $>200$ , Prandtl number  $\geq 1$  and  $(De^2 Pr)^{1/4} \geq 3.5$ . Another equation was also developed by Akiyama and Cheng (3) for Dean numbers ranging from 0 to the order of 100.

$$\frac{Nu}{(Nu)_o} = 0.234 (De^2 Pr)^{1/4} \left[ 1 - \frac{1.15}{(De^2 Pr)^{1/4}} + \frac{29.2}{(De^2 Pr)^{1/2}} - \frac{164}{(De^2 Pr)^{3/4}} + \frac{316}{(De^2 Pr)} \right] \quad (2.13)$$

where

$$(Nu)_o = 4.36 .$$

The restrictions concerning  $(De^2 Pr)$  and  $Pr$  for Equation (2.13) are the same as Equation (2.12).

It was shown by Kalb and Seader (19) that, for large Nusselt numbers, the extrapolation of Akiyama and Cheng's (2) numerical computations through the use of their similarity parameter  $De^2 Pr$  diverges from the numerical results of Kalb and Seader. A dimensional analysis performed by Kalb and Seader led them to the conclusion that this similarity parameter has a limited range of usefulness.

Kalb and Seader (18) have published their result which is based on a numerical solution of the constant property continuity, Navier-

Stokes, and thermal-energy equations. They proposed the following correlation to calculate the Nusselt number for laminar flow heat transfer in curved pipes.

$$Nu = 0.913 (De)^{0.476} (Pr)^{0.200} \quad (2.14)$$

The above equation is stated to be valid for  $80 < De < 1200$  and  $0.7 < Pr < 5$ .

Singh (37) measured the heat transfer to laminar flow inside helically-coiled tubes using water and Dowtherm G. Two coils having coil diameter to inside tube diameter ratios of 20.2 and 41.7 were tested over a Reynolds number range from 6 to the transition region. Singh proposed the following equation which includes corrections for curvature and natural convection effects.

$$Nu = \left\{ 0.224 + 1.369 \left( \frac{d_i}{D_c} \right) \right\} \left\{ Re \left[ 0.501 + 0.318 \left( \frac{d_i}{D_c} \right) \right] \right\} \left\{ 1 + 4.8 \left[ 1 - e^{-0.00946 (Gr/Re^2) (D_c/d_i)} \right] \right\} \left\{ Pr^{1/3} \left( \frac{\mu_b}{\mu_w} \right)^{0.14} \right\} \quad (2.15)$$

The physical properties of the fluid used in Equation (2.15) were evaluated at the bulk temperature except  $\mu_w$  which was evaluated at the wall temperature.

Equation (2.15) is reported to be valid for:

$$6 < Re < Re_{cr}$$

$$1 < De < 1.7 \times 10^3$$

$$2.3 < Pr < 250$$

$$241 < Gr < 9.22 \times 10^5$$

Oliver and Asghar (26) investigated experimentally the heat transfer to laminar flowing liquids in coils. Their results were correlated in terms of the Dean number to give a straightforward equation with the property of reducing to the Graetz-L           equation when the curvature ratio approaches zero. They proposed the following equations for Nusselt number:

$$\text{Nu} \left( \frac{\mu_w}{\mu_b} \right)^{0.14} = 1.75 \text{Gz}^{0.33} \left[ 1 + 0.118(\text{De})^{0.5} \right] \quad (2.16)$$

$$\text{Nu} \left( \frac{\mu_w}{\mu_b} \right)^{0.14} = 1.75 \text{Gz}^{0.33} \left[ 1 + 0.36(\text{De})^{0.25} \right] \quad (2.17)$$

The applicable range for Equation (2.16) is  $60 < \text{De} < 2000$  and for Equation (2.17) is  $4 < \text{De} < 60$ .

Janssen and Hoogendoorn (17) recently published their results of an experimental and numerical study of the convective heat transfer in coiled tubes with horizontal axes. They tested four coils having  $D_c/d_i$  ratios ranging from 10 to 100 over a Prandtl number range of 10 to 500 and Reynolds numbers from 20 to 4000. For the fully developed thermal region, the peripherally-averaged Nusselt number was given by the following correlations:

for  $20 < \text{De} < 100$

$$\text{Nu} = 0.9 (\text{Re}^2 \text{Pr})^{1/6} \quad (2.18)$$

for  $100 < \text{De} < 830$

$$\text{Nu} = 0.7 \text{Re}^{0.43} \text{Pr}^{1/6} \left( \frac{d_i}{D_c} \right)^{0.07} \quad (2.19)$$

and for  $\text{De} < 20$  and  $(\text{De}^2 \text{Pr})^{1/2} > 100$

$$\text{Nu} = 1.7 (\text{De}^2 \text{Pr})^{1/6} \quad (2.20)$$

## CHAPTER III

### EXPERIMENTAL EQUIPMENT

Liquid phase heat transfer was studied in a helical coil using ethylene glycol, distilled water and normal butyl alcohol. A sketch of the experimental set-up is shown in Figure 3. Since the experimental set-up and equipment used were essentially the same as that used by Farukhi (14) and Singh (37), some parts of this chapter and the following chapters are taken from their Ph.D. theses.

#### Description of Individual Units

##### Helical Coil

The helical coil used was 254 mm in diameter (tube-center to tube-center). The coil was fabricated from initially-straight Type 304 seamless stainless steel tubing 15.88 mm o.d. x 1.65 mm wall thickness. The axial (and heated) length of the helically coiled tube was 7.581 m. Straight tube sections were provided at the inlet and the exit of the coil. Dimensions of the helical coil are summarized in Table I.

The test section was thermally insulated by wrapping it with several layers of fiberglass tape and four layers of fiberglass wool insulation. The outside surface of insulation was then wrapped with vapor seal wrap so that the radiation losses would be minimized.

Some flattening of the tube resulted during the formation of the

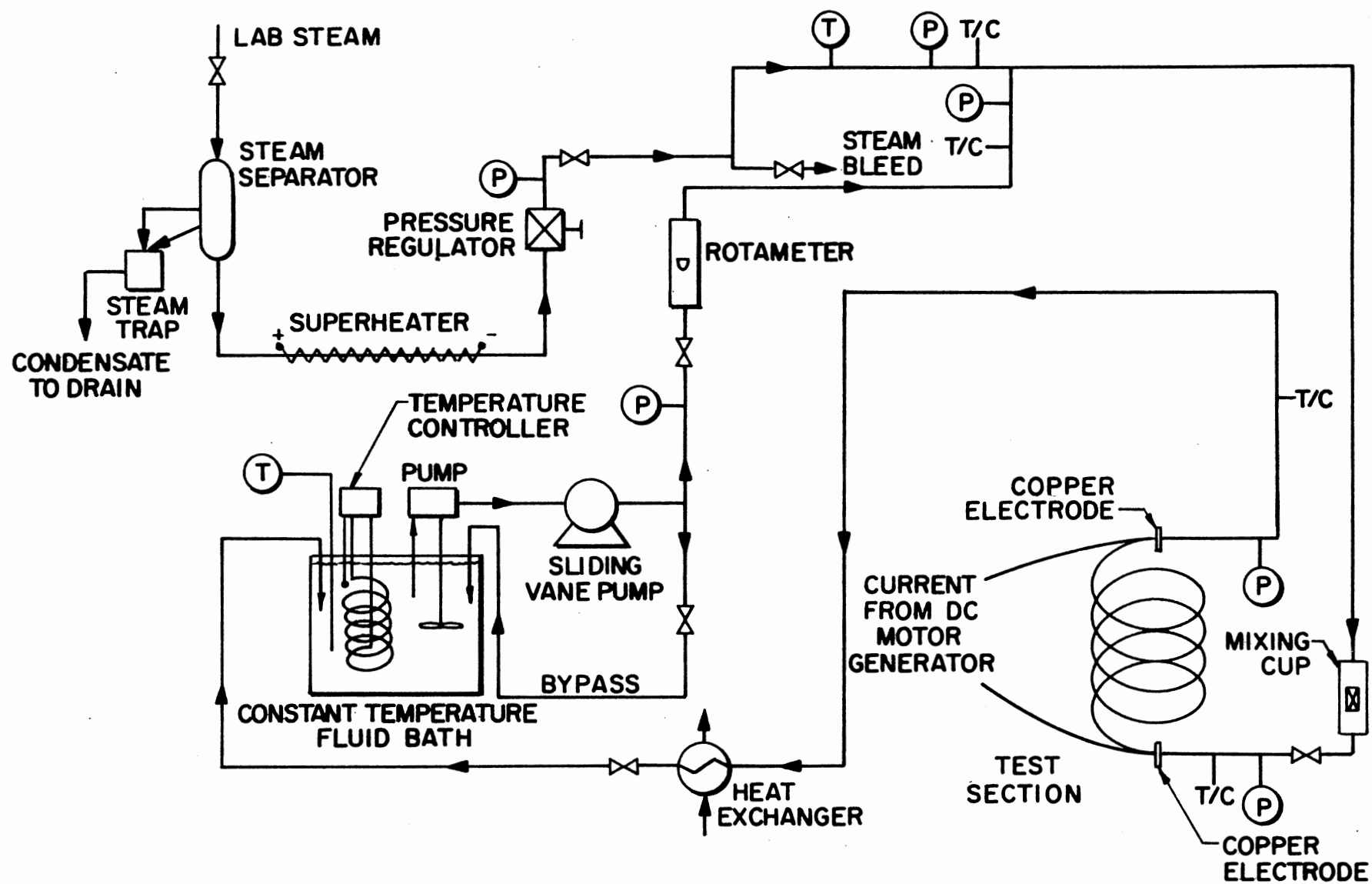


Figure 3. Schematic Diagram of Experimental Set-Up

TABLE I  
PHYSICAL DIMENSIONS OF THE HELICAL COIL

Item	Dimension
Coil diameter, tube-center-to-tube-center, $D_c$ , mm	254
Straight tube outside diameter, $d_o$ , mm	15.88
Straight tube inside diameter, $d_i$ , mm	12.57
Number of turns in helical coil	9.5
Ratio of coil diameter to straight tube inside diameter, $D_c/d_i$	20.2
Curvature ratio, $d_i/D_c$	0.0495
Axial and heated length of helical coil, m	7.581
Coil pitch, tube-center-to-tube-center, mm	16.73
Length of the straight tube preceding the inlet electrode, mm	1270
Length of the straight tube following the exit electrode, mm	609.6
Total length, mm	9460.6

helical coil. Hence, the longitudinal and the lateral outer tube diameters were measured at several different axial locations. These measurements are presented in Table V in Appendix A. The measurement intervals were selected to correspond to the intended thermocouple station locations on the helical coil.

A copper bar electrode was silver-soldered to the coil at each end of the heated length.

Experiments were performed with the axis of the coil in the vertical direction. The fluid entered the coil at the bottom and exited at the top.

#### Fluid Bath

The constant temperature bath used was a "Lo-Temprol" Model 154 circulating system manufactured by the Precision Scientific Company. The bath has a capacity of 2.75 gallons and is equipped with an ultra-sensitive Micro-Set thermo-regulator, a 250-500-1000 watt immersion type electric heater, a centrifugal pump and an impeller mounted on a common shaft and driven by an electric motor. The bath set-point temperature could be varied continuously from  $-10^{\circ}\text{C}$  to  $100^{\circ}\text{C}$  by adjusting the set-point on the thermo-regulator. The bath temperature was measured by means of a Brooklyn P-M mercury-in-glass thermometer having a range from 0 to  $220^{\circ}\text{F}$  and graduated in  $2^{\circ}\text{F}$  intervals. The circulating system has a guaranteed accuracy for maintaining the bath temperature to within  $0.06^{\circ}\text{C}$  of the set-point temperature (31).

#### Pump

A sliding vane pump was used to pump the fluid through the



experimental loop. The pump was manufactured by Eastern Industries, Inc. The pump model number is VW-5-A. The pump is a positive displacement pump having a rated maximum capacity of 1.2 gpm ( $75.7 \text{ cm}^3/\text{sec}$ ) of water and capable of developing a head of 138 feet (42 m).

#### DC Power Source

A Lincolnweld SA-750 AC motor driven DC generator was used to generate the DC current, which was fed to the helically-coiled tube through two copper bars silver-soldered to the tube. Resistance heating, due to the passage of the DC current through the tube wall, provided the heat to the fluid. All the experimental runs were conducted under approximately constant wall heat flux conditions. The DC power generator has a maximum rated output power of 30 kilowatts.

DC resistance heating was chosen over AC resistance heating because:

1. Complex AC induction and skin effects are avoided.
2. AC heating may cause cyclic temperature variations in the test section whereas DC heating provides a constant heat source.
3. Possible thermal stresses in the test section caused by the cyclic nature of the AC current are avoided.
4. The cyclic nature of the electrical forces in AC may induce vibrations in the test section. These vibrations do not exist when DC is used.
5. AC, because of its cyclic nature, may induce spurious emfs in the thermocouple wires resulting in erroneous readings.

A motor-generator was used as opposed to a rectifier because:

1. It was available

2. Its power output is relatively smooth and free from large magnitude superimposed sine waves.
3. It is more resistant to overload than rectifiers.
4. It is not as susceptible to transient voltage peaks that occur in switching the unit on and off as are rectifiers.

#### Heat Exchanger

A 1 shell-4 tube pass heat exchanger was used to cool the test fluid from the helical coil. The heat exchanger is a size 502, "BCF" type exchanger manufactured by the Kewanee-Ross Corporation (32).

#### Measuring Devices

##### Insulated Wire Thermocouples

Insulated wire thermocouples were used to measure the bulk fluid temperature and the outside wall temperature of the helically-coiled tube. The thermocouples were made from nylon insulated, 30 B&S gauge copper-constantan thermocouple wire. The thermocouples were fabricated in the laboratory by using the thermocouple welder.

The thermocouples were placed at eighteen stations on the helically-coiled tube. The thermocouple stations were located at different intervals. The intervals along the axial length of the tube were smaller near the inlet electrode in order to observe the effect of the developing thermal profile. Four thermocouples were placed 90 degrees apart on the tube cross-section at thermocouple stations 1 through 18. Figure 4 is a sketch of the thermocouple layout.

The thermocouple beads were fixed on the tube surface with Sauereisen cement. In order to electrically insulate the thermocouple beads

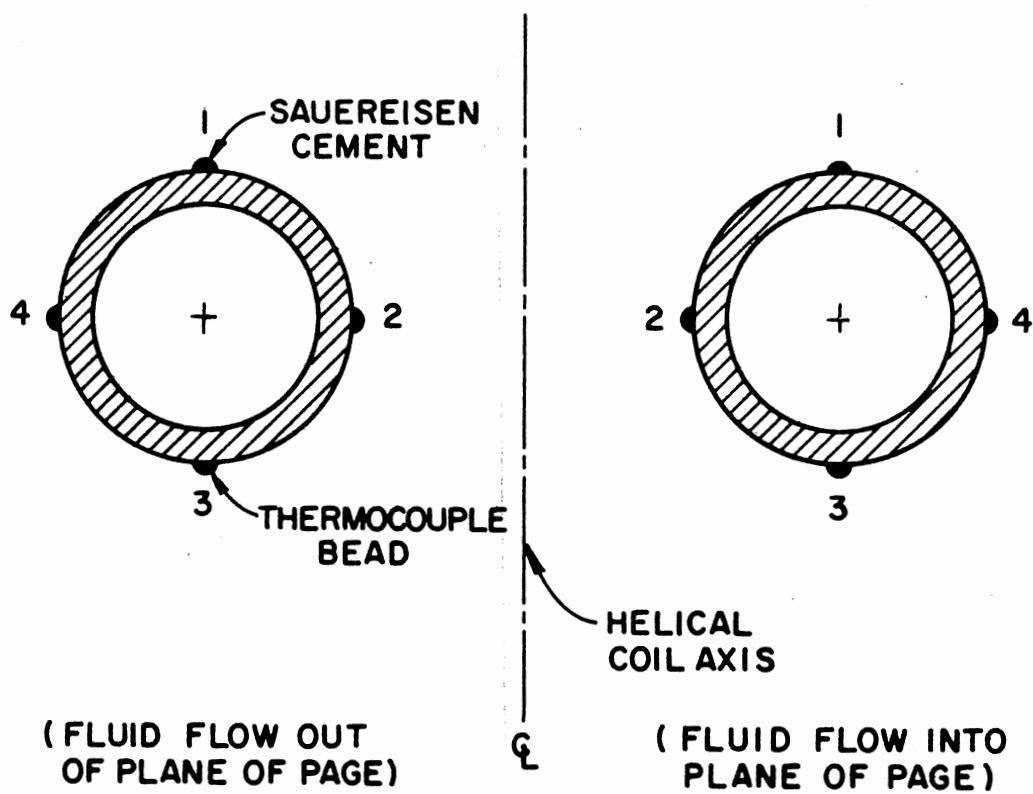


Figure 4. Layout of the Thermocouples on the Tube Cross-Section of the Helical Coil

from the heating current, a thin layer of Sauereisen cement was first placed at the intended thermocouple location and allowed to set before cementing the thermocouple to its intended location. The thermocouple wires from the thermocouple beads were held in place along the tube about 12 mm from the thermocouple beads by means of duct tape and a flexible hose clamp. The duct tape was placed between the clamp and the thermocouple wires to prevent any accidental short-circuiting of the thermocouple wire due to the sharp edges of the metal hose clamp. The thermocouple wires were then placed along the helical coil for about 50 mm and clamped again to the tube before being led off to the thermocouple selector switchboard.

Each thermocouple was tagged with two numbers: the first, running from 1 to 18, indicated the thermocouple station number; the second, running from 1 through 4, indicated the thermocouple location on the tube periphery. Location 1 was at the top of the tube and the others followed clockwise, facing the tube cross-section; that is, thermocouple 2 was closest to the coil axis. Thus, for example, a thermocouple tagged '5-3' indicates the thermocouple at station 5 and located 180 degrees from the top of the tube periphery, i.e., at the bottom of the tube at station 5.

All the surface thermocouples were connected to an array of barrier strips which in turn were connected to 18 rotary switches. The rotary switches were mounted on a panel and the connections were enclosed in a constant temperature box. The outputs from the rotary switches were brought to a master rotary switch which was connected to a Digital Thermocouple Indicator.

The thermocouples were calibrated in-situ by bleeding low pressure saturated steam through the coil. Details of the calibration procedure are given in Chapter IV.

#### Manometer

For each experimental run, the fluid pressure at the inlet and the exit of the helical coil was measured. The two pressure taps were connected to a manifold by a series of Whitey valves. The switching system was connected in such a manner that either of the two taps could be activated and read on a Meriam U-type manometer against atmospheric pressure.

#### Rotameter

A Brooks "Full-View" rotameter was used to indicate and meter the fluid flow rate. The rotameter specifications are given in Table VI in Appendix A.

#### DC Ammeter and Voltmeter

The current flowing through the coil was measured by a Weston model 931 DC ammeter in conjunction with a 50 millivolt shunt. The ammeter has a 0-750 amperes range. The 50 millivolt shunt was connected in the line carrying the current to the coil. The ammeter was connected across the shunt.

The voltage drop across the coil was measured by a Weston model 931 DC voltmeter. The voltmeter has a 0-50 volts range. The voltmeter was connected across the two copper electrodes.

The ammeter and the voltmeter were calibrated by the manufacturer and were guaranteed to be accurate to within one percent of their full range, that is  $\pm 7.5$  amperes and  $\pm 0.5$  volts, respectively.

#### Mercury-in-glass Thermometers

Mercury-in-glass thermometers were used to measure the bath fluid temperature and the room temperature. A Brooklyn "P-M" 0 to 220°F thermometer was used to measure the bath fluid temperature. The thermometer was graduated in 2°F intervals. A 23-inch long, 65 to 90°F ASTM Calorimeter Thermometer was used to measure the room temperature.

#### Digital Thermocouple Indicator

The thermocouple outputs were measured on a digital thermocouple indicator. The indicator is equipped with the circuitry that converts a thermocouple emf fed to the instrument into its corresponding temperature reading. The reading is displayed directly in degrees Fahrenheit on the digital readout panel in the thermocouple indicator.

The digital thermocouple indicator has the following stated accuracies:  $\pm 0.4^\circ\text{F}$  below  $0^\circ\text{F}$ ,  $\pm 0.3^\circ\text{F}$  above  $0^\circ\text{F}$  and the maximum linearization error is less than  $\pm 0.1^\circ\text{F}$ . Further details regarding the digital thermocouple indicator may be obtained from the Doric Owner's Manual (10).

#### Auxiliary Equipment

Auxiliary equipment was used for the calibration of the measuring devices. All measuring devices were calibrated except the DC ammeter

and voltmeter which had been previously calibrated by the School of Electrical Engineering Laboratories at Oklahoma State University. The results of the calibration were found to be within 1% accuracy of the full scale range. The description of the auxiliary equipment consists of two sections:

1. Rotameter calibration and fluid flow rate measurement equipment.
2. Digital thermocouple indicator calibration equipment.

#### Rotameter Calibration and Fluid Flow Rate Measurement Equipment

The rotameter calibration and fluid flow rate measurement equipment consisted of the following:

1. Stop Watch: A 60 minute stop watch with a main dial range of 60 seconds was used to time the fluid flow rate. The stop watch has a precision of 0.2 seconds.

2. Weighing Equipment: A 5 kilogram capacity Ohaus Pan Balance was used to weigh the amount of fluid collected for fluid flow rates below 1.0 gpm. The balance has a sensitivity of 0.5 grams. A set of calibrated weights was used in conjunction with the balance.

For fluid flow rates greater than 1.0 gpm, a single-beam platform weighing scale was used to weigh the amount of fluid collected. The scale has a capacity of 300 lbs and an accuracy of 0.125 lb. The beam is graduated in pounds and ounces.

3. Fluid Collecting Vessels: The fluid collecting vessels consisted of various capacity beakers and cylindrical jars. The vessels were used to collect the fluid for a given time interval, so that the mass flow rate could be determined.

Digital Thermocouple Indicator CalibrationEquipment

A Leeds and Northrup model 8687 volt potentiometer was used for the calibration of the digital thermocouple indicator. The potentiometer used has a maximum stated accuracy of  $\pm$  (0.03% of reading + 30 microvolts) (11).



## CHAPTER IV

### EXPERIMENTAL PROCEDURE

This chapter is subdivided into three sections: (1) Calibration procedure; (2) Start-up procedure; (3) Data gathering procedure.

#### Calibration Procedure

##### Thermocouple Calibration

The insulated wire thermocouples were calibrated in-situ by bleeding low pressure saturated steam through the coil.

After the helical coil was installed in the fluid flow circuit and prepared for obtaining experimental data (see Start-up Procedure below), the fluid flow circuit downstream of the helical coil was altered slightly to facilitate the collection of the steam condensate from the coil during the calibration process. The alteration involved is indicated in Figure 5.

Low pressure saturated steam was bled through the fluid flow circuit. The system was allowed to achieve steady state. Thermocouple readings, inlet and exit steam pressure, room temperature and the atmospheric pressure were recorded after 8, 21, and 27 hours of operation. In addition, the steam condensate flow rate was also measured.

Knowing the absolute pressure of the saturated steam at the inlet and exit of the coil, the steam temperature was determined from steam

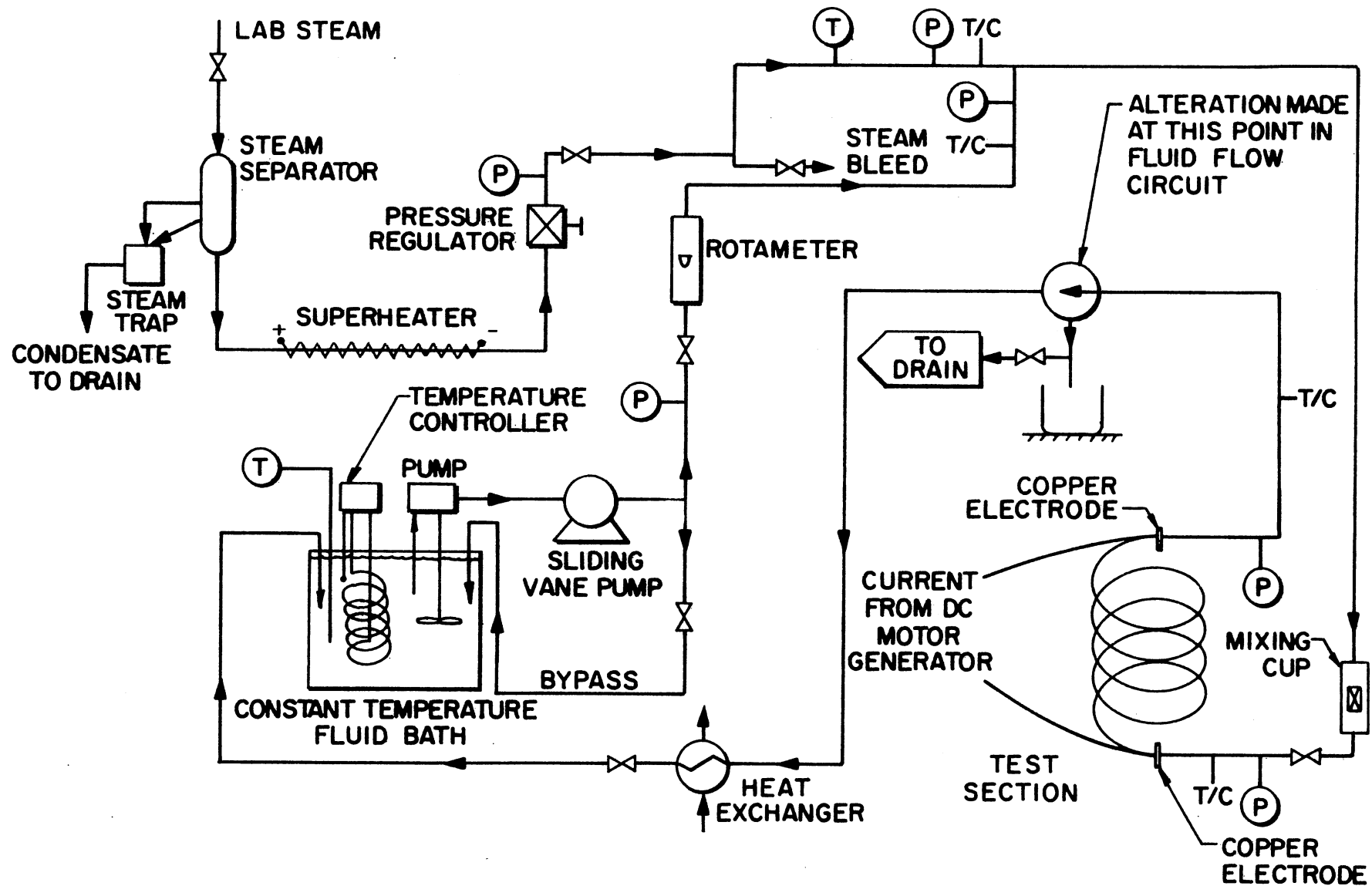


Figure 5. Sketch of the Experimental Set-Up for Thermocouple Calibration

tables and hence the deviation indicated by the thermocouples was determined. The steam temperature was assumed to drop linearly along the length of the helical coil. After 27 hours of operation, the temperature drop was  $1^{\circ}\text{C}$ . Knowing the condensate flow rate, the steam temperature in the coil, the room temperature and the total outer surface area of the coil, the average heat loss flux and the total heat loss at calibration conditions were determined. Thermocouple calibration data are presented in Appendix B.

Heat losses for each run were calculated by assuming that the losses were proportional to the difference between the test section temperature and the room temperature for each run as compared to the calibration run.

The thermocouple calibrations and the heat loss information obtained were incorporated into the computer programs for calculating the heat balance and the inside wall temperature.

#### Manometer Calibration

The differential reading of the U-type manometer was verified to be zero for the condition of no flow through the test section. Mercury was used as the indicator fluid in the manometer.

#### Rotameter Calibration

The rotameter used for measuring liquid flow rate in the heat transfer loop was calibrated for distilled water. The rotameter was calibrated from 10 percent to 100 percent of maximum flow in 10 percent increments. The rotameter was calibrated with the flow rate increasing

up to the maximum and then decreasing to the minimum flow rate.

The calibration procedure consisted of the following steps:

1. The fluid flow rate was adjusted to the desired float setting on the rotameter.
2. After operating for some time at the desired float setting, the fluid flowing in the system was collected in a previously weighed empty container for a measured time interval. The time interval ranged from 30 seconds up to three minutes, depending upon the flow rate being calibrated.
3. The bath fluid temperature was recorded and taken to be the temperature of the fluid in the rotameter.
4. The vessel containing the fluid collected was weighed to determine the weight of the fluid collected.

The above procedure was repeated three times for each float setting on the rotameter.

For ethylene glycol and n-butyl alcohol as test fluids, the rotameter was used as a guide to set the flow rate and the mass flow rate was measured (by the procedure outlined above) at the time of execution of the data run.

Calibration data for the rotameter are presented in Table VII in Appendix B.

#### Digital Thermocouple Indicator Calibration

The Digital Thermocouple Indicator was calibrated periodically. The calibration procedure is detailed in Section IV of the Owner's Manual (10).

### Start-up Procedure

Experimental data were obtained for one helical coil with a diameter of 254 mm using three different fluids.

After the test section was installed in the fluid flow loop and the thermocouple wires were connected to the switches on the thermocouple selector switchboard, the fluid flow loop was tested for possible leaks by flowing fluid at the anticipated maximum flow rate through the loop. Any leaks detected were eliminated. The fluid flow loop was then insulated with fiberglass tape and fiberglass wool insulation and prepared for obtaining experimental data.

The following step-by-step procedure was followed to gather experimental data for each run:

1. The impeller and the heater in the fluid bath were activated and the fluid in the bath was brought to the desired operating temperature (90°F).
2. The DC generator was started, with the polarity switch in the "Off" position, and allowed to warm up for 30 minutes.
3. Cooling water was started to the heat exchanger located downstream of the test section.
4. The Digital Thermocouple Indicator was activated.
5. The pump was started and the fluid was allowed to circulate in the by-pass line.
6. The flow control valve located upstream of the rotameter was opened and the fluid was allowed to flow through the test section.

7. After about five minutes, the polarity switch was thrown to the "Electrode Negative" position thereby causing the DC current to flow through the test section.

#### Data Gathering Procedure

The data gathering procedure consisted of the following steps:

1. The fluid flow rate was adjusted to the desired value by means of the flow control valve.

2. The DC current was adjusted to the desired value by varying the output control switch on the control box of the generator. Fine control of the current was accomplished by adjusting the external rheostat connected to the generator.

3. The cooling water flow rate to the heat exchanger was adjusted so that the bath fluid temperature remained constant.

4. The experimental set-up was then operated for at least one and one-half hours to allow the system to achieve steady state. Minor adjustments were made to the current, the fluid flow rate and the cooling water flow rate, as was deemed necessary.

5. After about three hours of operation, the following experimental data were taken:

- a. The test section surface temperatures (indicated by the insulated wire thermocouples cemented on the test section).
- b. The inlet and exit bulk fluid temperature.
- c. The fluid flow rate indicated by the rotameter.
- d. The DC current flowing through the test section and the voltage drop across the test section.

- e. The room and bath fluid temperature.
- f. The coil inlet and exit fluid pressure, as indicated by the U-type manometer.

All of the thermocouple outputs were measured on the Digital Thermocouple Indicator.

6. The entire set of data, as indicated in Step 5 above was measured again to ascertain if steady state had been achieved. The time span between the two sets of measurements was approximately half an hour.

7. Steady state was deemed to have been achieved if the two sets of temperature measurements agreed within  $\pm 0.3^{\circ}\text{F}$ .

If steady state had not been achieved, Steps 5 and 6 were repeated after about one hour of continued operation.

Except for a few data cases, steady state was achieved when data were measured after about three hours of operation for a given set of fluid flow rate and current settings.

The fluid flow rate and/or the current was changed to a new set of conditions and the entire Data Gathering Procedure was repeated for the new set of input conditions.

For each of the ethylene glycol and n-butyl alcohol runs, the mass flow rate of the fluid was measured, after obtaining the temperature and pressure data as indicated in Steps 5 and 6 of the Data Gathering Procedure section.

The distilled water used in the experiments was changed frequently to minimize the buildup of solids content in the water.

Each time the fluid was changed, the fluid flow loop was cleaned with acetone. After draining the acetone, air was blown in the fluid

flow loop until no more acetone can be detected in the effluent.

Some runs were repeated after several weeks to see if the results changed due to surface aging; no change was noted.



## CHAPTER V

### DATA REDUCTION

Experimental data were gathered for the helical coil using ethylene glycol, distilled water and n-butyl alcohol. A total of 60 runs was made; 26 runs with ethylene glycol, 14 runs with distilled water and 20 runs with n-butyl alcohol as the working fluid. The raw experimental data are presented in Appendix C. Computer programs which were originally written by Singh (37) were modified to reduce the experimental data using the IBM 370/158 computer. Computer program listings are given in Appendix G.

The physical quantities measured for each experimental run are listed under Item 5 in the Data Gathering Procedure in Chapter IV. The outer surface temperatures were measured at 72 locations along the length of the test section. The locations of the thermocouples are given in Table V in Appendix A.

The physical properties of the fluid were evaluated at the bulk fluid temperature at each thermocouple station. The bulk fluid temperature was assumed to increase linearly along the axial length of the coil, starting from the inlet electrode.

Average bulk fluid temperatures for the entire coil, for each data run, were taken to be the arithmetic average of the inlet and exit bulk fluid temperatures. To correct for wall (non-isothermal transport) effects, the fluid viscosity was also evaluated at the average inside

wall temperature so that a viscosity gradient correction factor could be incorporated into the correlations.

Data reduction consisted of the following steps:

1. Calculation of the error percentage in heat balance.
2. Calculation of the local inside wall temperatures and the inside wall radial heat fluxes.
3. Calculation of the local heat transfer coefficients.
4. Calculation of the dimensionless axial distances and the dimensionless inside wall temperatures.
5. Calculation of the relevant dimensionless numbers.

Details regarding each of the above steps follow.

#### Calculation of the Error Percentage in Heat Balance

The error percentage in the heat balance for each data run was calculated as follows:

Heat input rate, Joules/sec =  $Q_{\text{input}}$

$$Q_{\text{input}} = (I) (V) - Q_{\text{loss}} \quad (5.1)$$

where

$I$  = current in coil, amperes;

$V$  = voltage drop across coil, volts;

$Q_{\text{loss}}$  = heat loss, Joules/sec (calculated from calibration data).

Heat output rate, Joules/sec =  $Q_{\text{output}}$

$$Q_{\text{output}} = (W) (C_p) [(t_b)_{\text{out}} - (t_b)_{\text{in}}]$$

where

$W$  = mass flow rate of fluid flowing through the coil, gm/sec;

$C_p$  = specific heat of the fluid at the average bulk fluid temperature in the coil, cal/gm - K;

$(t_b)_{out}$  = bulk fluid temperature at the coil exit, K;

$(t_b)_{in}$  = bulk fluid temperature at the coil inlet, K;

$$\Delta Q = Q_{input} - Q_{loss} - Q_{output} \quad (5.3)$$

$$\text{Percentage error in heat balance} = \frac{\Delta Q}{Q_{input}} \{100\} \quad (5.4)$$

The inlet and the exit fluid temperatures were corrected based on the thermocouple calibrations given in Table VIII in Appendix B.

#### Calculation of the Local Inside Wall

##### Temperature and the Inside Wall

##### Radial Heat Flux

Computer programs originally written by Owhadi (27) and Crain (6) and later used by Singh (37) were modified to determine the inside wall temperatures from the measured outside wall temperatures. The computer program was modified to correct the measured outside wall temperatures, based on the surface thermocouple calibrations. The calibration data for the surface thermocouples on the helical coil are given in Table IX in Appendix B.

Briefly, the modified computer program corrects the outside wall temperatures and then, using the corrected outside wall temperatures, computes the inside wall temperatures by a trial-and-error solution. The program also computes the inside wall radial heat flux at each thermocouple location on the helical coil. Details regarding the computer program are given in Reference (6). A listing of the modified computer program, called MAH#02, is given in Appendix G of this thesis.

## Calculation of the Local Heat Transfer Coefficient

Knowing the inside wall temperature, the inside wall radial heat flux and the bulk fluid temperature, the local heat transfer coefficient was calculated as follows:

$$h_i = \frac{(Q/A)_i}{[(t_w)_i - t_b]} \quad (5.5)$$

where

$h_i$  = local inside heat transfer coefficient,  
J/sec-m<sup>2</sup>-K;

$(Q/A)_i$  = local inside wall heat flux, J/sec-m<sup>2</sup>;

$(t_w)_i$  = local inside wall temperature, K;

$t_b$  = bulk fluid temperature at the thermocouple station, K.

The average bulk fluid temperature at the thermocouple station was obtained by measuring the "mixing-cup" bulk fluid temperatures at the coil inlet and exit and by assuming that the fluid temperature rise was linear along the length of the helical coil.

## Calculation of the Dimensionless Axial Distance and the Dimensionless Inside Wall Temperature

The dimensionless axial distance and the dimensionless inside wall temperatures were calculated for each thermocouple for each data run:

1. To get the temperature profiles across the coil for each thermocouple location on a common basis for ease of comparison.

2. To facilitate a comparison of the experimental data with the results presented by Dravid et al. (13).

The dimensionless axial distance and the dimensionless wall temperatures were defined exactly as Dravid et al. (13) defined them, namely:

$$\text{Dimensionless axial distance} = z = \frac{\text{Axial distance along helical coil from inlet electrode, mm}}{\text{Tube inside radius, mm}} \quad (5.6)$$

and

$$\text{Dimensionless wall temperature} = T_w = \frac{[t_w - (t_b)_{\text{inlet}}]}{dt_b/dz} \quad (5.7)$$

where

$$\frac{dt_b}{dz} = \frac{[(t_b)_{\text{exit}} - (t_b)_{\text{inlet}}]}{\frac{\text{Total heated length, mm}}{\text{Tube inside radius, mm}}} \quad (5.8)$$

#### Calculation of the Relevant Dimensionless Numbers

The dimensionless numbers calculated at the average bulk fluid temperature at each station were the Reynolds, Prandtl, Dean and Graetz number. The Nusselt number was also calculated for each thermocouple position at each station. In addition, the Grashof and Rayleigh numbers were calculated for each station using the circumferentially-averaged inside wall temperature and the average bulk fluid temperature at the station to define the  $\Delta t$  term. The definition of the dimensionless numbers evaluated are given in Table II.

All the experimental data gathered were reduced using the above procedures. Sample calculations for one data run are given in Appendix E.

TABLE II  
DEFINITION OF THE DIMENSIONLESS  
NUMBERS EVALUATED

Dimensionless Number	Symbol	Definition
Reynolds	Re	$\frac{(d_i) (G)}{\mu}$
Prandtl	Pr	$\frac{(C_p) (\mu)}{k}$
Dean	De	$(Re) (\sqrt{d_i/D_c})$
Nusselt	Nu	$\frac{(h) (d_i)}{(k)}$
Graetz	Gz	$\frac{(W) (C_p)}{(k) (L)}$
Grashof	Gr	$\frac{(d_i^3) (\rho^2) (g) (\beta) (\Delta t)}{\mu^2}$
Rayleigh	Ra	$(Gr) (Pr)$

The inside wall heat transfer coefficients were calculated for each thermocouple location on the coil and the Nusselt number profile for each thermocouple station was digitally plotted for the four thermocouple locations on the tube periphery for each data run. The thermocouple locations are shown in Figure 4 in Chapter III.

## CHAPTER VI

### RESULTS AND DISCUSSION

Experimental data were gathered for Reynolds numbers ranging from 30 to 5500 and Prandtl numbers ranging from 2.24 to 113.1, using a helical coil with a curvature ratio of 0.0495. The test fluids were ethylene glycol, distilled water and normal butyl alcohol. All the experimental runs were conducted under approximately constant wall heat flux conditions. The difference in wall thickness of the tube, caused during the formation of the helical coil, caused the circumferential variation in the wall heat flux. The latter was also partially due to the inherent circumferential temperature gradient resulting from the helix flow behavior. However, the heat input per unit length of tube was constant giving rise to a linear increase in the bulk temperature. The results of this study together with a discussion of the results are presented in this chapter.

H. Ito's (16) equation for the critical Reynolds number for fluid flow at the start of turbulence was used to determine the upper limit of the Reynolds number for these tests. The equation is:

$$Re_{cr} = 2 \times 10^4 (d_i / D_c)^{0.32} \quad (6.1)$$

For a curvature ratio of 0.0495, the critical Reynolds number is 7644.

#### General Discussion

Values of the Reynolds, Dean and Prandtl numbers and the average



values of the heat flux, the heat transfer coefficient and the Nusselt number for the inside wall were computed for each thermocouple station for each data run. These values are summarized in Appendix F for all the experimental data runs.

The average heat transfer coefficient and the average heat flux at a thermocouple station were defined as follows:

$$h = \text{average heat transfer coefficient} = \frac{1}{4} \sum_{i=1}^4 \left[ \frac{(Q/A)_i}{(t_w)_i - t_b} \right] \quad (6.2)$$

$$\text{Average heat flux} = \frac{1}{4} \sum_{i=1}^4 (Q/A)_i \quad (6.3)$$

where  $i$  indicates the peripheral location on the tube cross section at a given thermocouple station. The average heat transfer coefficient obtained from Equation (6.2) was then used to determine the average Nusselt number for the thermocouple station. The physical properties of the fluid used in the determination of the Reynolds, Prandtl and Nusselt numbers were evaluated at the bulk temperature at the thermocouple station,  $t_b$ .

In addition to Equation (6.2), the average heat transfer coefficient at a thermocouple station was also computed as follows:

$$h' = \text{average heat transfer coefficient} = \frac{(\overline{Q/A})}{\overline{t_w} - t_b} \quad (6.4)$$

where

$$(\overline{Q/A}) = \frac{1}{4} \sum_{i=1}^4 (Q/A)_i \quad (6.5)$$

and

$$\bar{t}_w = \frac{1}{4} \sum_{i=1}^4 (t_w)_i \quad (6.6)$$

where  $i$  in Equations (6.5) and (6.6) has the same definition as in Equation (6.2). In Appendix F,  $H1$  and  $H2$  represent the average heat transfer coefficient using Equations (6.2) and (6.4) respectively.  $h$  and  $h'$  become equal if the peripheral distribution of inside wall temperatures is uniform; however, for a nonuniform distribution of inside wall temperatures  $h$  becomes larger than  $h'$ .

#### Comparison with a Straight Tube Under Similar Flow Conditions

The peripheral average heat transfer coefficient at each thermocouple station along the helical coil was calculated using Equations (6.2) and (6.4) and was compared to the correlation (Equation (6.7)) developed by Morcos and Bergles (23). The Morcos and Bergles correlation is chosen because it takes into account the effect of the natural convection in straight tubes.

$$Nu_f = \left\{ (4.36)^2 + \left[ 0.055 \left( \frac{Gr_f Pr_f^{1.35}}{Pw^{0.25}} \right)^{0.4} \right]^2 \right\}^{1/2} \quad (6.7)$$

for

$$Re_f < 1200;$$

$$3 \times 10^4 < Ra_f < 10^6;$$

$$4 < Pr_f < 175; \text{ and}$$

$$2 < Pw < 66$$

where

$$P_w = \frac{h d_i^2}{k_w t} ; \quad (6.8)$$

$t$  = tube wall thickness; and

$k_w$  = thermal conductivity of tube wall.

The average heat transfer coefficient used in Equation (6.8) is defined as in Equation (6.4).

As anticipated, higher heat transfer coefficients were obtained for fluid flow in a helically-coiled tube than in an equivalent straight tube under similar flow conditions. This fact has been known historically and has been indicated by earlier investigators in the field (Dravid et al. (13), Kalb and Seader (18) and Singh (37), to mention a few). The heat transfer coefficients were about two to four times the value for the straight tube under similar operating conditions. The higher heat transfer coefficients have been attributed to the presence of a superimposed secondary flow due to centrifugal action. However, as mentioned earlier, the contribution of natural convection cannot be ignored depending on the flow conditions and the physical properties.

Figure 6 shows some typical heat transfer coefficient profiles at thermocouple station 15 plotted as a function of the peripheral location. The following observations may be made from Figure 6.

1. At the higher Reynolds numbers, the heat transfer coefficient is highest at position 4 and lowest at position 2, while the heat transfer coefficients at positions 1 and 3 are comparable. This indicates that at higher Reynolds numbers, secondary flow due to centrifugal action tends to predominate.

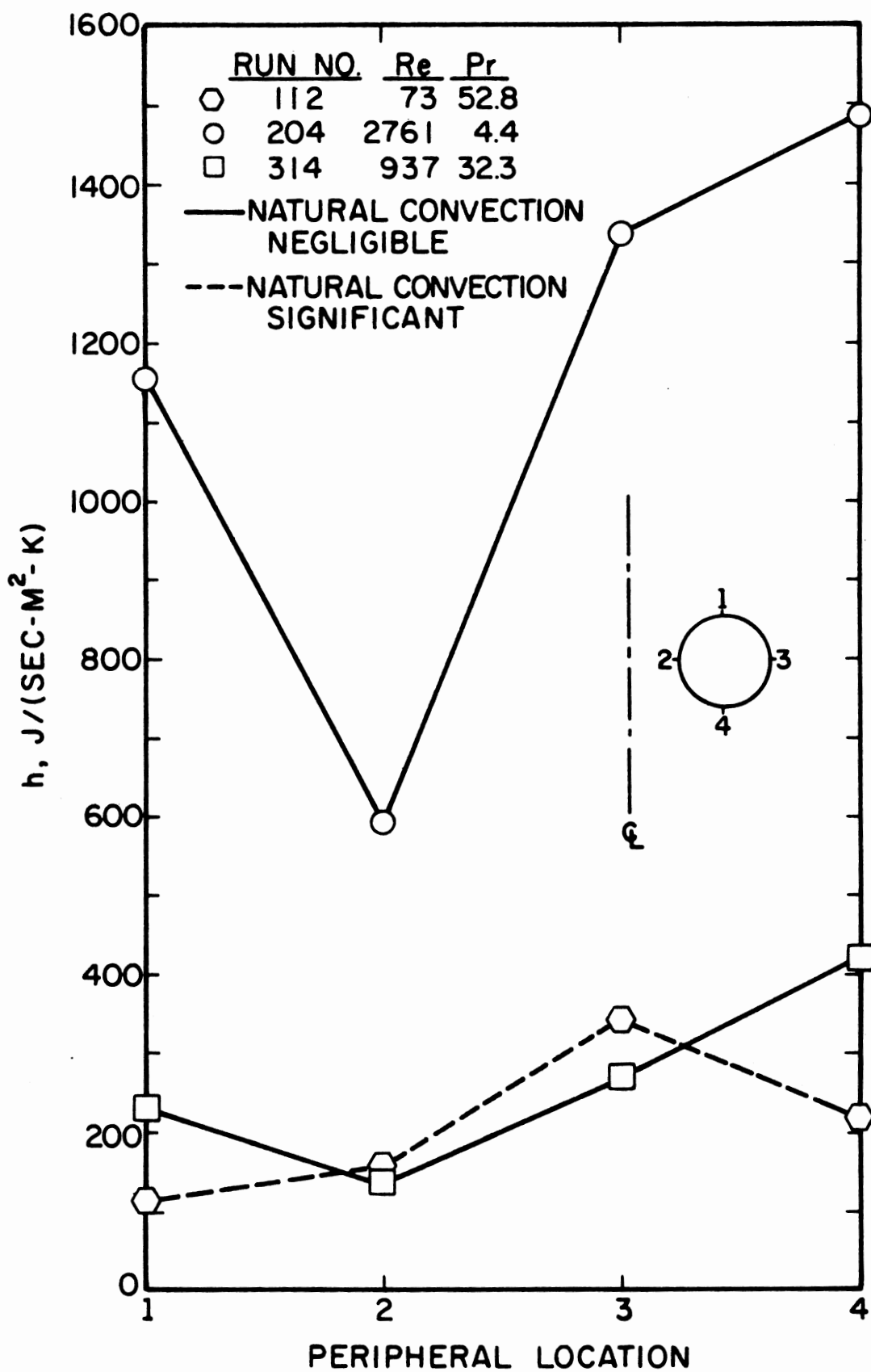


Figure 6. Heat Transfer Coefficient Profile

2. At the lower Reynolds numbers, the heat transfer coefficient is highest at position 3 and lowest at position 1 while the heat transfer coefficients at positions 2 and 4 are comparable. This strongly indicates that natural convection is the dominating factor in the flow pattern.

### Axial Temperature Profiles

In the following discussion, unless otherwise mentioned, the physical properties in the Prandtl and Dean numbers are based on the mean of the inlet and outlet temperatures. The dimensionless temperature is defined by Equation (5.7) and has been calculated as described in Appendix E. The variation of the dimensionless wall temperature was plotted against the dimensionless axial distance.

Figures 7, 8, and 9 show the comparison for the three fluids used in the present work with Dravid's (12). The present experimental work corresponds to the same system and almost the same Dean number. In Figure 7, the present experimental result yielded lower dimensionless temperatures than that obtained by Dravid's, which is expected due to the difference in Prandtl numbers. It should be noted that Dravid used the boundary condition of an isothermal periphery with axially constant wall heat flux, while in the present work, the "constant heat flux" condition was used. The difference between these two boundary conditions does not seem to have great influence on the value of the dimensionless temperature as can be seen from Figures 8 and 9. Figures 7 through 9 are direct comparisons between Dravid's experimentally obtained dimensionless temperature and the present work.

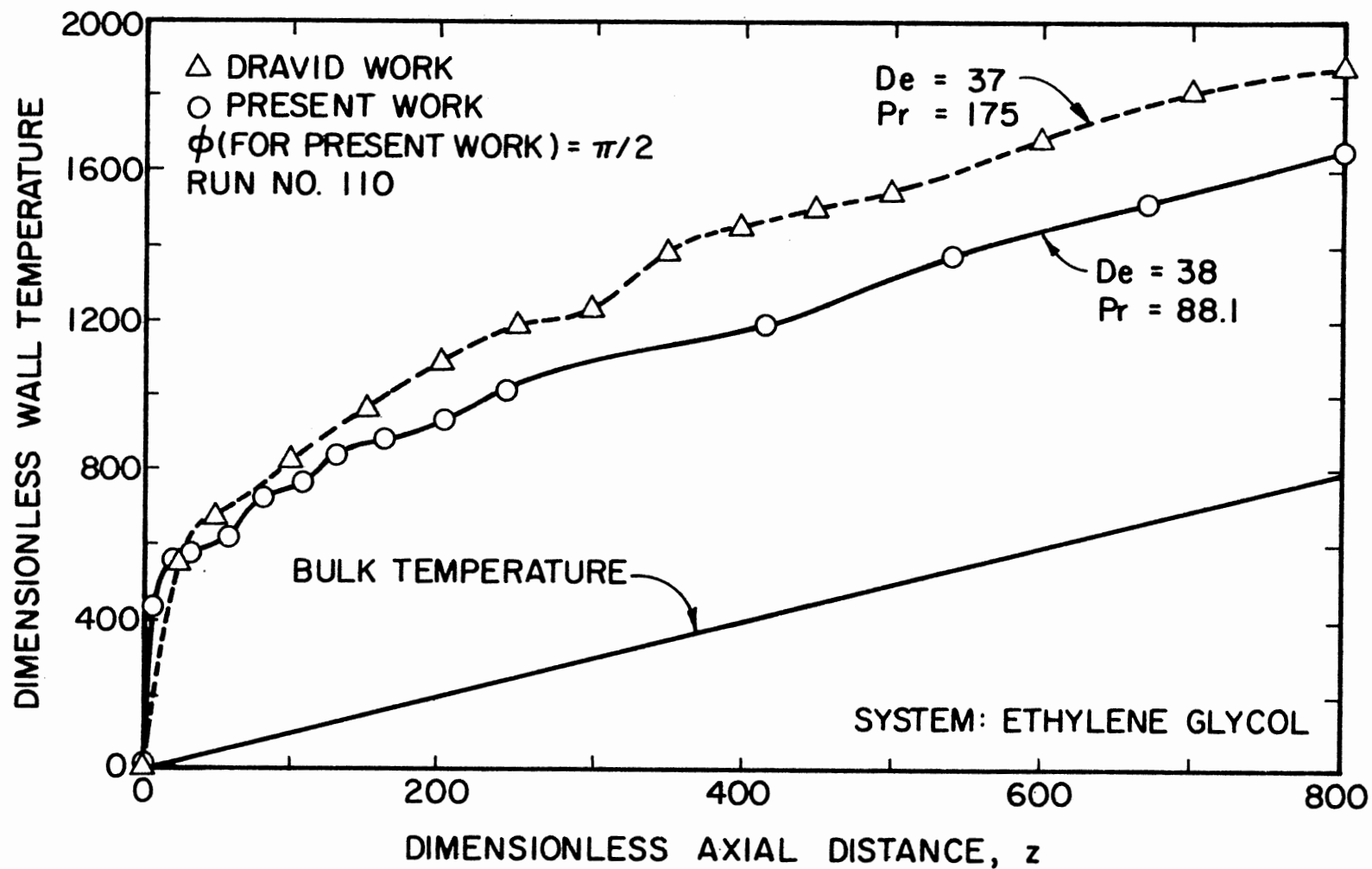


Figure 7. Comparison of the Variation of Wall Temperature for Ethylene Glycol

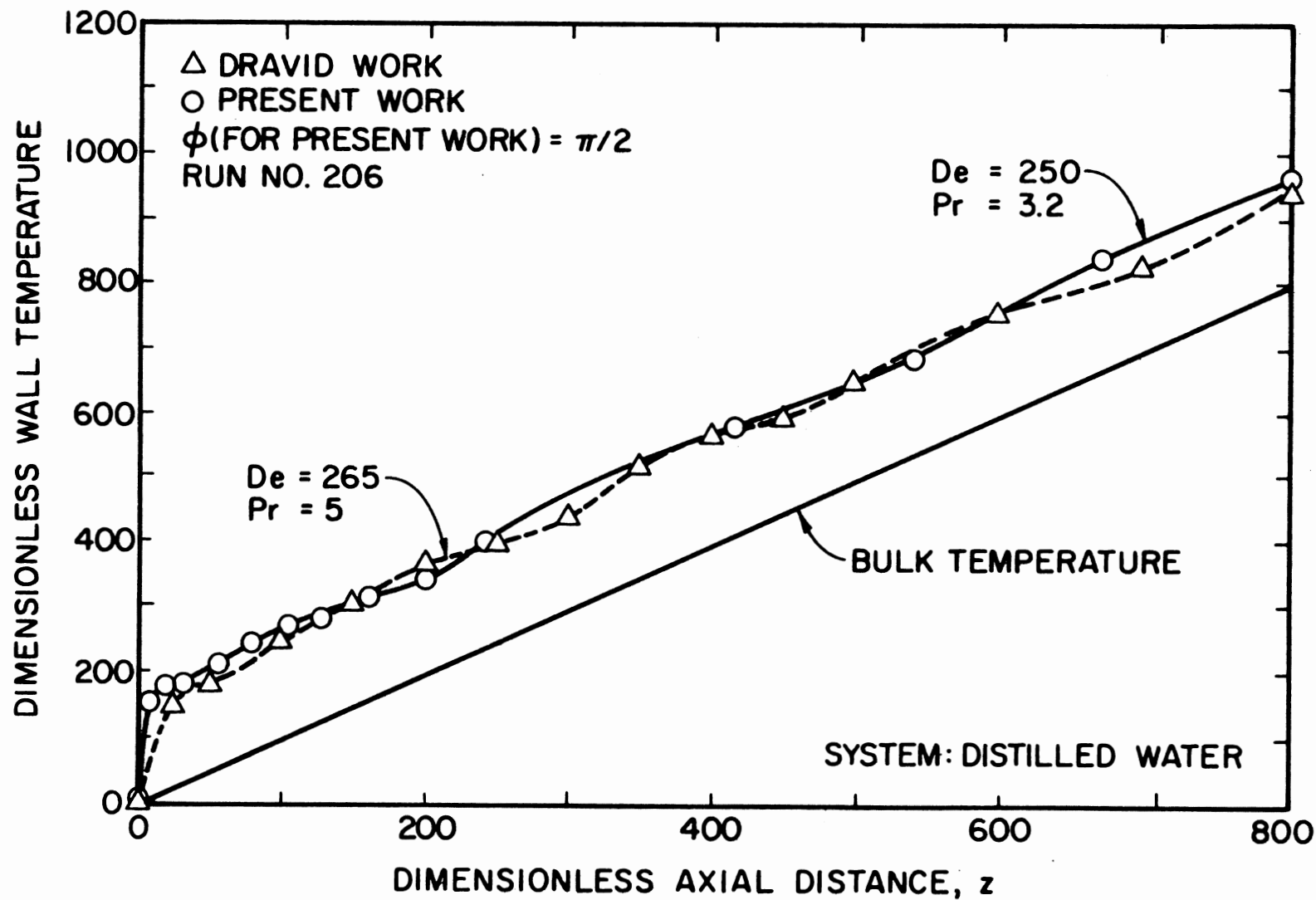


Figure 8. Comparison of the Variation of Wall Temperature for Distilled Water

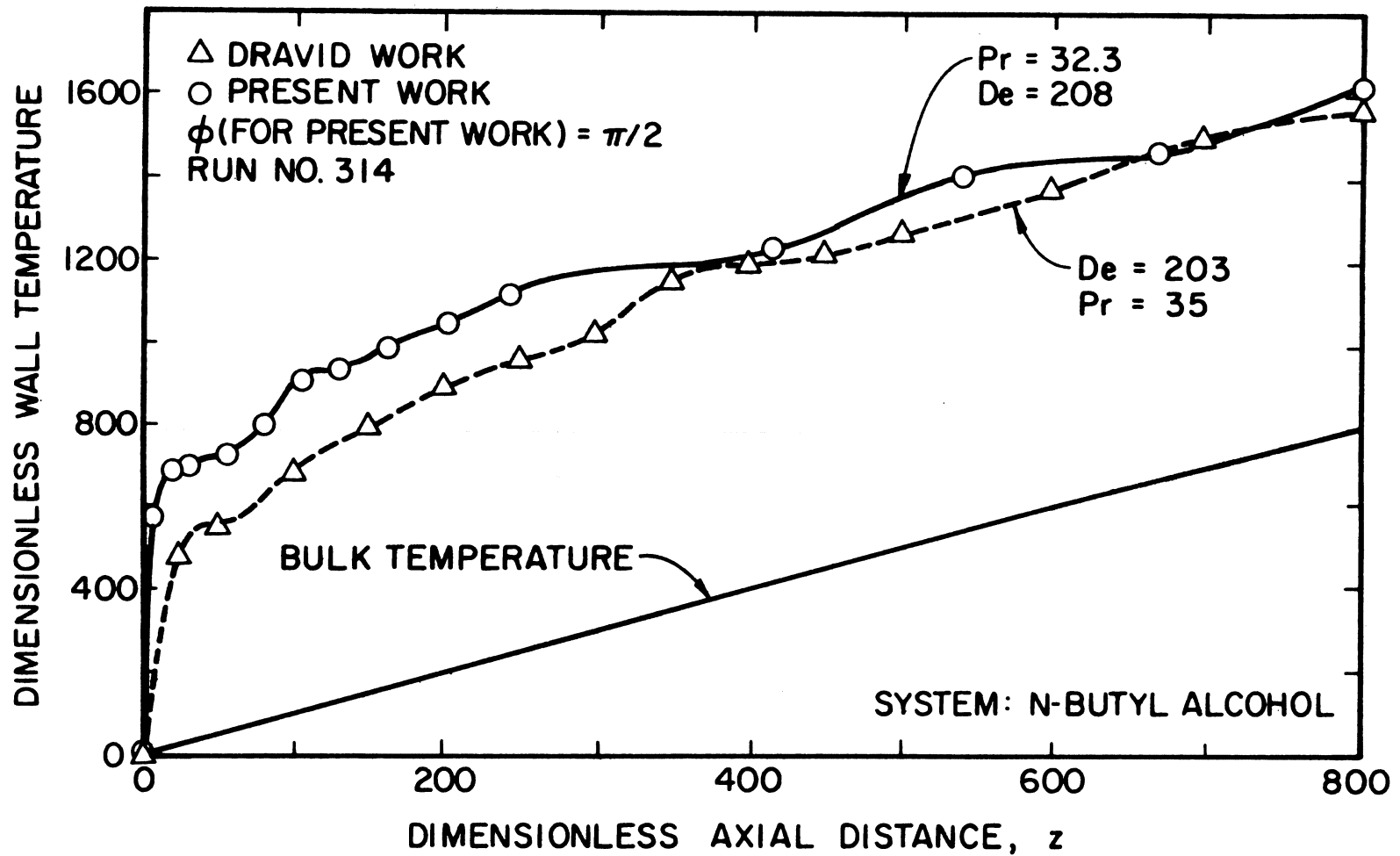


Figure 9. Comparison of the Variation of Wall Temperature for N-Butyl Alcohol



Figures 10 through 12 show the axial variation of the wall temperature at four values of  $\phi$  for the three fluids used with Reynolds numbers of 2363, 73 and 491, respectively. In Figure 10, where Reynolds number is high, it can be seen that the top line is for the inside position,  $\phi=90$  degrees, and the bottom line is for the outside position,  $\phi=270$  degrees. However, in Figure 11 where Reynolds number is low, the top line is for the top position,  $\phi=0$  degree, and the bottom line is for the bottom position,  $\phi=180$  degrees. The top lines in Figures 10 and 11 correspond to the lowest heat transfer positions in the coil, while the bottom lines in Figures 10 and 11 correspond to the highest heat transfer positions in the coil. In the case where the secondary flow is dominating, the centrifugal action causes the fluid to sweep position 4,  $\phi=270$  degrees, thereby increasing the heat transfer coefficient at that thermocouple location. The recirculating fluid tends to accumulate at position 2,  $\phi=90$  degrees, thereby decreasing the heat transfer coefficient at position 2. In the case of low Reynolds numbers, the natural convection effect predominates in the heat transfer process. The gravity force due to the difference in density causes the motion of the fluid element in the vertical direction and causes the highest heat transfer coefficient to move from position 4 to position 3, and the lowest heat transfer coefficient to move to position 1 from position 2. The fluid flow patterns postulated to be responsible for the above behaviors are sketched in Figures 1 and 2.

In Figure 12, it can be seen that at about  $z$  equal to 1050 the lines labeled  $\phi=0$  degree (top position) and  $\phi=270$  degrees (outside position) start to cross the  $\phi=90$  degrees and the  $\phi=180$  degrees lines, respectively. This is an indication that at this point the controlling

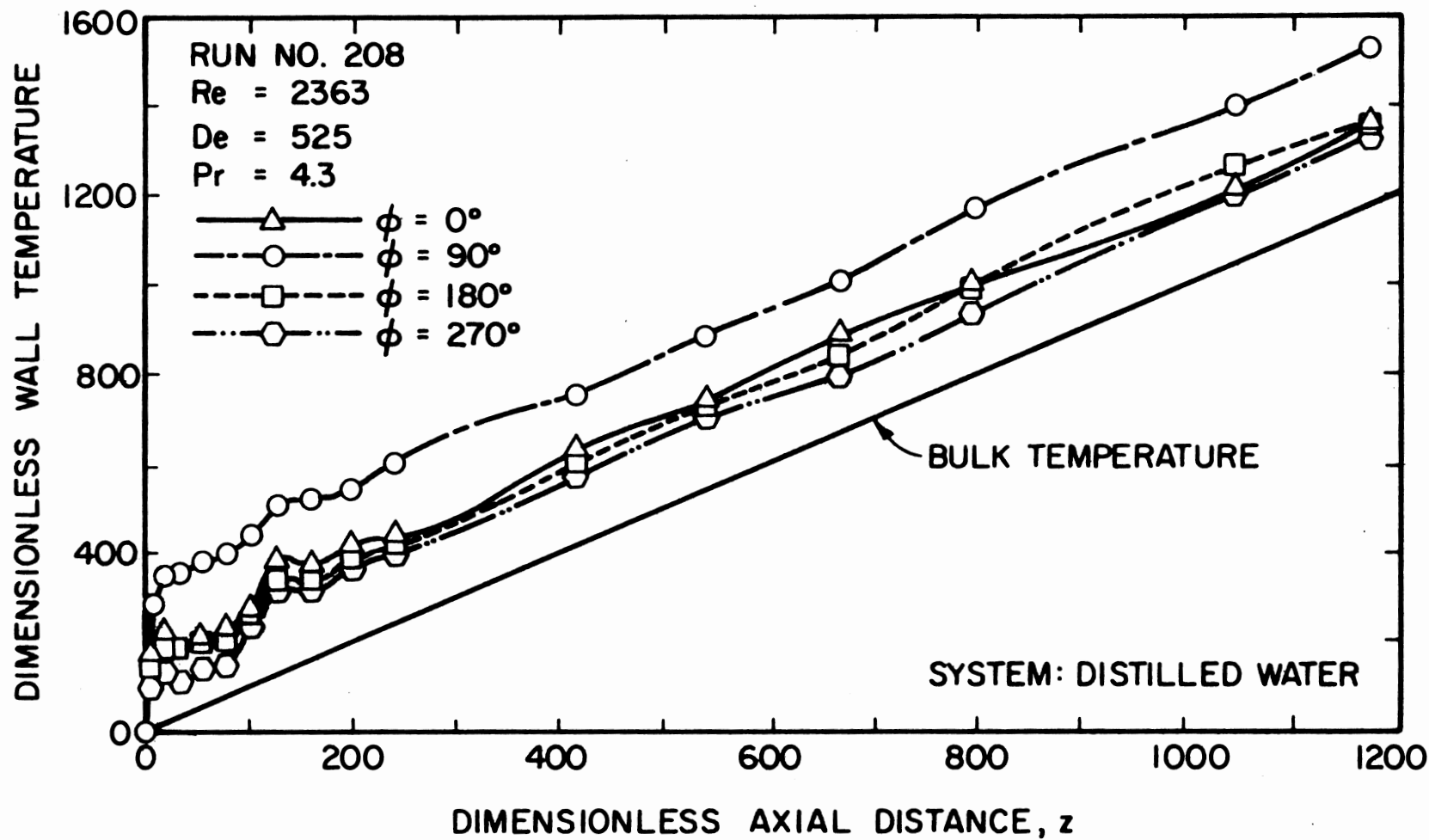


Figure 10. Axial Wall Temperature Profiles for Distilled Water

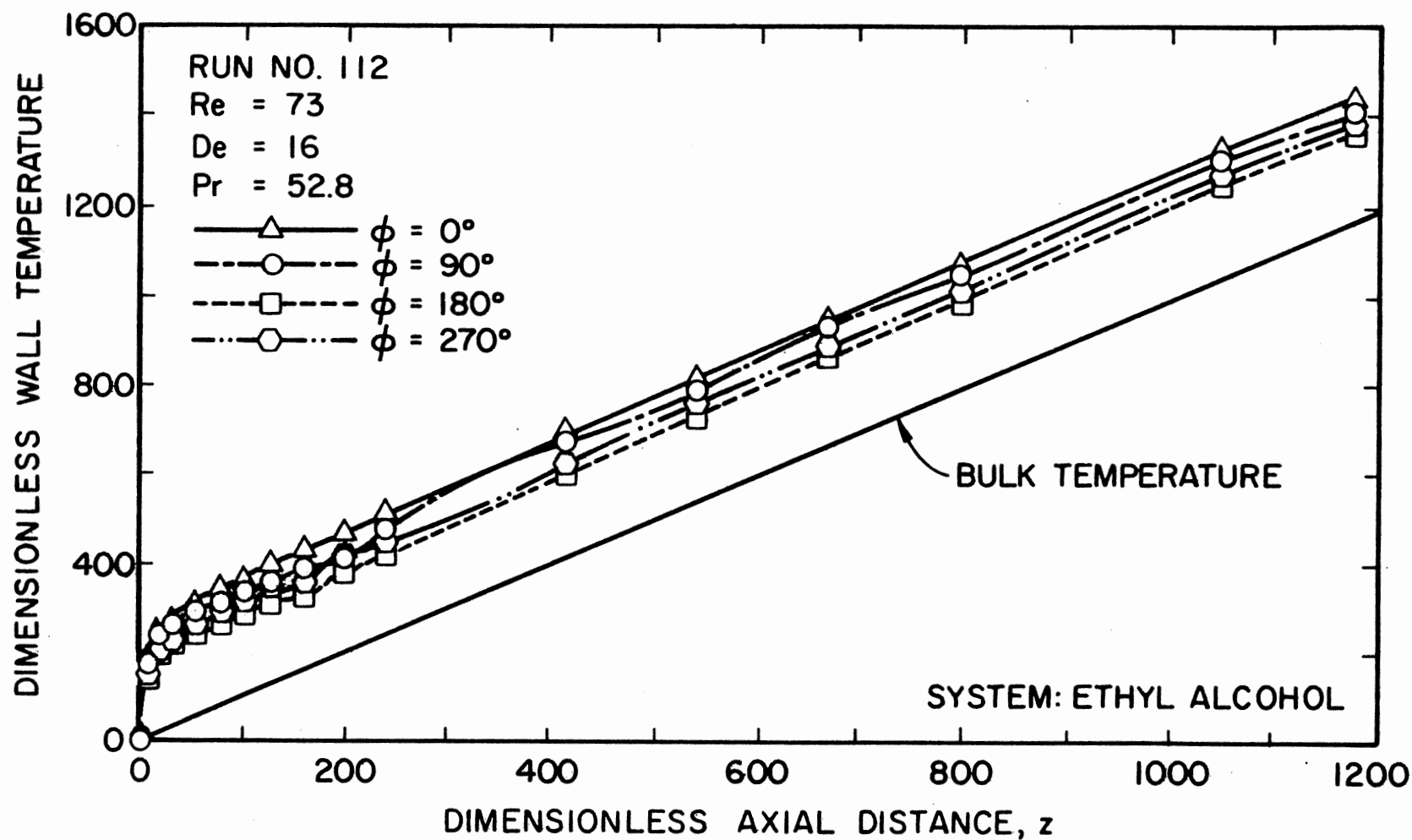


Figure 11. Axial Wall Temperature Profiles for Ethylene Glycol

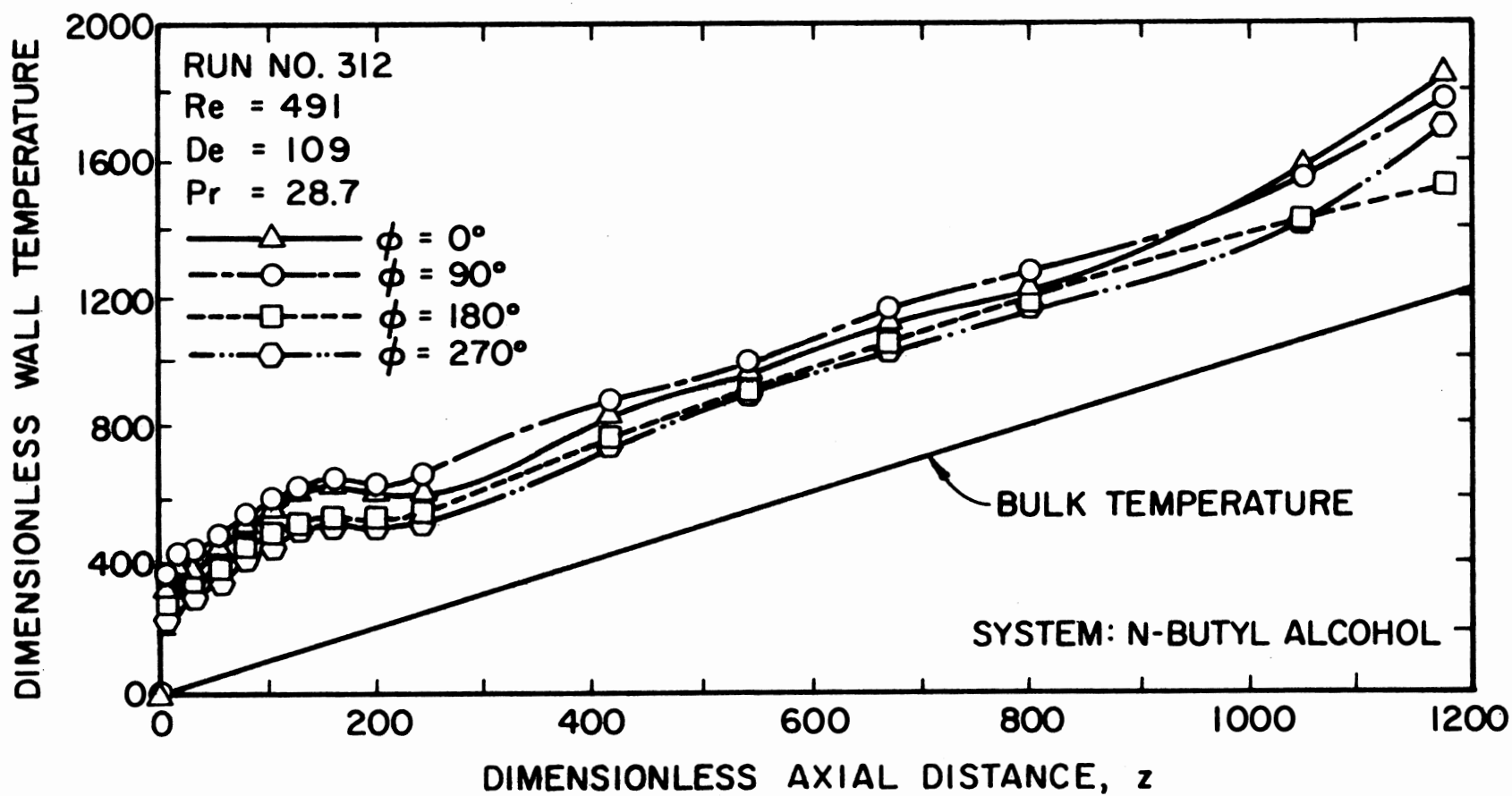


Figure 12. Axial Wall Temperature Profiles for N-Butyl Alcohol

factor has changed, and natural convection is becoming important, due to the changes in the physical properties. This phenomenon can be explained by examining the Grashof number quantitatively. For example, at an axial distance of 800, the Grashof number is 45,000, while the value of Grashof number at an axial distance of 1180 is 84,000. The increase in the Grashof number apparently caused the change in the controlling mechanism.

Figure 13 shows the effect of Dean number on the dimensionless temperature for ethylene glycol at  $\phi$  equal to  $\pi/2$  ( $90^\circ$ ) position 2), which is the inside peripheral location. Figures 14 and 15 show similar plots for distilled water and n-butyl alcohol.

In Figures 7 through 15 the axial temperature profiles show large amplitude oscillations, as reported by Dravid (12), which decay and damp out in the fully-developed region. The achievement of the fully-developed temperature field is indicated by the wall temperatures rising steadily, parallel to the linearly-increasing bulk temperature.

Cyclic variations are apparent in the early portion of each curve and the intensity of the oscillations increases with increasing Dean number. It is to be noted that throughout this thesis, an increase in the Dean number is caused by an increase in the Reynolds number, because the curvature ratio  $d_1/D_c$  is constant.

These oscillations are a consequence of the secondary flow as analyzed by Dravid (12) and Patankar et al. (29). This phenomenon can be explained by following an element of fluid in the entrance region of the tube. The development of the hydrodynamic and the thermal boundary layers will take place as the fluid enters the curved portion of the tube. Element e (see Figure 16) by virtue of secondary flow will enter

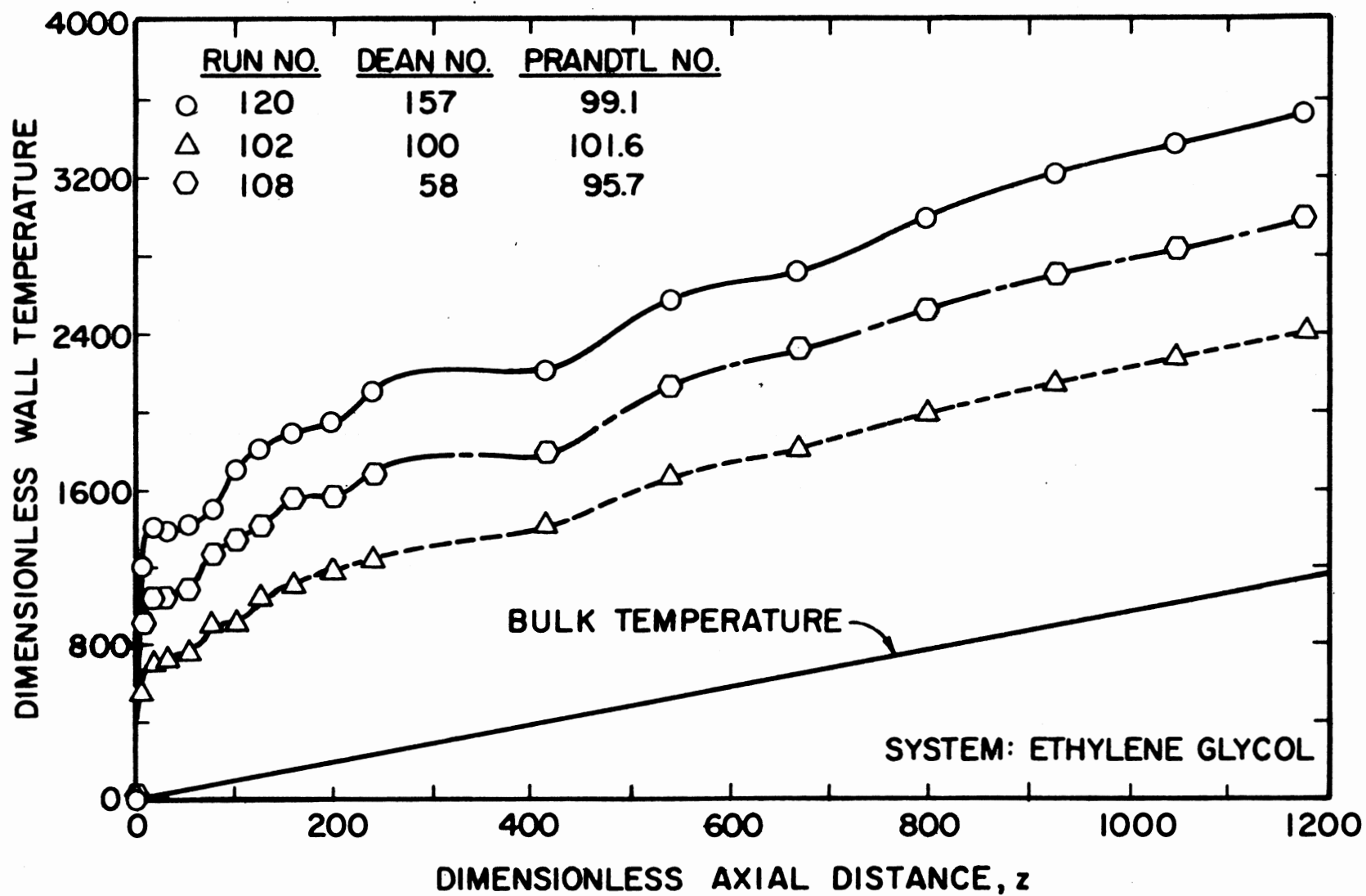


Figure 13. Variation of Wall Temperature at  $\phi = 90^\circ$  with Axial Distance for Ethylene Glycol

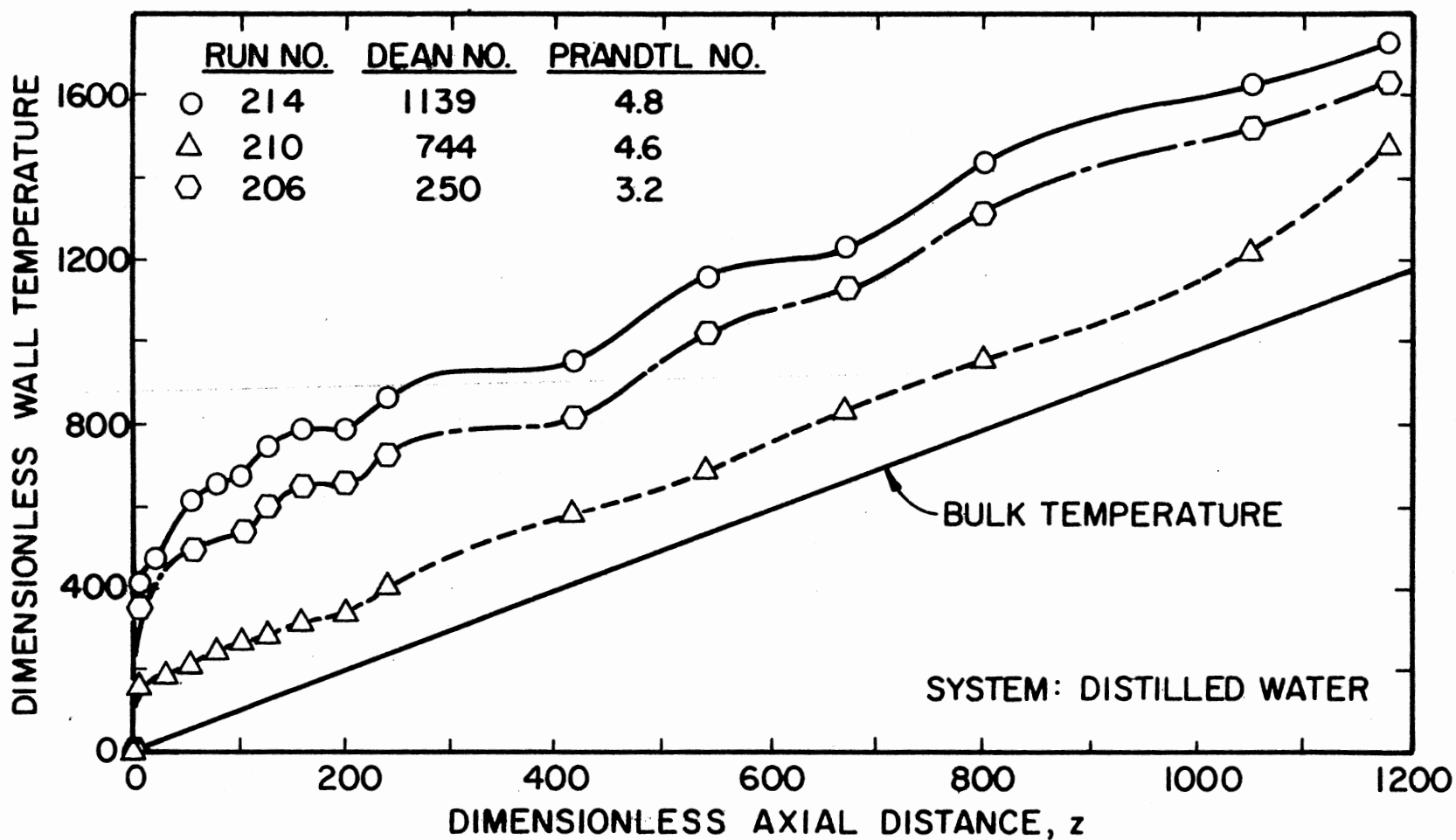


Figure 14. Variation of Wall Temperature at  $\phi = 90^\circ$  with Axial Distance for Distilled Water

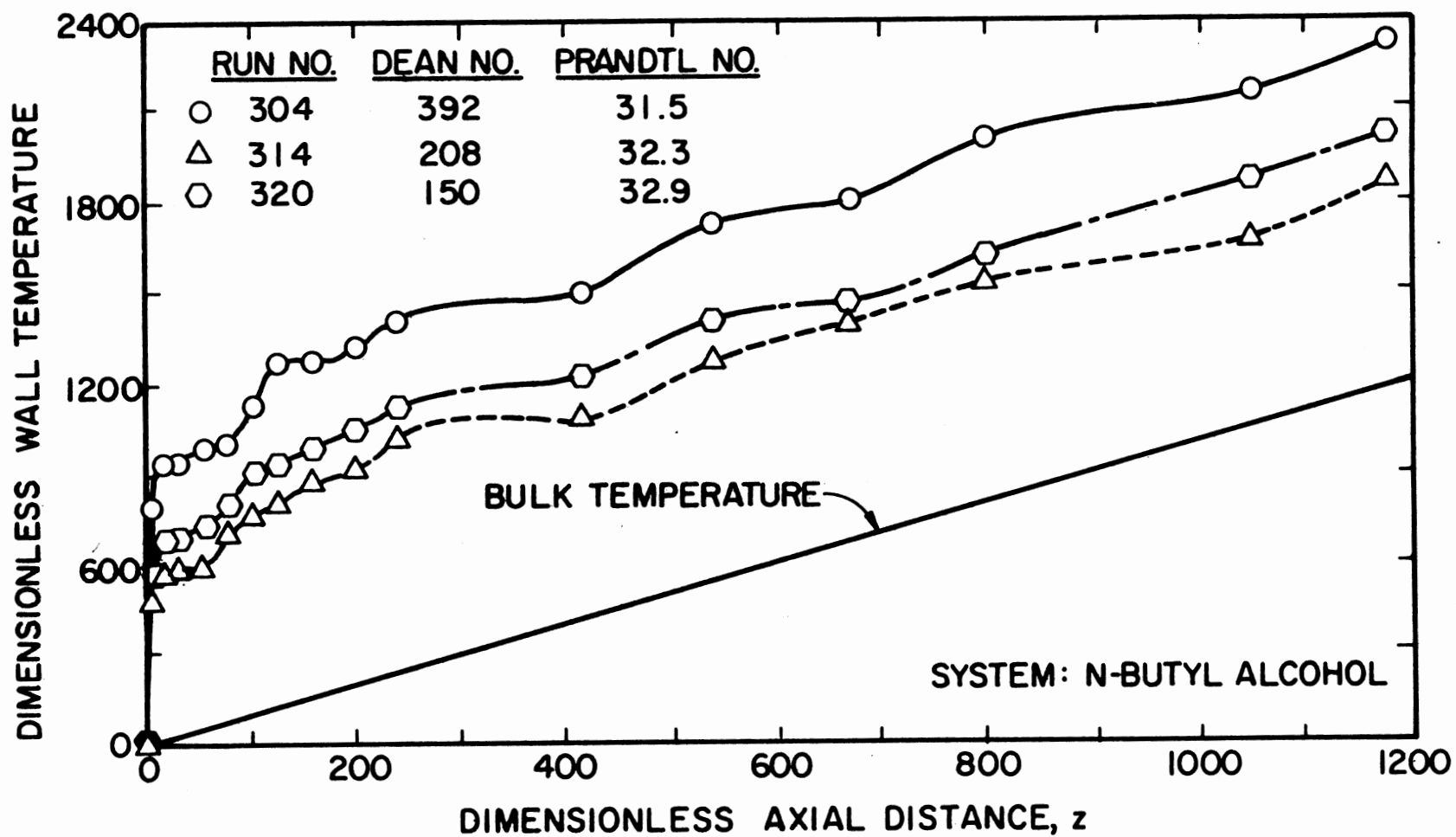


Figure 15. Variation of Wall Temperature at  $\phi = 90^\circ$  with Axial Distance for N-Butyl Alcohol



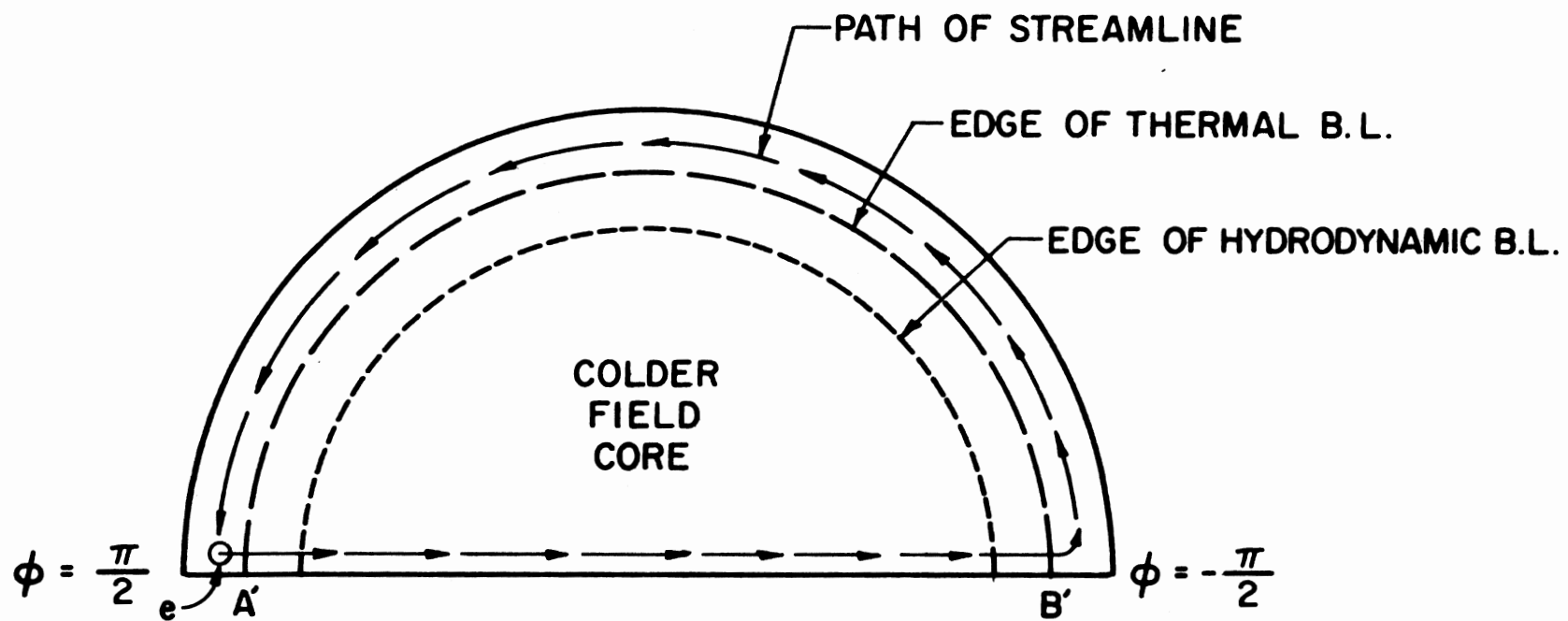


Figure 16. Schematic Diagram of the Interaction Between Secondary Flow and Thermal Boundary Layer

the core region which is colder than element e. All the elements of fluid preceding element e on the streamline A'B' are, therefore, colder than element e. Hence, wall temperature at B' will not change until element e reaches B'. Element e will generate a step change in the temperature and remain at a new value of wall temperature until all the elements on the streamline preceding element e passed point B'. Element e then follows a circumferential path as shown in Figure 16, and absorbs heat from the tube wall. This cyclic nature of the flow causes the oscillatory behavior of the wall temperature. However, when element e passes through the core region, heat is transmitted by conduction in the direction normal to the streamline A'B', hence, subsequent oscillations are damped. Finally, when temperature profiles are fully developed, oscillations are not observed.

#### Testing of Literature Correlations

Available literature correlations in the laminar flow for helical coils were tested against the experimental results to determine how well the two agreed. The average absolute percent deviation (AAPD) was used as a measure to determine the degree of fit of the literature correlations to the experimental data. Table III summarizes the results of the tests when the literature correlations are applied to all the experimental data, while Table IV summarizes the results of the tests when the literature correlations are applied to the experimental data within the applicable range of each correlation.

The comparison between the experimental results and the literature correlations were calculated for stations 15, 16, 17 and 18, where the flow is fully developed. The AAPD is defined as follows:

TABLE III

COMPARISON OF LITERATURE CORRELATIONS TO THE PRESENT EXPERIMENTAL DATA

Investigator(s)	References(s)	Basis	Applicable Range	AAPD			
				Station Number			
				15	16	17	18
Akiyama and Cheng	2,3	Theor.	$100 < De < 200$ $Pr > 1$ $(De^2 Pr)^{1/4} > 3.5$	43.1	40.3	48.5	46.9
Berg and Bonilla	5	Exp.	$Re < Re_{cr}$	50.8	52.4	52.5	52.0
Dravid, et al.	13	Theor. & Exp.	$50 < De < 2000$ $5 < Pr < 175$	15.2	18.9	16.3	16.2
Janssen and Hoogendoorn	17	Theor. & Exp.	$De < 830$	14.6	18.1	15.5	15.7
Kalb and Seader	18	Theor.	$80 < De < 1200$ $0.7 < Pr < 5$	22.4	20.3	23.9	25.3
Kubair and Kuloor	21	Exp.	$80 < Re < 6000$ $20 < Pr < 100$ $10 < Gz < 1000$	99.8	83.1	79.2	68.4
Mori and Nakayama	25	Theor.	$De > 30, Pr \rightarrow \infty$ $De > 60, Pr > 1$	92.5	85.7	100.0	99.4
Oliver and Asghar	26	Exp.	$4 < De < 2000$	21.4	24.5	23.8	24.2
Schmidt	33	Exp.	$100 < Re < Re_{cr}$	42.3	37.6	46.0	46.2
Seban and McLaughlin	34	Exp.	$12 < Re < 5600$ $100 < Pr < 657$	26.9	30.5	28.5	28.5

TABLE III (Continued)

Investigator(s)	References(s)	Basis	Applicable Range	AAPD			
				Station Number			
				15	16	17	18
Shchukin	35	Exp.	26<De<7000 7<Pr<369	35.5	33.4	37.2	37.6
Singh	37	Exp.	6<Re<Re <sub>cr</sub> 2.3<Pr<250 1<De<1700 241<Gr<9.22x10 <sup>5</sup>	68.7	64.3	75.0	73.9
Present Work	--	Exp.	92<Re<5500 2.2<Pr<101 760<Gr<10 <sup>6</sup>	7.6	8.8	10.1	10.1

TABLE IV

COMPARISON OF LITERATURE CORRELATIONS TO THE PRESENT EXPERIMENTAL DATA WITHIN  
THE APPLICABLE RANGE OF THE CORRELATIONS

Investigator(s)	Reference(s)	Basis	Applicable Range	AAPD			
				Station Number			
				15	16	17	18
Akiyama and Cheng	2,3	Theor.	$100 < De < 200$ $Pr > 1$ $(De^2 Pr)^{1/4} > 3.5$	38.5	35.0	42.5	40.3
Berg and Bonilla	5	Exp.	$Re < Re_{cr}$	50.8	52.4	52.5	52.0
Dravid, et al.	13	Theor. & Exp.	$50 < De < 2000$ $5 < Pr < 175$	13.3	18.2	16.3	14.9
Janssen and Hoogendoorn	17	Theor. & Exp.	$De < 830$	13.6	17.0	14.5	14.9
Kalb and Seader	18	Theor.	$80 < De < 1200$ $0.7 < Pr < 5$	11.4	11.8	13.3	14.1
Kubair and Kuloor	21	Exp.	$80 < Re < 6000$ $20 < Pr < 100$ $10 < Gz < 1000$	116.2	90.6	91.0	75.6
Mori and Nakayama	25	Theor.	$De > 30, Pr \rightarrow \infty$ $De > 60, Pr > 1$	94.1	87.0	101.5	99.4
Oliver and Asghar	26	Exp.	$4 < De < 2000$	21.4	24.5	23.8	24.2
Schmidt	33	Exp.	$100 < Re < Re_{cr}$	43.3	37.6	46.0	46.2
Seban and McLaughlin	34	Exp.	$12 < Re < 600$ $100 < Pr < 657$	Not Applicable			

TABLE IV (Continued)

Investigator(s)	Reference(s)	Basis	Applicable Range	AAPD			
				Station Number			
				15	16	17	18
Shchukin	35	Exp.	26<De<7000 7<Pr<369	40.6	36.6	43.9	45.4
Singh	37	Exp.	6<Re<Re <sub>cr</sub> 2.3<Pr<250 1<De<1700 241<Gr<9.22x10 <sup>5</sup>	68.7	64.3	75.0	73.9
Present Work	--	Exp.	92<Re<5500 2.2<Pr<101 760<Gr<10 <sup>6</sup>	7.6	8.8	10.1	10.1

$$AAPD = \frac{\sum_{i=1}^n \left[ \left| \frac{(\text{Calculated Value}) - (\text{Experimental Value})}{\text{Experimental Value}} \right| (100) \right]}{n} \quad (6.9)$$

where  $n$  is the total number of data points evaluated. It may be noted from Table IV that Kalb and Seader's (18) correlation comes closest to fitting the experimental data within the stated range of validity of the correlation, followed by Janssen and Hoogendoorn (17). All of the literature correlations tested break down when extended to the straight tube case, i.e., when  $D_c$  tends to infinity. With the exception of Singh (37), all investigators either neglected or did not incorporate the natural convection effect in their correlations.

In order to improve the prediction of the heat transfer coefficient over the existing correlations, an attempt was made to find a correlation which would reduce to the straight tube case when  $D_c$  tends to zero, and also would account for the natural convection effect.

#### Development of Correlation

Experimental data in the laminar flow regime were gathered using ethylene glycol, distilled water and normal butyl alcohol.

As indicated earlier in this chapter, higher heat transfer coefficients were obtained for fluid flow in helical coils. The heat transfer coefficients were about two to four times the value for the straight tube under otherwise similar operating conditions. The higher heat transfer coefficients have been attributed to the presence of a superimposed secondary flow due to centrifugal action. Little attention

had been given to the possible effects of natural convection.

In general, the experimental results indicated that the heat transfer coefficient was the highest at position 4 and lowest at position 2 on the tube periphery. Referring to Figure 6, for an average Reynolds number of 2761, the heat transfer coefficient at position 4 was 2.5 times the value at position 2, while the heat transfer coefficients at positions 1 and 3 were comparable and intermediate between the values at 2 and 4. This was attributed to the presence of the secondary flow caused by centrifugal action. The fluid flow pattern postulated to be responsible for the above behavior is sketched in Figure 1. Referring to Figure 1, the secondary flow causes the fluid to sweep position 4, thereby increasing the heat transfer coefficient at 4, but the recirculating fluid tends to accumulate at position 2 thereby decreasing the heat transfer coefficient at 2. Also, the fact that the heat transfer coefficients at positions 1 and 3 were comparable suggests that the secondary flow pattern was symmetrical about a horizontal plane through the tube center.

It was also observed that as the fluid velocity through the helical coil was decreased below approximately 3 cm/sec, the highest heat transfer coefficient moved from position 4 to position 3, and the lowest heat transfer coefficient moved to position 1 from position 2, while the heat transfer coefficients at positions 2 and 4 were comparable and intermediate between the values at 1 and 3. In this case, it is believed that natural convection has become the dominant factor (next to primary forced convection) in the heat transfer process. The fluid flow pattern postulated to exist in the helically-coiled tube



for heat transfer to the fluid at low Reynolds number is shown in Figure 2.

To aid in the development of the correlation, the average Nusselt number is presented in Figures 17 through 19 for the fluids used in this study. These figures show the variation of the average Nusselt number with Graetz number. The parameter Dean number is evaluated at the average inlet and exit bulk temperatures. The Hausen (15) correlation for laminar flow in a straight tube is also shown in the above plots. The oscillations in each curve are a result of the oscillations in the wall temperatures. These oscillations were also reported by Seban and McLaughlin (34) and Dravid (12).

The local heat transfer coefficient does not decrease continuously with axial distance, but undergoes cyclic oscillations with increasing axial distance. These oscillations damp out as the region of fully developed temperature field is approached. Dravid (12) had pointed out that these oscillations arise because of the fact that even at high Dean numbers the fluid core is not well-mixed.

It should be noted that there are three phenomena that contribute towards the heat transfer process, namely, forced flow, secondary flow due to the curvature and natural convection effects. Evaluating the effects of these three factors experimentally could be tedious and difficult. However, one could assume that the three phenomena do not interact and the contribution of each one could be expressed as a product form given by the following equation:

$$Nu = \left( \begin{array}{l} \text{forced convection} \\ \text{for straight tube} \end{array} \right) \left( \begin{array}{l} \text{coil tube secondary} \\ \text{flow contribution} \end{array} \right) \left( \begin{array}{l} \text{coiled tube natural} \\ \text{convection contribution} \end{array} \right) \quad (6.10)$$

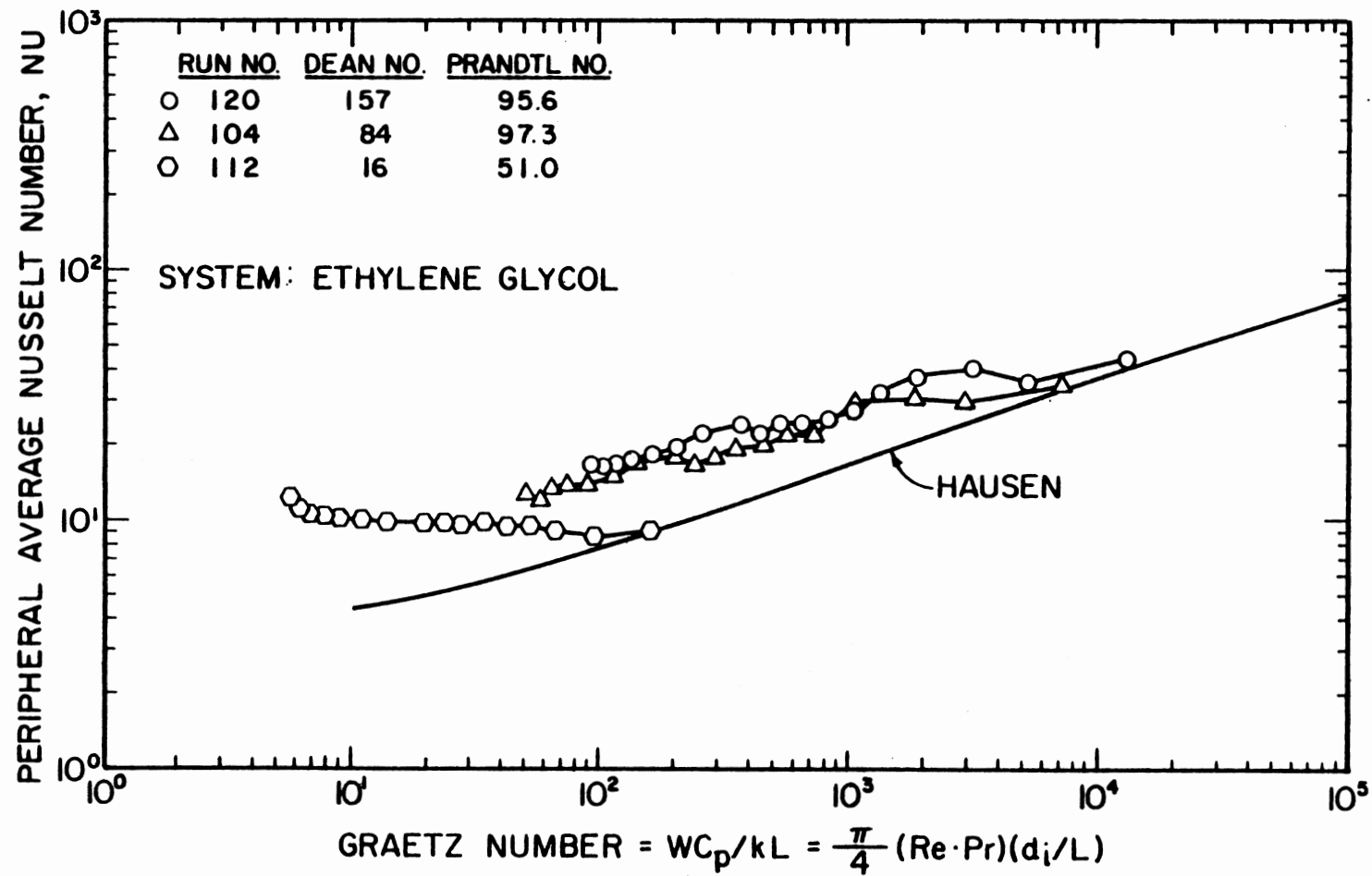


Figure 17. Variation of the Peripheral Average Nusselt Number with Graetz Number for Ethylene Glycol

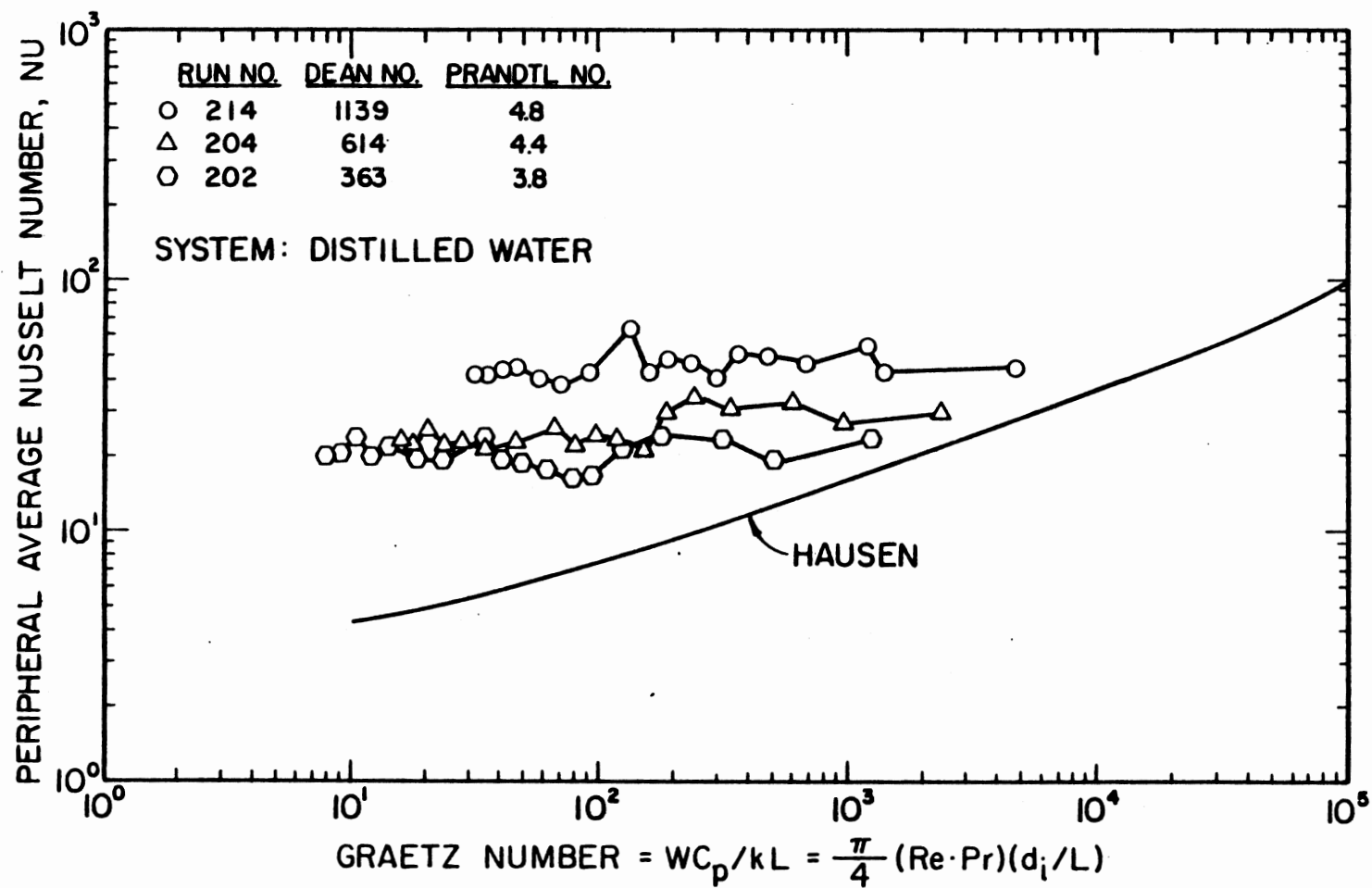


Figure 18. Variation of the Peripheral Average Nusselt Number with Graetz Number for Distilled Water

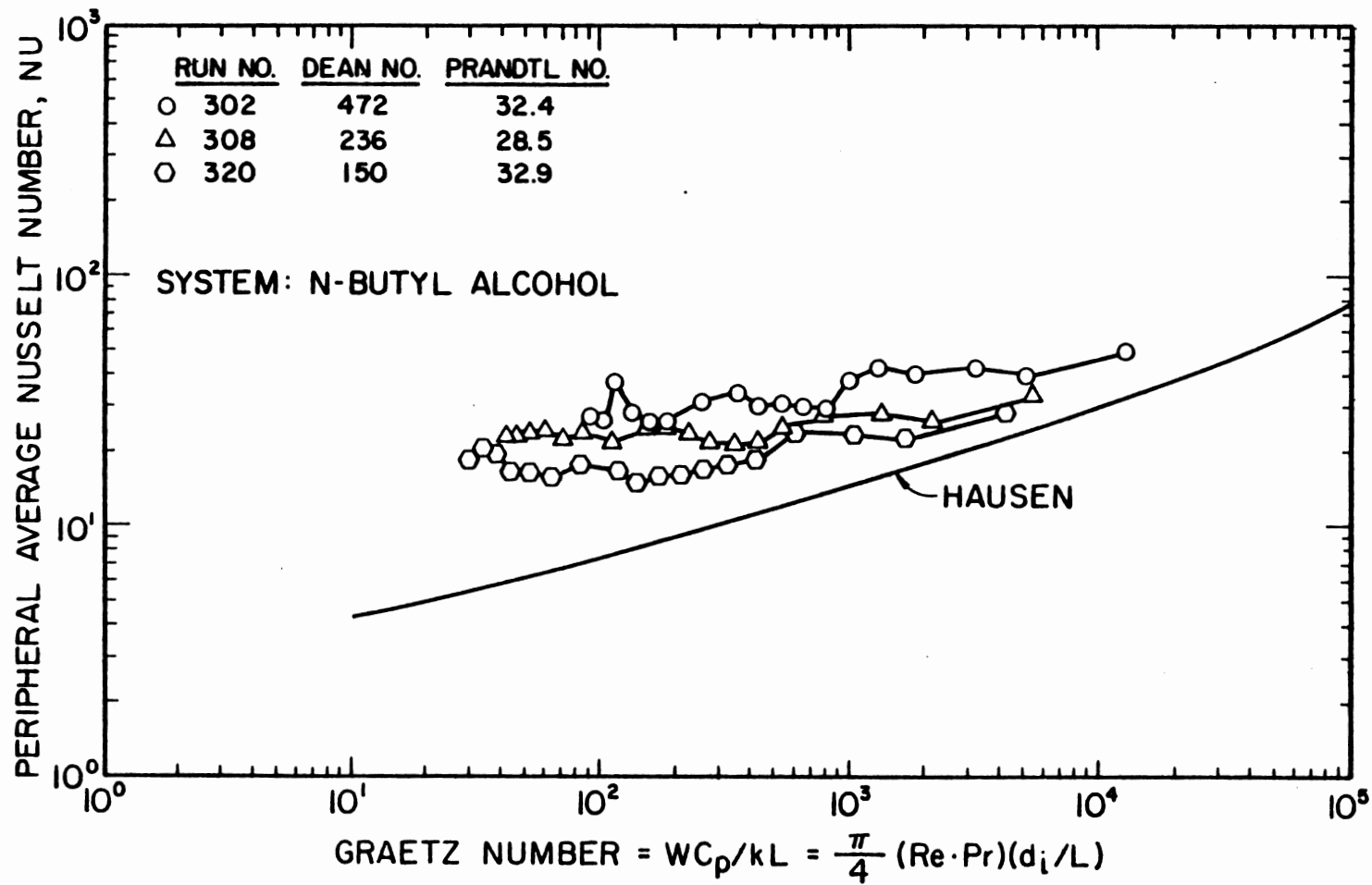


Figure 19. Variation of the Peripheral Average Nusselt Number with Graetz Number for N-Butyl Alcohol

The forced convection term is rewritten as an equation for a straight tube so that one could include an experimental correlation that includes a natural convection factor affecting flow in a straight tube. Then, the other two terms give the effects of curvature and natural convection in a helical coil. Hence, Equation (6.10) is rewritten as:

$$\text{Nu} = \left( \begin{array}{c} \text{straight tube} \\ \text{correlation} \end{array} \right) \left( \begin{array}{c} \text{coiled tube} \\ \text{secondary flow} \\ \text{contribution} \end{array} \right) \left( \begin{array}{c} \text{coiled tube} \\ \text{natural convection} \\ \text{contribution} \end{array} \right) \quad (6.11)$$

The data were divided into four groups based on the ratio of the local heat transfer coefficients for the top (position 1) and the bottom (position 3) thermocouple positions on the tube periphery. The four groups are defined as follows:

$$\frac{h_1}{h_3} \geq 0.9 \quad \text{natural convection is negligible.}$$

$$0.9 > \frac{h_1}{h_3} \geq 0.7 \quad \text{natural convection exists but not significant.}$$

$$0.7 > \frac{h_1}{h_3} \geq 0.5 \quad \text{natural convection is becoming significant.}$$

$$0.5 > \frac{h_1}{h_3} \quad \text{natural convection is significant if not predominant.}$$

Figure 6 shows some typical heat transfer coefficient profiles at thermocouple station 15 plotted as a function of the peripheral location.

Attempts were made to correlate the data using the curved tube factor,  $[1 + f(\text{Re}\sqrt{d_1/D_c})]$ , with the goal that the correlation developed would reduce to the straight tube correlation when  $D_c$  tended to infinity.

Another factor was considered in developing the correlation was the natural convection contribution. The factor should be made up of some combination of the dimensionless groups (Grashof and Reynolds numbers), that reflect the relative magnitude of the natural convection effect, with the goal that this factor would reduce to 1 as the Grashof number tended to zero.

The secondary flow contribution was evaluated by considering the data points of thermocouple stations 15, 16, 17 and 18 having  $h_1/h_3$  ratios greater than or equal to 0.9. As mentioned earlier, points having  $h_1/h_3 \geq 0.9$  were considered to show a negligible natural convection contribution. Hence, the secondary flow contribution factor was found to be:

$$1 + 0.0276 \text{ De}^{0.75} \text{ Pr}^{0.197} \quad (6.12)$$

The ratio of the local heat transfer coefficients for the top (position 1) and the bottom (position 3) thermocouple positions, for thermocouple stations 15, 16, 17 and 18 was plotted against the ratio of  $\text{Gr}/(\text{De}^2)$  in Figure 20. As it was expected, at higher values of  $\text{Gr}/(\text{De}^2)$ , the ratio of the local heat transfer coefficients,  $h_1/h_3$ , decreases.

The natural convection contribution was then evaluated. A detailed examination of the experimental data indicated that the natural convection contribution should satisfy the following criteria:

1. The contribution should be larger than 1 for data points having  $h_1/h_3 < 0.5$  but should tend to unity for data points where  $h_1/h_3 \geq 0.9$ .

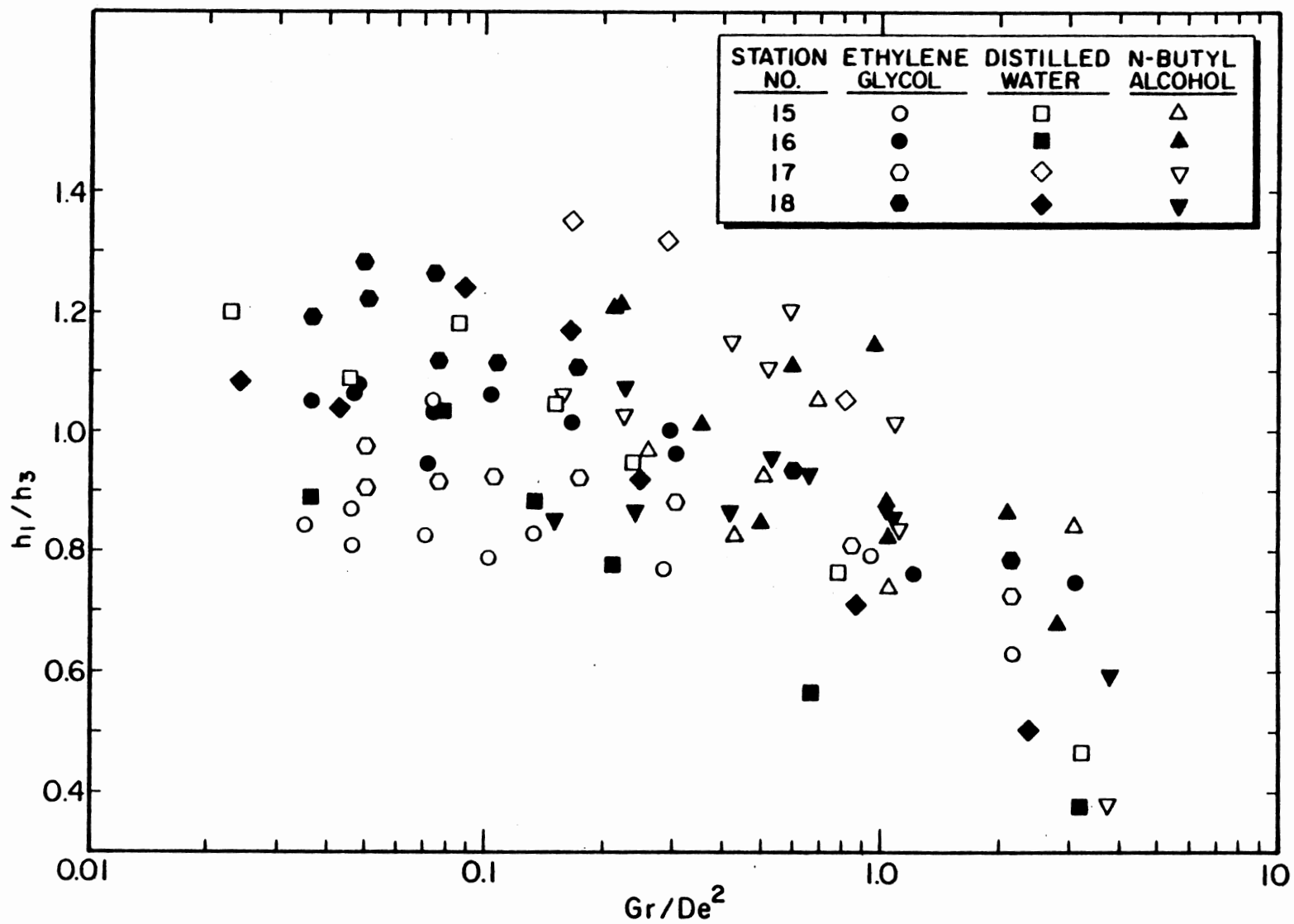


Figure 20. Local Heat Transfer Coefficient\_Ratio Versus  $Gr/(De^2)$

2. The factor should be made up of some combination of the dimensionless groups (Grashof and Reynolds) that reflect the magnitude of the natural convection effect.

The factor was found to be:

$$1 + 0.9348 \left( \frac{Gr}{De^2} \right)^{2.78} e^{-1.33Gr/(De^2)} \quad (6.13)$$

The Sieder-Tate (36) viscosity correction factor was also incorporated into the proposed correlation as a measure of the interaction of the viscosity gradient of the temperature field on the velocity distribution.

Hence, the final correlation to predict the peripherally-averaged Nusselt number for the fully developed fluid flow in a helically coiled tube in the laminar flow regime may be written as:

$$Nu = \left\{ 4.36 + 2.84 \left( \frac{Gr}{Re^2} \right)^{3.94} \right\} \left\{ 1 + 0.0276 De^{0.75} Pr^{0.197} \right\} \left\{ 1 + 0.9348 \left( \frac{Gr}{De^2} \right)^{2.78} e^{-1.33Gr/(De^2)} \right\} \left( \frac{\mu_b}{\mu_w} \right)^{0.14} \quad (6.14)$$

The physical properties of the fluid used in Equation (6.14) were evaluated at the bulk temperature except  $\mu_w$  which was evaluated at the average inside wall temperature at the thermocouple station. Equation (6.14) is valid for:

$$92 < Re < 5500$$

$$2.2 < Pr < 101$$

$$760 < Gr < 10^6 .$$



Test results of the fit of Equation (6.14) to the experimental data are given in Tables III and IV. Figure 21 is a plot of error ratio versus Dean number for thermocouple station 15.

The limiting cases of Equation (6.14) are as follows:

1. For the limiting case of  $d_i/D_c$  tending to zero, Dean number tends to zero, and Equation (6.14) reduces to:

$$Nu = \left\{ 4.36 + 2.84 \left( \frac{Gr}{Re^2} \right)^{3.95} \right\} \left( \frac{\mu_b}{\mu_w} \right)^{0.14} \quad (6.15)$$

2. For Grashof number tends to zero, Equation (6.14) reduces to:

$$Nu = 4.36 (1 + 0.0276 De^{0.75} Pr^{0.197}) \left( \frac{\mu_b}{\mu_w} \right)^{0.14} \quad (6.16)$$

From Tables III and IV, it may be noted that the correlation developed best fits the present experimental data. Also when the correlation is extended to the straight tube case, it results in Equation (6.15), which predicts Nusselt numbers for the straight tube in the fully developed region.

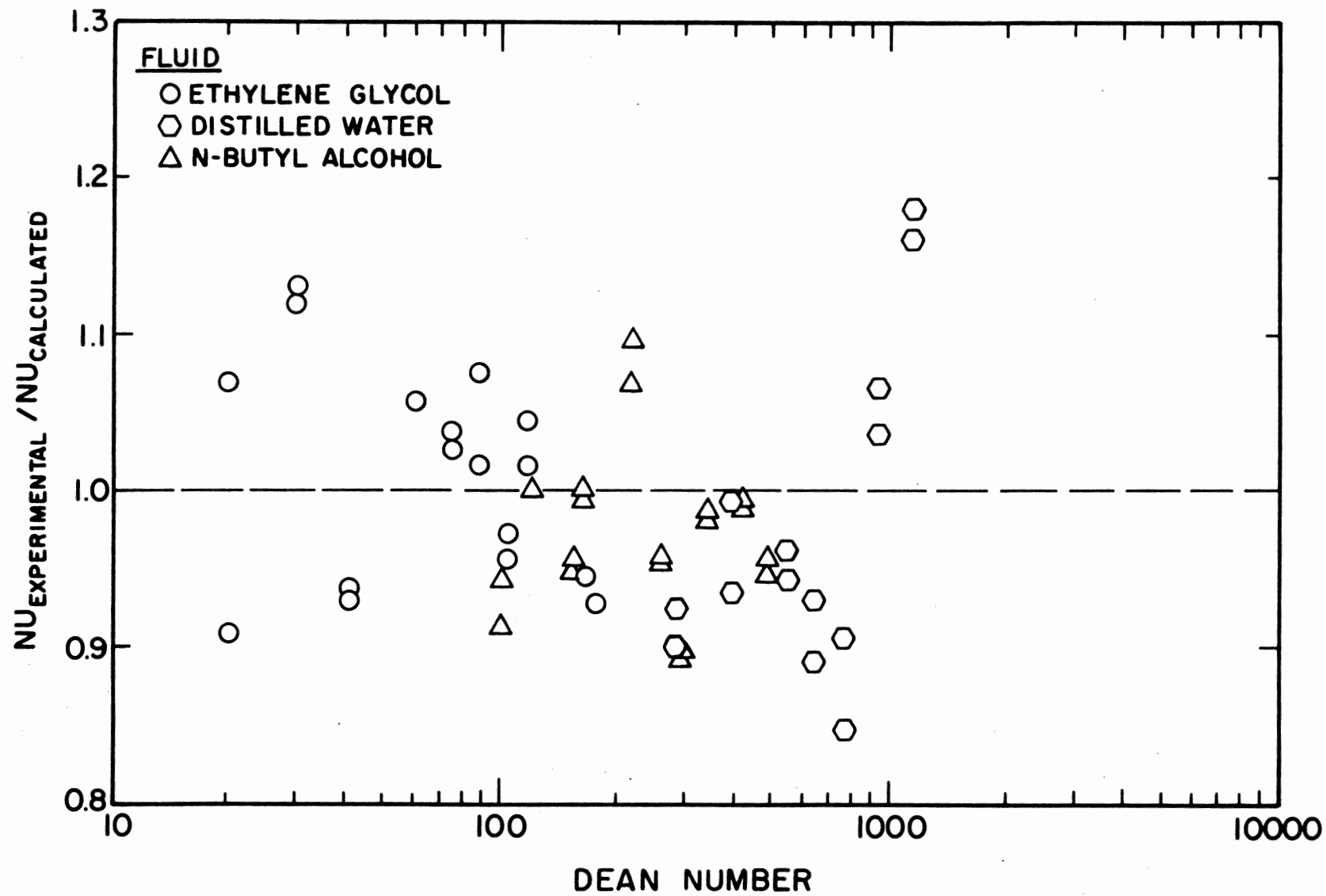


Figure 21. Error Ratio Versus Dean Number for Thermocouple Station 15

## CHAPTER VII

### CONCLUSIONS AND RECOMMENDATIONS

Experimental measurements of the heat transfer coefficient for laminar flow inside a helical coil were made. Three fluids, ethylene glycol, distilled water and normal butyl alcohol, were studied using a helical coil with a  $D_c/d_i$  ratio of 20.2.

The following conclusions were arrived at as a result of the total study:

1. Higher heat transfer coefficients were obtained for fluid flow in a helically coiled tube than that in an equivalent straight tube under similar fluid flow conditions. The reason for this is the existence of a so-called secondary flow resulting from the tube curvature.

2. At low Reynolds numbers or high Grashof numbers, the natural convection effect became an important factor in the heat transfer process. The relative intensity of natural convection was diminished as the Reynolds number increased. It was determined that the higher heat transfer coefficients obtained for flow in a helical coil were due not only to the presence of the superimposed secondary flow due to centrifugal action, but also due to the existence of natural convection. A measure of the extent to which the natural convection effects contributed to the increase of the average heat transfer coefficient has been incorporated into the empirical correlation developed to predict the average Nusselt number (Equation (6.14)).

3. The axial temperatures show large oscillations with axial distance, which damp out in the fully-developed region. Consequently, the oscillatory behavior was also present in the Nusselt number. The Nusselt number approaches an asymptotic value as the fully developed temperature field is approached.

4. A correlation for the peripherally-averaged Nusselt number, for the fully-developed region was developed. The correlation developed allows for the contribution of the natural convection effect to the heat transfer process. The correlation is a function of Dean, Grashof, Prandtl and Reynolds numbers, Equation (6.14). The correlation fits the experimental results better than any of the literature correlations tested.

5. The developed correlation is of a form that, when the coil diameter tends to infinity, results in a valid equation (Equation (6.15)) for predicting Nusselt numbers for the straight tube in the fully developed region.

Several gaps still exist in the complete understanding of the mechanism of heat transfer in a helical coil. The following recommendations are made, based on the results of this study, for future research in the area:

1. Equation (6.14) was developed for the case when a fluid is heated in a helical coil. It is felt that the same correlation should apply when a fluid is cooled in a helically-coiled tube. However, it is recommended that an experimental study be performed when a fluid is cooled in a helical coil to establish the validity of this premise.

2. Further research needs to be performed using helical coils with widely varying curvature ratios.

3. Experimental studies should also be performed with the axis in the horizontal direction.

# BIBLIOGRAPHY

1. Adler, M., "Stromung in Gekrummten Rohren", Z. Angew. Math. Mech., 14, 257 (1934).
2. Akiyama, M., and K. C. Cheng, "Boundary Vorticity Method for Laminar Forced Convection Heat Transfer in Curved Pipes", Int. J. Heat Mass Transfer, 14, 1659 (1971).
3. Akiyama, M. and K. C. Cheng, "Graetz Problem in Curved Pipes with Uniform Wall Heat Flux", Appl. Sci. Res., 29, 401 (1974).
4. ASME Steam Tables, The American Society of Mechanical Engineers, New York, N.Y. (1967).
5. Berg, R. R., and C. F. Bonilla, "Heating of Fluids in Coils", Trans. N.Y. Acad. Sci., 13, 12 (1950).
6. Crain, Berry, Jr., "Forced Convection Heat Transfer to a Two-Phase Mixture of Water and Steam in a Helical Coil", Ph.D. Thesis, Oklahoma State University, Stillwater, Oklahoma (1973).
7. Curme, G. O., Jr., and F. Johnston, eds. Glycols. New York: Reinhold Publishing Corporation (1952).
8. Dean, W. R., "Note on the Motion of Fluid in a Curved Pipe", Phil. Mag., 4, 208-223 (1927).
9. Dean, W. R., "The Streamline Motion of Fluid in a Curved Pipe", Phil. Mag., 5, 673-695 (1928).
10. Digital Thermocouple Indicators Owner's Manual, Manual 350-4440-03, Doric Scientific, San Diego, Ca.
11. Directions for 8687 Volt Potentiometer, Manual No. 177126, Issue 5, Leeds & Northrup Co., Pa.
12. Dravid, A. N., "Effect of Secondary Fluid Motion on Laminar Flow Heat Transfer in Helically Coiled Tubes", Sc. D. Thesis, Massachusetts Institute of Technology, Cambridge, Mass. (1969).
13. Dravid, A. N., K. A. Smith, E. W. Merrill, and P.L.T. Brain, "Effect of Secondary Fluid Motion on Laminar Flow Heat Transfer in Helically Coiled Tubes", AIChE J., 17, No. 5 1114 (1971).

14. Farukhi, M. N., "An Experimental Investigation of Forced Convective Boiling at High Qualities Inside Tubes Preceded by 180 Degree Bends", Ph.D. Thesis, Oklahoma State University, Stillwater, Oklahoma (1974).
15. Hausen, H., "Darstellung des Wärmeüberganges in Rohren durch verallgemeinerte Potenzbeziehungen", Z. Ver. Dt. Ing., Beihefte Verfahrenstechnik, No. 4, 91 (1943).
16. Ito, H., "Theoretical and Experimental Investigation Concerning the Flow Through Curved Pipes", Mem. Inst. High Speed Mechanics, Tohoku Univ., Japan, 14, 137 (1959).
17. Janssen, L.A.M., and C.J. Hoogendoorn, "Laminar Convective Heat Transfer in Helical Coiled Tubes", Int. J. Heat Mass Transfer, 21, 1197 (1978).
18. Kalb, C. E., and J. D. Seader, "Heat and Mass Transfer Phenomena for Viscous Flow in Curved Circular Tubes", Int. J. Heat Mass Transfer, 15, 801 (1972) [Also see errata in Int. J. Heat Mass Transfer, 15, 2680 (1972)].
19. Kalb, C. E., and J. D. Seader, "Fully Developed Viscous-Flow Heat Transfer in Curved Circular Tubes with Uniform Wall Temperature", AIChE Journal, 20, 340 (1974).
20. Koutsky, J. A., and R. J. Adler, "Minimization of Axial Dispersion by Use of Secondary Flow in Helical Tubes", Can. J. Chem. Eng., 42, 239 (1964).
21. Kubair, V., and N. R. Kuloor, "Heat Transfer to Newtonian Fluids in Coiled Pipes in Laminar Flow", Int. J. Heat Mass Transfer, 9, 63 (1966).
22. Morcos, S. M., and A. E. Bergles, "Combined Forced and Free Laminar Convection in Horizontal Tubes", Technical Report HTL-1, ISU-ERI, Ames 74008, Iowa State University (1974).
23. Morcos, S. M., and A. E. Bergles, "Experimental Investigation of Combined Forced and Free Laminar Convection in Horizontal Tubes", Transactions of ASME, Journal of Heat Transfer, 97, 212 (1975).
24. Mori, Y., and W. Nakayama, "Study on Forced Convective Heat Transfer in Curved Pipes--First Report", Int. J. Heat Mass Transfer, 8, 67 (1965).
25. Mori, Y., and W. Nakayama, "Study on Forced Convective Heat Transfer in Curved Pipes--Third Report", Int. J. Heat Transfer, 10, 681 (1967).

26. Oliver, D. R., and S. M. Asghar, "Heat Transfer to Newtonian and Viscoelastic Liquids During Laminar Flow in Helical Coils", Trans. Inst. Chem. Eng., 54, 218 (1976).
27. Owahdi, A., K. J. Bell and B. Crain, Jr., "Forced Convection Boiling Inside Helically Coiled Tubes", Intl. J. of Heat and Mass Transfer, 11, 1779 (1968).
28. Özisik, M. N., and H. C. Topakoglu, "Heat Transfer for Laminar Flow in a Curved Pipe", Trans. ASME, J. Heat Transfer, 90, 313 (1968).
29. Patankar, S. V., V. S. Pratap and D. B. Spalding, "Prediction of Laminar Flow and Heat Transfer in Helically Coiled Pipes", J. Fluid Mech., 62, 539 (1974).
30. Perry, J. H., ed., Chemical Engineering Handbook, 4th edition, McGraw-Hill Book Company, New York (1973).
31. Precision Scientific Company Catalog 65, October (1967).
32. Ross Type BCF Exchangers Bulletin 1.1K6, Copyrighted 1957 by American Radiator and Standard Sanitary Corp.
33. Schmidt, E. F., "Wärmeübergang und Druckverlust in Rohrschlangen", Chemie Ingenieur Technik, 13, 781 (1967).
34. Seban, R. A., and E. F. McLaughlin, "Heat Transfer in Tube Coils with Laminar and Turbulent Flow", Int. J. Heat Mass Transfer, 6, 387 (1963).
35. Shchukin, V. K., "Correlation of Experimental Data on Heat Transfer in Curved Pipes", Teploenergetika, 16, No. 2, 50 (1969).
36. Sieder, E. N., and G. E. Tate, "Heat Transfer and Pressure Drop of Liquids in Tubes", Ind. Eng. Chem., 28, 1429 (1936).
37. Singh, S. P., "Liquid Phase Heat Transfer in Helically Coiled Tubes", Ph.D. Thesis, Oklahoma State University, Stillwater, Oklahoma (1973).
38. Srinivasan, P. S., S. S. Nandapurkar, and F. A. Holland, "Pressure Drop and Heat Transfer in Coils", Trans. Inst. Chem. Engrs., 218, CE113 (1968).
39. Tarbell, J. M., and M. R. Samuels, "Momentum and Heat Transfer in Helical Coils", The Chemical Engineering J., 5, 117 (1973).
40. Union Carbide Corporation, Glycol, New York: Author (1971).
41. Weast, R. C., ed., CRC Handbook of Chemistry and Physics, 52nd edition, The Chemical Rubber Company, Cleveland, Ohio (1972).



42. Weissman, M. H., and L. F. Mockros, "Gas Transfer to Blood Flowing in Coiled Circular Tubes", J. Engrg. Mech. Div., Proc. ASCE, 94, No. EM3, 857 (1968).
43. White, C. M., "Streamline Flow Through Curved Pipes", Proc. Roy. Soc. London, A, 123, 645 (1929).

**APPENDIX A**

**EQUIPMENT DATA**

TABLE V  
MEASURED OUTSIDE TUBE DIAMETER AFTER  
FORMATION OF HELICAL COIL

Station Number	Axial Distance from Inlet Electrode, cm	Coiled Tube Outside Diameter, cm	
		Longitudinal	Lateral
1	5.08	1.6129	1.5824
2	12.70	1.6180	1.5748
3	20.32	1.6180	1.5748
4	35.56	1.6129	1.5748
5	50.80	1.6104	1.5723
6	66.04	1.6129	1.5697
7	81.28	1.6154	1.5697
8	101.60	1.6129	1.5697
9	127.00	1.6104	1.5723
10	152.40	1.6104	1.5697
11	181.61	1.6129	1.5646
12	261.62	1.6104	1.5723
13	340.36	1.6104	1.5723
14	421.64	1.6129	1.5723
15	502.92	1.6104	1.5748
16	584.20	1.6129	1.5697
17	660.40	1.6129	1.5723
18	741.68	1.6129	1.5748
Average Values		1.6128	1.5724

TABLE VI  
ROTAMETER SPECIFICATIONS

---

Rotameter model number	1110-08H2B1A
Rotamete tube number	R-8M-25-4
Float number	8-RV-14
Maximum water flow rate, gpm	1.45

---

## APPENDIX B

### CALIBRATION DATA

TABLE VII  
CALIBRATION DATA FOR THE ROTAMETER FOR DISTILLED WATER

Rotameter Setting % Maximum Flow	Mass Flow Rate, gm/sec
10.0	9.8
20.0	17.7
30.0	26.5
40.0	33.8
50.0	42.0
60.0	48.0
70.0	57.5
80.0	65.5
90.0	73.2
100.0	81.4

Bath fluid temperature =  $32.4^{\circ}\text{C}$ .

For ethylene glycol and n-butyl alcohol, the flow rate was measured for each individual data run; the rotameter was used merely as an indication of flow rate.

TABLE VIII  
CALIBRATION DATA FOR INLET AND OUTLET THERMOCOUPLES  
DURING IN-SITU CALIBRATION OF SURFACE THERMO-  
COUPLES ON THE HELICAL COIL

Thermocouple Location	Saturated Steam Temperature, °F	Thermocouple Correction, °F	Average Room Temperature, °F
Inlet	211.80	0.10	81.2
Outlet	211.02	1.12	

Note:

1. The inlet thermocouple was located 1499 mm upstream from the inlet electrode and the outlet thermocouple was located 902 mm downstream from the exit electrode.
2. The saturated steam temperature was determined from Steam Tables (4) at the absolute pressure of steam at the indicated location. The absolute pressure was determined by reading the atmospheric pressure.
3. The correction correlation for inlet and outlet bulk fluid temperatures are:

$$\left[ (t_b)_{in} \right]_{corrected} = (t_b)_{in} + 0.10 \frac{[(t_b)_{in} - t_{room}]}{(211.8 - 81.2)}$$

and

$$\left[ (t_b)_{out} \right]_{corrected} = (t_b)_{out} + 1.12 \frac{[(t_b)_{out} - t_{room}]}{(211.02 - 81.2)}$$

4. The temperature corrections were computed after 27 hours of continuous operation.

TABLE IX  
CALIBRATION DATA FOR SURFACE THERMOCOUPLES

Thermocouple Station Number	$\Delta$ = Temperature Correction, °F Peripheral Location			
	1	2	3	4
1	1.58	0.68	1.08	0.78
2	0.57	0.47	0.57	0.97
3	0.97	0.67	0.97	0.17
4	0.46	0.26	0.66	0.96
5	0.94	0.54	1.04	0.84
6	1.23	0.83	0.73	0.73
7	1.02	0.52	1.32	0.62
8	0.70	0.60	0.60	0.80
9	0.98	0.78	0.78	0.68
10	1.56	0.56	0.76	0.96
11	1.74	0.74	0.84	0.74
12	1.28	0.88	1.18	1.58
13	1.22	1.12	1.12	0.92
14	1.15	0.75	0.95	0.65
15	1.79	1.89	2.09	1.19
16	1.23	1.13	1.23	1.63
17	1.17	1.57	1.67	1.47
18	2.00	1.10	2.00	2.10

Note:

1. For correction of the surface thermocouples the effect of pressure drop along the coil is included.
2. The temperature corrections indicated above were the corrections required to be added to the temperature indicated by the thermocouples when low pressure saturated steam was bled through the coil.
3. The correction for surface temperatures is:

$$(t)_{\text{corrected}} = t_{\text{read}} + \Delta \frac{(t_{\text{read}} - t_{\text{room}})}{(t_{\text{s-s.}} - 81.2)}$$

where  $t_{\text{s-s.}}$  is the temperature of the saturated steam.

4. The temperature corrections are computed after 27 hours of continuous operation.



TABLE X  
CALIBRATION DATA FOR HEAT LOSS FROM TEST SECTION

---

Average temperature of steam in test section	= 211.4°F
Room temperature during calibration	= 81.2°F
Amount of mass of steam condensed	= 0.60 lb/hr
Heat of vaporization of water at 211.4°F ( $\lambda$ )	= 970.67 Btu/lb

---

$$\left\{ \begin{array}{l} \text{Heat loss from} \\ \text{heat transfer loop} \end{array} \right\} = q = m \lambda$$

$$= 0.6 \times 970.67$$

$$= 582.4 \text{ Btu/hr}$$

So, heat loss during experimental run,  $q_{\text{loss}}$ ; Btu/hr

$$q_{\text{loss}} = \frac{582.4 (t_{\text{avg}} - t_{\text{room}})}{(211.4 - 81.2)}$$

or, heat loss from the test section,  $Q_{\text{loss}}$ ; Btu/hr

$$Q_{\text{loss}} = \left( \frac{\ell}{L_{\text{total}}} \right) q_{\text{loss}}$$

where

$\ell$  = length of test section (heated section)

and

$L$  = total length of heat transfer loop

$$t_{\text{avg}} = (1/2) \left[ (t_b)_{\text{in}} + (t_b)_{\text{out}} \right], \text{ } ^\circ\text{F}$$

## APPENDIX C

### EXPERIMENTAL DATA

<u>Run Number</u>	<u>Test Fluid</u>
101-126	Ethylene Glycol
201-214	Distilled Water
301-320	Normal Butyl Alcohol

Only those experimental data which were referred to are presented here. The rest of the experimental data are available at:

School of Chemical Engineering  
Oklahoma State University  
Stillwater, Oklahoma 74074 U.S.A.  
Attn: Dr. Kenneth J. Bell

FLUID : ETHYLENE GLYCOL

RUN NUMBER	102	104	108	110	112	120
THERMOCOUPLE #	TEMP., F	TEMP., F	TEMP., F	TEMP., F	TEMP., F	TEMP., F
1-1	94.3	94.2	95.0	96.9	100.9	97.3
1-2	96.2	96.0	96.4	98.1	101.3	101.2
1-3	93.1	93.4	94.0	96.0	99.8	95.6
1-4	91.9	92.2	92.7	94.7	99.6	93.7
2-1	94.7	95.1	95.9	98.4	106.8	98.4
2-2	97.3	97.4	98.5	100.9	106.7	103.1
2-3	94.0	94.0	95.1	97.3	103.8	97.3
2-4	93.0	93.0	93.9	95.9	103.7	95.5
3-1	93.8	94.2	95.3	97.7	108.4	97.0
3-2	97.3	97.6	98.7	101.3	107.9	102.8
3-3	94.1	94.6	95.5	97.9	105.1	97.4
3-4	92.5	93.1	93.7	95.7	105.1	94.6
4-1	94.5	95.0	96.5	99.5	112.3	97.9
4-2	97.6	97.9	99.2	102.2	110.6	103.3
4-3	94.7	94.9	96.4	99.2	107.0	98.0
4-4	93.1	93.3	94.7	97.3	108.6	95.4
5-1	96.5	97.1	98.5	101.6	114.6	99.5
5-2	99.1	99.6	101.2	104.4	112.3	104.0
5-3	96.2	96.5	97.9	100.9	108.1	98.9
5-4	95.1	95.3	96.4	99.2	110.0	97.0
6-1	96.6	96.8	98.4	102.1	116.3	100.6
6-2	99.7	99.8	101.3	105.2	113.8	105.9
6-3	96.8	96.9	98.3	101.9	109.6	101.3
6-4	95.6	95.7	96.9	100.1	111.7	99.2
7-1	98.0	98.4	100.7	104.6	118.6	102.7
7-2	100.4	100.7	103.0	106.9	115.7	107.1
7-3	97.0	97.3	99.7	103.0	111.5	101.2
7-4	96.2	96.7	98.8	102.1	115.1	99.9
8-1	98.5	98.7	101.1	105.2	121.1	102.9
8-2	101.5	101.6	103.9	107.8	118.2	107.9
8-3	98.0	98.2	100.2	103.8	113.7	102.4
8-4	97.1	97.2	99.0	102.5	115.7	101.0
9-1	98.0	99.6	102.1	106.3	124.2	104.2
9-2	101.6	102.2	104.8	108.9	120.0	108.4
9-3	98.2	99.0	101.3	105.2	117.5	102.1
9-4	97.6	98.4	100.4	104.2	120.7	102.0
10-1	99.4	100.0	102.7	107.4	127.2	104.0
10-2	102.6	103.1	105.8	110.7	125.1	110.0
10-3	99.6	100.1	102.7	107.2	120.8	105.4
10-4	98.5	99.1	101.3	105.5	123.1	103.0

FLUID : ETHYLENE GLYCOL

THERMOCOUPLE #	TEMP., F	TEMP., F	TEMP., F	TEMP., F	TEMP., F	TEMP., F
11-1	100.0	100.4	103.2	108.3	129.8	104.0
11-2	102.2	102.4	105.2	110.2	128.0	108.4
11-3	100.1	100.4	102.6	107.4	124.8	105.1
11-4	98.5	98.7	100.9	105.6	126.7	101.0
12-1	100.5	101.5	105.5	111.7	141.4	106.5
12-2	103.4	104.1	108.0	114.5	140.6	111.0
12-3	101.5	102.0	105.7	111.8	134.9	106.5
12-4	99.8	100.5	104.1	109.8	136.5	104.5
13-1	103.1	104.0	108.6	115.5	151.9	109.6
13-2	106.1	106.8	111.3	118.4	149.7	114.5
13-3	103.7	104.5	108.5	115.4	145.5	110.3
13-4	102.3	103.0	107.2	113.6	147.7	108.3
14-1	105.4	106.2	111.1	119.1	162.5	112.0
14-2	107.7	108.5	113.4	121.6	161.8	116.0
14-3	105.2	106.1	110.6	118.4	156.2	111.7
14-4	104.3	105.2	109.7	117.0	158.2	110.2
15-1	107.1	108.1	113.4	122.1	172.3	114.2
15-2	109.2	110.2	115.4	124.2	170.2	118.4
15-3	106.0	107.0	112.0	120.6	165.7	113.2
15-4	105.4	106.6	111.5	119.6	168.1	112.3
16-1	107.5	108.7	114.4	123.5	182.3	115.2
16-2	110.8	111.9	117.7	127.2	181.0	120.8
16-3	107.8	108.9	114.5	123.7	176.7	115.8
16-4	107.2	108.2	113.7	122.3	178.6	114.7
17-1	109.6	111.0	117.4	125.3	192.8	118.4
17-2	111.8	113.1	119.4	127.7	190.4	122.1
17-3	109.2	110.5	116.6	124.5	186.4	117.4
17-4	108.3	109.5	115.6	122.6	188.1	116.2
18-1	109.8	111.2	118.5	123.5	201.5	117.6
18-2	113.2	114.4	121.3	126.9	199.1	123.8
18-3	110.7	111.9	118.4	123.4	195.5	119.7
18-4	109.1	110.4	117.1	121.4	196.7	116.7
INLET FLUID TEMPERATURE, F	88.5	88.7	88.4	88.6	87.2	88.9
EXIT FLUID TEMPERATURE, F	98.4	99.0	105.0	114.3	182.9	100.7
BATH FLUID TEMPERATURE, F	90.0	90.0	90.0	90.0	90.0	90.0
AMMETER READING, I., AMPS	90.00	90.00	88.00	89.00	86.00	123.00
VOLTMETER READING, V., VOLTS	7.30	7.30	7.20	7.25	7.20	10.30
FLUID FLOW RATE, LB/HR	420.40	350.70	226.10	135.00	31.80	638.40
INLET FLUID PRESSURE, PSIG	11.16	9.00	7.40	3.20	0.95	18.70
EXIT FLUID PRESSURE, PSIG	7.44	5.70	4.90	1.60	0.20	12.00
ROOM TEMPERATURE, F	90.2	84.0	82.2	84.4	83.7	84.0
RUN NUMBER	102	104	108	110	112	120

FLUID : DISTILLED WATER

RUN NUMBER	202	204	206	208	210	214
THERMOCOUPLE #	TEMP., F	TEMP., F	TEMP., F	TEMP., F	TEMP., F	TEMP., F
1-1	95.8	93.2	98.2	93.0	92.7	92.3
1-2	99.1	96.2	100.1	96.1	95.2	94.2
1-3	94.0	92.6	95.1	92.1	92.1	91.8
1-4	92.6	91.5	93.5	91.0	91.4	91.4
2-1	97.4	94.2	100.3	94.4	93.1	92.5
2-2	100.7	97.5	101.8	97.9	96.3	94.9
2-3	95.5	93.3	97.0	93.2	92.6	92.2
2-4	94.0	92.3	95.8	92.0	91.9	91.6
3-1	96.0	93.4	99.5	93.2	92.8	92.1
3-2	100.6	97.9	102.0	97.9	96.8	95.2
3-3	95.6	93.6	97.1	93.3	92.7	91.9
3-4	93.6	91.7	95.4	91.4	91.4	91.2
4-1	97.5	94.2	102.6	94.1	93.3	92.5
4-2	102.0	98.7	104.2	98.7	97.7	96.5
4-3	96.6	94.1	98.6	94.0	93.4	92.8
4-4	94.4	92.6	97.4	92.2	92.0	91.8
5-1	98.9	94.7	105.2	94.6	93.8	93.0
5-2	103.0	99.1	106.5	99.1	98.1	97.0
5-3	97.8	94.2	101.3	94.1	93.5	92.8
5-4	96.2	92.6	100.0	92.4	92.1	91.7
6-1	101.1	95.4	106.6	95.8	94.2	93.1
6-2	105.3	99.7	108.3	100.2	98.5	97.2
6-3	100.2	95.0	102.4	95.7	93.8	93.0
6-4	99.2	93.9	100.5	94.7	92.6	92.0
7-1	103.7	97.8	109.5	98.7	95.8	94.1
7-2	106.5	101.2	109.5	102.1	99.6	98.0
7-3	101.1	96.5	103.9	97.2	94.9	93.7
7-4	100.3	96.1	104.1	96.9	94.0	92.8
8-1	103.9	97.9	111.2	98.6	96.6	94.6
8-2	107.8	102.0	111.7	102.5	100.5	98.5
8-3	102.3	96.7	105.9	97.5	95.6	93.6
8-4	101.1	96.5	105.5	96.9	95.2	92.8
9-1	105.8	98.4	114.4	99.7	97.0	94.7
9-2	108.4	102.1	113.6	103.0	100.6	98.5
9-3	103.9	97.5	109.5	98.6	96.1	93.9
9-4	102.8	97.3	109.2	98.3	95.8	93.3
10-1	106.5	99.4	116.3	100.1	97.7	95.1
10-2	111.1	103.9	117.9	104.7	101.9	99.4
10-3	105.1	98.9	111.5	99.7	97.1	94.8
10-4	104.6	98.7	111.3	99.2	96.9	94.0

FLUID : DISTILLED WATER

THERMOCOUPLE #	TEMP., F	TEMP., F	TEMP., F	TEMP., F	TEMP., F	TEMP., F
11-1	106.7	99.8	117.6	101.3	97.8	94.8
11-2	117.2	102.6	119.3	103.9	100.6	97.5
11-3	107.4	100.3	116.4	101.2	98.5	95.4
11-4	105.2	98.7	115.1	100.0	96.8	93.6
12-1	113.7	103.2	129.1	105.4	99.9	97.0
12-2	118.5	106.7	131.0	108.8	103.5	100.4
12-3	113.6	102.7	124.4	104.5	100.0	97.1
12-4	111.6	101.7	123.9	103.6	98.5	95.8
13-1	119.9	106.5	138.5	108.4	103.1	98.8
13-2	123.9	110.5	138.8	112.3	107.1	102.7
13-3	119.2	106.2	133.5	108.0	103.2	98.9
13-4	117.3	105.7	133.4	107.3	102.4	97.6
14-1	126.6	109.5	148.5	112.3	105.8	100.4
14-2	130.1	113.0	149.7	115.7	109.1	103.6
14-3	123.9	109.0	142.6	111.1	105.5	100.3
14-4	122.3	107.9	141.4	109.9	104.6	98.9
15-1	131.4	112.0	156.9	115.2	107.5	101.4
15-2	135.4	116.4	157.8	119.7	112.2	105.7
15-3	130.1	112.1	152.7	115.0	108.1	101.7
15-4	128.5	110.9	151.4	113.6	106.9	100.0
16-1	136.6	114.4	166.2	118.5	109.8	102.7
16-2	138.7	116.9	165.2	120.4	112.1	105.0
16-3	134.1	113.9	161.6	117.8	109.6	102.5
16-4	134.6	114.3	162.1	117.8	109.7	102.0
17-1	141.8	117.3	183.6	121.2	111.7	103.9
17-2	146.2	121.7	177.5	125.9	116.0	108.0
17-3	141.6	118.3	171.1	122.3	112.8	105.0
17-4	139.6	117.0	172.2	120.7	111.6	103.2
18-1	147.6	120.0	204.3	124.9	113.7	105.5
18-2	152.5	124.5	196.6	129.5	118.1	109.3
18-3	146.3	120.4	180.2	124.8	114.5	105.6
18-4	145.5	119.5	194.4	124.0	113.6	104.8
INLET FLUID TEMPERATURE, F	88.5	88.5	88.2	88.1	88.5	89.1
EXIT FLUID TEMPERATURE, F	142.1	115.9	176.1	120.5	110.1	102.9
BATH FLUID TEMPERATURE, F	90.0	90.0	90.0	90.0	90.0	90.0
AMMETER READING, I, AMPS	118.00	116.00	118.00	115.00	116.00	118.00
VOLTMETER READING, V, VOLTS	10.00	9.80	10.00	9.70	9.70	9.80
FLUID FLOW RATE, LB/HR	74.55	143.85	43.94	120.39	179.69	285.22
INLET FLUID PRESSURE, PSIG	1.30	2.25	4.50	3.00	2.25	2.30
EXIT FLUID PRESSURE, PSIG	1.20	2.05	4.42	2.80	2.00	1.80
ROOM TEMPERATURE, F	82.2	82.4	84.6	79.5	81.1	79.0
RUN NUMBER	202	204	206	208	210	214

FLUID : NORMAL BUTYL ALCOHOL

RUN NUMBER	302	304	308	312	314	320
THERMOCOUPLE #	TEMP., F	TEMP., F	TEMP., F	TEMP., F	TEMP., F	TEMP., F
1-1	99.6	101.2	105.8	100.3	96.3	94.2
1-2	103.7	105.7	110.1	102.0	98.5	95.5
1-3	97.6	99.2	102.8	98.6	95.1	93.3
1-4	95.8	96.9	100.0	97.0	93.6	92.3
2-1	102.2	104.0	109.3	102.8	98.1	95.4
2-2	106.7	108.8	113.8	104.4	100.6	96.9
2-3	100.3	102.0	106.7	100.7	97.0	94.6
2-4	97.9	99.3	104.0	99.7	95.7	93.8
3-1	100.2	102.0	107.4	102.4	97.2	94.8
3-2	107.0	108.9	113.9	104.8	100.7	97.1
3-3	100.7	102.5	107.0	101.3	97.3	94.9
3-4	97.2	98.7	103.2	99.7	95.3	93.7
4-1	101.8	103.7	109.6	104.8	98.3	95.4
4-2	107.6	110.0	115.2	106.3	101.3	97.3
4-3	101.6	103.4	108.1	102.5	97.8	95.1
4-4	98.3	99.7	104.5	101.2	95.8	93.9
5-1	102.0	104.0	113.0	107.5	99.9	97.4
5-2	107.9	110.2	117.7	108.7	102.5	98.9
5-3	101.3	103.2	110.9	104.9	99.1	96.8
5-4	98.1	99.8	108.3	103.8	97.7	96.0
6-1	103.0	106.2	116.1	108.9	101.5	97.9
6-2	108.8	112.8	121.6	110.2	104.5	99.8
6-3	102.7	106.8	114.8	106.3	101.1	97.6
6-4	99.8	103.4	112.0	105.2	99.7	96.7
7-1	108.0	111.2	118.8	111.2	102.7	99.1
7-2	112.2	115.9	122.3	111.5	105.0	100.4
7-3	105.5	108.7	114.6	107.4	101.3	98.1
7-4	104.5	107.4	113.0	107.2	100.3	97.5
8-1	107.6	110.7	118.7	111.6	103.2	99.9
8-2	113.0	115.9	124.5	112.5	105.9	101.4
8-3	105.9	108.3	117.1	108.1	102.3	99.1
8-4	104.6	106.8	113.5	107.2	101.2	98.3
9-1	106.9	111.3	117.9	110.9	104.9	100.4
9-2	113.2	116.9	121.5	111.6	106.9	102.0
9-3	107.1	110.1	115.4	107.8	103.2	99.9
9-4	104.8	108.7	114.4	107.6	102.7	99.2
10-1	107.5	112.8	118.3	110.7	103.9	101.8
10-2	114.9	118.8	124.2	113.0	108.2	103.5
10-3	108.3	111.7	117.2	108.8	104.8	100.9
10-4	105.5	109.6	113.4	108.1	102.7	100.4



FLUID : NORMAL BUTYL ALCOHOL

THERMOCOUPLE #	TEMP., F	TEMP., F	TEMP., F	TEMP., F	TEMP., F	TEMP., F
11-1	106.4	111.2	119.7	112.0	103.4	100.9
11-2	111.0	114.7	122.9	113.6	105.9	102.5
11-3	107.9	110.3	119.0	112.0	104.5	101.6
11-4	105.1	107.8	116.6	110.5	102.7	100.3
12-1	110.9	115.8	127.8	119.1	107.1	102.4
12-2	115.7	120.6	132.6	120.9	110.1	104.4
12-3	110.2	114.2	126.2	116.8	107.4	102.7
12-4	107.6	112.0	124.0	115.7	105.7	101.4
13-1	115.6	120.1	131.5	123.8	110.0	105.4
13-2	120.8	125.2	136.1	125.0	113.2	107.2
13-3	115.1	118.5	129.3	122.1	110.6	105.4
13-4	113.3	116.7	126.8	121.8	108.5	104.6
14-1	117.0	121.5	138.1	129.2	111.7	107.4
14-2	122.3	127.0	142.4	131.0	114.3	109.0
14-3	118.2	120.9	134.8	127.1	111.1	107.2
14-4	115.1	117.6	132.5	126.1	108.7	105.8
15-1	117.4	122.9	141.1	132.8	113.9	108.9
15-2	125.0	130.8	146.5	134.7	116.7	110.8
15-3	120.1	125.7	140.1	131.8	113.5	108.9
15-4	115.8	120.7	136.5	130.6	111.8	107.8
16-1	115.6	123.7	146.0	136.8	116.5	109.4
16-2	125.7	131.5	149.9	137.6	117.7	111.3
16-3	118.5	125.0	144.4	134.9	115.8	109.5
16-4	114.1	122.0	143.0	134.2	114.9	108.4
17-1	124.1	126.1	151.1	146.3	118.2	110.9
17-2	129.7	134.1	156.4	145.0	121.2	112.9
17-3	124.2	129.5	150.9	140.4	118.6	111.2
17-4	121.5	124.1	147.8	140.2	116.6	109.7
18-1	125.9	131.7	155.8	155.8	120.8	113.7
18-2	131.8	137.8	161.7	153.7	123.9	115.7
18-3	124.5	130.5	154.4	144.1	120.6	113.5
18-4	123.3	129.1	152.7	150.2	119.5	112.8
INLET FLUID TEMPERATURE, F	88.8	88.8	88.6	88.5	88.3	88.5
EXIT FLUID TEMPERATURE, F	108.6	114.1	134.3	132.8	109.5	106.1
BATH FLUID TEMPERATURE, F	90.0	90.0	90.0	90.0	90.0	90.0
AMMETER READING, I., AMPS	111.00	113.00	113.00	78.00	78.00	60.00
VOLTMETER READING, V., VOLTS	9.60	9.80	9.80	6.70	6.70	5.20
FLUID FLOW RATE, LB/HR	317.44	254.26	134.42	62.78	139.78	103.34
INLET FLUID PRESSURE, PSIG	4.00	3.40	1.80	1.00	2.00	2.20
EXIT FLUID PRESSURE, PSIG	2.50	2.20	1.20	0.58	1.40	1.84
ROOM TEMPERATURE, F	83.6	84.8	84.7	85.8	82.9	86.4
RUN NUMBER	302	304	308	312	314	320

## **APPENDIX D**

### **PHYSICAL PROPERTIES**

### A. Ethylene Glycol

The following correlations, which were developed by Morcos and Bergles (22) based on the data reported in References (7,40), were used to compute the physical properties of ethylene glycol.

#### 1. Density in gm/cm<sup>3</sup>

$$\rho = 1.0/[0.924848 + 6.2796 \times 10^{-4} (T-65) + 9.2444 \times 10^{-7} (T-65)^2 + 3.057 \times 10^{-9} (T-65)^3]$$

where T = temperature in °C

Temperature range: 4.5°C to 171°C

Maximum error: 0.18%.

#### 2. Viscosity in centipoise

$$\mu = \exp \left[ 3.80666 - 1.79809 \left( \frac{T-40}{60} \right) + 0.38590 \left( \frac{T-40}{60} \right)^2 - 0.05878 \left( \frac{T-40}{60} \right)^3 + 0.004173 \left( \frac{T-40}{60} \right)^4 \right]$$

where T = temperature, °F

Temperature range: 40°F to 300°F

Maximum error: 0.56%.

#### 3. Specific heat in Btu/lbm-°F

$$C_p = 0.553 + 0.04150 \left( \frac{T-60}{80} \right) + 0.0035 \left( \frac{T-60}{80} \right)^2$$

where T = temperature in °F

Temperature range: 40°F to 300°F

Maximum error: 0.12%.

$$1 \text{ Btu/lbm-}^\circ\text{F} = 4.185 \text{ Joules/gm-}^\circ\text{C}$$

#### 4. Thermal conductivity in Btu/hr-ft-°F

$$k = 0.1825 - 2.3 \times 10^{-4} (T)$$

where T = temperature, °F

Temperature range: 40°F to 350°F

Maximum error: There is no difference between the computed value and the input data within the accuracy of computation.

$$1 \text{ Btu/hr-ft-}^{\circ}\text{F} = \frac{1}{57.83} \text{ Joules/sec-cm-}^{\circ}\text{C}$$

5. Coefficient of thermal expansion in 1/°C

$$\beta = - \frac{1}{\rho} \frac{d\rho}{dT}$$

$$\beta = \rho [6.2796 \times 10^{-4} + 1.84888 \times 10^{-6} (T-65) + 9.171 \times 10^{-9} (T-65)^2]$$

where  $\rho$  = density in gm/cm<sup>3</sup>

and T = temperature, °C

Temperature range: 4.5°C to 171°C

Maximum error: 0.18%.

## B. Distilled Water

The following correlations, which were developed by Singh (37) based on the CRC Handbook of Chemistry and Physics (41), were used to compute the physical properties of distilled water.

1. Density in gm/cm<sup>3</sup>

$$\rho = 0.999986 + 0.1890 \times 10^{-4} (T) - 0.5886 \times 10^{-5} (T)^2 + 0.1548 \times 10^{-7} (T)^3$$

where T = temperature, °C

Temperature range: 0°C to 100°C

Average Absolute Percent Deviation (AAPD) = 0.00637%.

## 2. Viscosity in centipoise

$$\log_{10} \left( \frac{\mu_T}{\mu_{20}} \right) = \frac{1.3272(20-T) - 0.001053(20-T)^2}{T + 105}$$

where  $T$  = temperature,  $^{\circ}\text{C}$

and  $\mu_{20}$  = viscosity of water at  $20^{\circ}\text{C} = 1.002 \text{ cp}$ .

Temperature range:  $20^{\circ}\text{C}$  to  $100^{\circ}\text{C}$

AAPD = 0.00338%.

3. Specific heat in  $\text{Btu/lbm-}^{\circ}\text{F}$ 

$$C_p = 1.01881 - 0.4802 \times 10^{-3} (T) + 0.3274 \times 10^{-5} (T)^2 - 0.604 \times 10^{-8} (T)^3$$

where  $T$  = temperature,  $^{\circ}\text{F}$

Temperature range:  $32^{\circ}\text{F}$  to  $212^{\circ}\text{F}$

AAPD = 0.04455%.

$$1 \text{ Btu/lbm-}^{\circ}\text{F} = 4.185 \text{ Joules/gm-}^{\circ}\text{C}$$

4. Thermal conductivity in  $\text{Btu/hr-ft-}^{\circ}\text{F}$ 

$$k = 0.30289 + 0.7029 \times 10^{-3} (T) - 0.1179 \times 10^{-5} (T)^2 - 0.604 \times 10^{-8} (T)^3$$

where  $T$  = temperature,  $^{\circ}\text{F}$

Temperature range:  $44^{\circ}\text{F}$  to  $206^{\circ}\text{F}$

AAPD = 0.04404%.

$$1 \text{ Btu/hr-ft-}^{\circ}\text{F} = \frac{1}{57.83} \text{ Joules/sec-cm-}^{\circ}\text{C}$$

5. Coefficient of thermal expansion in  $1/^{\circ}\text{C}$ 

$$\beta = - \frac{1}{\rho} \frac{d\rho}{dT}$$

$$\beta = \frac{-1}{\rho} [0.1890 \times 10^{-4} - 1.1772 \times 10^{-5} (T) + 0.4644 \times 10^{-7} (T)^2]$$

where  $\rho$  = density in  $\text{gm/cm}^3$

and  $T$  = temperature,  $^{\circ}\text{C}$

Temperature range: 0°C to 100°C

AAPD = 0.00637%.

### C. N-Butyl Alcohol

#### 1. Density in gm/cm<sup>3</sup>

Data are taken from the FPRI Computer Library. The following expression, as a function of temperature, T, was obtained.

$$\rho = 0.824605 - 0.700505 \times 10^{-3} (T) - 0.101516 \times 10^{-5} (T)^2 + 0.29629 \times 10^{-8} (T)^3$$

where T = temperature, °C

Temperature range: 0°C to 86°C

Maximum error: 0.10%.

#### 2. Viscosity in centipoise

Data are reported on page F-38 in Reference (41).

$$\mu = \exp \left[ -6.92545 + \frac{2.3839 \times 10^3}{T + 273.15} - \frac{1.08564 \times 10^4}{(T + 273.15)^2} \right]$$

where T = temperature, °C

Temperature range: -50°C to 100°C

Maximum error: 1.26%.

#### 3. Specific heat in Btu/lbm-°F

$$C_p = 0.53 + 0.16101 \times 10^{-2} (T-50) - 0.167946 \times 10^{-5} (T-50)^2 + 0.783422 \times 10^{-8} (T-50)^3$$

where T = temperature in °F

The data for the above correlation were taken from page 3-129 in Reference (30).

Temperature range:  $50^{\circ}\text{F}$  to  $212^{\circ}\text{F}$  -

Maximum error: 0.71%.

$$1 \text{ Btu/lbm-}^{\circ}\text{F} = 4.185 \text{ Joules/gm-}^{\circ}\text{C}$$

4. Thermal conductivity in  $\text{Btu/hr-ft-}^{\circ}\text{F}$

Data are taken from the FPRI Computer Library. The following expression was obtained:

$$k = 0.09307 - 0.84619 \times 10^{-4} (T) + 0.158015 \times 10^{-6} (T)^2$$

where  $T$  = temperature in  $^{\circ}\text{F}$

Temperature range:  $-93^{\circ}\text{F}$  to  $347^{\circ}\text{F}$

Maximum error = 1.28%.

$$1 \text{ Btu/hr-ft-}^{\circ}\text{F} = \frac{1}{57.83} \text{ Joules/sec-cm-}^{\circ}\text{C}$$

5. Coefficient of thermal expansion in  $1/^{\circ}\text{C}$

$$\beta = - \frac{1}{\rho} \frac{d\rho}{dT}$$

$$\beta = - \frac{1}{\rho} [-0.700505 \times 10^{-3} - 0.203032 \times 10^{-5} (T) + 0.888882 \times 10^{-8} (T)^2]$$

where  $\rho$  = density in  $\text{gm/cm}^3$

and  $T$  = temperature,  $^{\circ}\text{C}$

Temperature range:  $0^{\circ}\text{C}$  to  $86^{\circ}\text{C}$

Maximum error: 0.10%.

#### D. Stainless Steel

The following correlations, which were developed by Singh (37), were used to compute the physical properties of stainless steel Type 304.

1. Electrical resistivity in  $\text{Ohms-ft}^2/\text{ft}$

$$\varepsilon = 2.1675 \times 10^{-6} + 0.11492 \times 10^{-8} (T) \\ + 0.70965 \times 10^{-12} (T)^2 - 0.84327 \times 10^{-17} (T)^3$$

where T = temperature, °F

2. Thermal conductivity in Btu/hr-ft-°F

$$k = 7.8034 + 0.51691 \times 10^{-2} (T) - 0.88501 \times 10^{-6} (T)^2$$

where T = temperature, °F

$$1 \text{ Btu/hr-ft-}^\circ\text{F} = \frac{1}{57.83} \text{ Joules/sec-cm-}^\circ\text{C}$$



## APPENDIX E

### SAMPLE CALCULATIONS

Calculations for experimental data run 108 are presented as a sample calculation. Experimental data values for run 108 are presented on pages 95 and 96 in Appendix C. The sample calculations given here are based on the following assumptions and conditions:

1. Electrical resistivity and thermal conductivity of tube walls are functions of temperature.
2. Peripheral and radial wall conduction exist.
3. Axial conduction is negligible.
4. Steady state conditions exist.

Computer programs originally written by Singh (37) were modified to perform the calculations for all the data runs on the IBM 370/158 computer.

#### Calculation of the Error Percentage in Heat Balance

Heat input rate, Joules/sec =  $Q_{\text{input}}$

$$Q_{\text{input}} = \left\{ \begin{array}{c} \text{current} \\ \text{in coil} \end{array} \right\} \left\{ \begin{array}{c} \text{voltage drop} \\ \text{across coil} \end{array} \right\}$$

$$= (88.0) (7.2) = 633.6 \text{ Joules/sec}$$

Heat loss rate, Joules/sec =  $Q_{\text{loss}}$

Calibration data for heat losses from the test section are given in Table X in Appendix B.

$$Q_{\text{loss}} = \left( \frac{7581}{9460.1} \right) \frac{(582.4)(1054.18)}{(211.4-81.2)} \left( \frac{1}{3600} \right) (t_{\text{avg}} - t_{\text{room}})$$

The inlet and outlet bulk fluid temperatures measured by the thermocouples were corrected, based on their calibration. Calibration data for these thermocouples are given in Table VIII in Appendix B.

$$\begin{aligned}
 \left\{ \begin{array}{l} \text{corrected inlet} \\ \text{fluid temperature} \end{array} \right\} &= (t_b)_{in} + (0.1) \frac{[(t_b)_{in} - t_{room}]}{(211.8-81.2)} \\
 &= 88.4 + (0.1) \frac{(88.4-82.2)}{(211.8-81.2)} \\
 &= 88.4^{\circ}\text{F} = 31.52^{\circ}\text{C}
 \end{aligned}$$

$$\begin{aligned}
 \left\{ \begin{array}{l} \text{corrected outlet} \\ \text{fluid temperature} \end{array} \right\} &= (t_b)_{out} + (1.12) \frac{[(t_b)_{out} - t_{room}]}{(211.02-81.2)} \\
 &= 105.0 + (1.12) \frac{(105.0-82.2)}{(211.02-81.2)} \\
 &= 105.20^{\circ}\text{F} = 40.85^{\circ}\text{C}
 \end{aligned}$$

$$\begin{aligned}
 \left\{ \begin{array}{l} \text{average bulk} \\ \text{fluid temperature} \end{array} \right\} &= t_{avg} = \frac{1}{2} [(t_b)_{in} + (t_b)_{out}] \\
 t_{avg} &= \frac{1}{2} (88.4 + 105.2) \\
 &= 96.8^{\circ}\text{F} = 36.18^{\circ}\text{C}
 \end{aligned}$$

$$\begin{aligned}
 Q_{loss} &= \frac{(7581)}{(9460.6)} \frac{(582.4)}{(211.4-81.2)} \frac{(1054.18)}{(3600)} (96.8-82.2) \\
 &= 15.32 \text{ Joules/sec}
 \end{aligned}$$

$$\text{Heat output rate, Joules/sec} = Q_{output}$$

$$Q_{output} = (W) (C_p) [(t_b)_{out} - (t_b)_{in}]$$

From Appendix D, for ethylene glycol

$$\begin{aligned}
 C_p &= 0.553 + 0.04150 \left( \frac{T-60}{80} \right) + 0.0035 \left( \frac{T-60}{80} \right)^2 \\
 &\text{at } T = 96.8^{\circ}\text{F}
 \end{aligned}$$

$$C_p = 0.553 + 0.04150 \left( \frac{96.8-60}{80} \right) + 0.0035 \left( \frac{96.8-60}{80} \right)^2$$

$$= 0.573 \text{ Btu/lbm-}^{\circ}\text{F} = 0.573 \text{ cal/gm-K}$$

$$W = 28.49 \frac{\text{g}}{\text{sec}} = 226.1 \frac{\text{lb}}{\text{hr}}$$

$$Q_{\text{output}} = (226.1)(0.573)(105.2-88.4)$$

$$= 2176.5 \text{ Btu/hr}$$

$$= 2176.5 \left( \frac{1054.18}{3600} \right)$$

$$= 637.3 \text{ Joules/sec}$$

$$\begin{aligned} \text{Percentage error in heat balance} &= \frac{Q_{\text{input}} - Q_{\text{loss}} - Q_{\text{output}}}{Q_{\text{input}}} \\ &= \frac{633.6 - 15.32 - 637.3}{633.6} \times 100 \\ &= -3.0\% \end{aligned}$$

Similarly the heat balances for all data runs were calculated.

The results of these calculations are presented in Tables XI, XII, and XIII for the three fluids used.

#### Calculation of the Local Inside Wall

##### Temperatures and the Inside Wall

##### Radial Heat Flux

As indicated in Chapter V, a numerical solution developed by Owhadi (27) and Crain (6) was used to compute the inside wall temperatures and the inside wall radial heat flux at each thermocouple location. The trial-and-error solution is complex and hence a sample calculation will not be given here; however, Tables XIV to XVII give the uncorrected outside surface temperatures, the corrected outside

TABLE XI  
HEAT BALANCE FOR ETHYLENE GLYCOL

Run Number	Average Reynolds Number	Average Prandtl Number	$Q_{in}$ ( $\frac{\text{Joules}}{\text{sec}}$ )	$Q_{out}$ ( $\frac{\text{Joules}}{\text{sec}}$ )	$Q_{lost}$ ( $\frac{\text{Joules}}{\text{sec}}$ )	Heat Flux ( $\frac{\text{Joules}}{\text{sec-m}^2}$ )	Heat Balance Error %
101	449	102.28	657.0	664.9	2.45	2186	-1.63
102	452	101.61	657.0	700.9	3.45	2183	-7.06
103	380	100.09	657.0	599.8	10.62	2159	7.40
104	381	100.82	657.0	611.6	10.41	2159	5.50
105	323	97.77	633.6	617.2	10.10	2082	0.96
106	323	97.68	633.6	621.9	9.83	2083	0.23
107	260	95.73	633.6	636.9	15.43	2064	-3.05
108	260	95.73	633.6	636.9	15.33	2065	-3.03
109	171	87.99	645.3	597.4	17.98	2095	4.82
110	171	88.06	645.3	590.5	18.03	2095	5.96
111	73	52.72	619.2	536.9	54.30	1886	5.01
112	73	52.76	619.2	535.2	54.35	1886	5.32
113	515	103.86	649.7	620.8	5.97	2150	3.57
114	514	103.96	649.7	612.4	5.82	2150	4.95
115	122	78.55	657.0	581.2	22.18	2120	8.76
116	122	78.75	657.0	579.6	22.02	2121	9.05

TABLE XI (Continued)

Run Number	Average Reynolds	Average Prandtl	$Q_{in}$ ( $\frac{\text{Joules}}{\text{sec}}$ )	$Q_{out}$ ( $\frac{\text{Joules}}{\text{sec}}$ )	$Q_{lost}$ ( $\frac{\text{Joules}}{\text{sec}}$ )	Heat Flux ( $\frac{\text{Joules}}{\text{sec-m}^2}$ )	Heat Balance Error %
117	776	100.50	1240.3	1248.0	4.19	4128	-1.02
118	774	100.76	1240.3	1237.8	6.24	4121	-0.37
119	707	99.09	1266.9	1275.8	10.89	4194	-1.63
120	707	99.09	1266.9	1276.2	11.41	4193	-1.70
121	174	60.58	1302.0	1144.3	46.40	4193	9.21
122	174	60.50	1302.0	1147.5	46.18	4194	8.95
123	211	74.05	1248.0	1113.1	35.32	4050	8.49
124	211	73.88	1248.0	1115.6	35.37	4050	8.27
125	454	101.64	682.5	728.6	12.04	2239	-8.38
126	454	101.64	682.5	714.4	11.83	2240	-6.38
The Absolute Average Percentage Error							5.03

TABLE XII  
HEAT BALANCE FOR DISTILLED WATER

Run Number	Average Reynolds Number	Average Prandtl Number	$Q_{in}$ ( $\frac{\text{Joules}}{\text{sec}}$ )	$Q_{out}$ ( $\frac{\text{Joules}}{\text{sec}}$ )	$Q_{lost}$ ( $\frac{\text{Joules}}{\text{sec}}$ )	Heat Flux ( $\frac{\text{Joules}}{\text{sec-m}^2}$ )	Heat Balance Error %
201	1635	3.82	1180.0	1184.0	35.33	3823	-3.36
202	1635	3.82	1180.0	1179.6	35.02	3824	-2.96
203	2757	4.44	1136.8	1151.5	20.88	3727	-3.12
204	2761	4.43	1136.8	1164.2	20.94	3726	-4.22
205	1127	3.21	1180.0	1140.5	50.64	3772	-0.97
206	1127	3.21	1180.0	1140.5	50.33	3773	-0.94
207	2364	4.32	1115.5	1149.0	26.27	3638	-5.32
208	2363	4.32	1115.5	1152.5	26.22	3638	-5.62
209	3345	4.59	1125.2	1142.2	19.08	3694	-3.19
210	3344	4.59	1125.2	1147.5	19.24	3693	-3.67
211	4077	4.69	1156.4	1158.2	21.18	3791	-1.98
212	4080	4.68	1156.4	1164.7	21.13	3791	-2.54
213	5119	4.78	1156.4	1167.3	18.06	3802	-2.49
214	5119	4.78	1156.4	1167.3	17.96	3802	-2.48
The Absolute Average Percentage Error							3.06

TABLE XIII  
HEAT BALANCE FOR N-BUTYL ALCOHOL

Run Number	Average Reynolds Number	Average Prandtl Number	$Q_{in}$ ( $\frac{\text{Joules}}{\text{sec}}$ )	$Q_{out}$ ( $\frac{\text{Joules}}{\text{sec}}$ )	$Q_{lost}$ ( $\frac{\text{Joules}}{\text{sec}}$ )	Heat Flux ( $\frac{\text{Joules}}{\text{sec-m}^2}$ )	Heat Balance Error %
301	2121	32.42	1065.6	1114.8	16.07	3505	-6.1
302	2123	32.39	1065.6	1126.3	15.96	3505	-7.12
303	1763	31.50	1107.4	1155.1	17.77	3639	-5.9
304	1764	31.48	1107.4	1159.7	17.61	3639	-6.28
305	1437	30.72	1086.4	1109.8	22.16	3554	-4.58
306	1438	30.71	1086.4	1113.5	22.10	3554	-4.58
307	1063	28.48	1107.4	1131.7	28.57	3603	-4.85
308	1063	28.47	1107.4	1134.3	28.30	3604	-5.05
309	711	31.15	514.8	515.4	19.46	1654	-4.03
310	712	31.13	514.8	513.8	19.20	1655	-3.63
311	491	28.71	522.6	513.5	26.56	1657	-3.53
312	491	28.70	522.6	512.4	26.30	1657	-3.26
313	935	32.37	522.6	533.6	16.86	1689	-5.42
314	937	32.32	522.6	531.3	16.92	1689	-5.00
315	1285	33.27	522.6	538.6	12.47	1704	-5.50



TABLE XIII (Continued)

Run Number	Average Reynolds Number	Average Prandtl Number	$Q_{in}$ ( $\frac{\text{Joules}}{\text{sec}}$ )	$Q_{out}$ ( $\frac{\text{Joules}}{\text{sec}}$ )	$Q_{lost}$ ( $\frac{\text{Joules}}{\text{sec}}$ )	Heat Flux ( $\frac{\text{Joules}}{\text{sec-m}^2}$ )	Heat Balance Error %
316	1286	33.26	522.6	535.1	12.21	1704	-4.79
317	425	31.10	312.0	312.9	16.56	987	-5.81
318	426	31.04	312.0	315.2	16.56	987	-6.55
319	677	32.88	312.0	322.5	11.58	1003	-7.17
320	678	32.86	312.0	324.4	11.53	1003	-7.73
The Absolute Average Percentage Error							5.33

$$\begin{aligned}
 \text{Inside surface area} &= \pi d_i L = \pi (1.257) (758.1) = 2.994 \times 10^3 \text{ cm}^2 \\
 &= 0.2994 \text{ m}^2
 \end{aligned}$$

TABLE XIV  
UNCORRECTED OUTSIDE SURFACE TEMPERATURES FOR RUN 108

Thermocouple Station Number	Uncorrected Outside Surface Temperatures, °F Peripheral Location*			
	1	2	3	4
1	95.00	96.40	94.00	92.70
2	95.90	98.50	95.10	93.90
3	95.30	98.70	95.50	93.70
4	96.50	99.20	96.40	94.70
5	98.50	101.20	97.90	96.40
6	98.40	101.30	98.30	96.90
7	100.70	103.00	99.70	98.80
8	101.10	103.90	100.20	99.00
9	102.10	104.80	101.30	100.40
10	102.70	105.80	102.70	101.30
11	103.20	105.20	102.60	100.90
12	105.50	108.00	105.70	104.10
13	108.60	111.30	108.50	107.20
14	111.10	113.40	110.60	109.70
15	113.40	115.40	112.00	111.50
16	114.40	117.70	114.50	113.70
17	117.40	119.40	116.60	115.60
18	118.50	121.30	118.40	117.10

\* See the position of each thermocouple in Figure 4.

TABLE XV  
CORRECTED OUTSIDE SURFACE TEMPERATURES FOR RUN 108

Thermocouple Station Number	Corrected Outside Surface Temperature, °F Peripheral Location			
	1	2	3	4
1	95.16	96.47	94.10	92.76
2	95.96	98.56	95.16	93.99
3	95.40	98.78	95.60	93.72
4	96.55	99.23	96.47	94.79
5	98.62	101.28	98.03	96.49
6	98.55	101.42	98.39	96.98
7	100.84	103.08	99.88	98.88
8	101.20	104.00	100.28	99.10
9	102.25	104.94	101.41	100.50
10	102.95	105.90	102.82	101.44
11	103.48	105.33	102.73	101.01
12	105.73	108.17	105.91	104.37
13	108.85	111.55	108.73	107.38
14	111.36	113.58	110.81	109.84
15	113.83	115.88	112.48	111.77
16	114.70	118.01	114.81	114.09
17	117.72	119.85	117.04	115.98
18	119.06	121.63	118.96	117.66

TABLE XVI  
CALCULATED INSIDE WALL TEMPERATURES FOR RUN 108

Thermocouple Station Number	Inside Wall Temperature, °F Peripheral Location			
	1	2	3	4
1	94.98	96.28	93.90	92.57
2	95.76	98.39	94.94	93.80
3	95.19	98.63	95.39	93.54
4	96.35	99.06	96.27	94.60
5	98.42	101.11	97.82	96.30
6	98.35	101.25	98.18	96.80
7	100.65	102.91	99.66	98.71
8	101.00	103.84	100.06	98.91
9	102.05	104.77	101.19	100.31
10	102.74	105.73	102.61	101.25
11	103.29	105.14	102.53	100.81
12	105.52	107.99	105.71	104.18
13	108.64	111.37	108.51	107.19
14	111.15	113.39	110.59	109.65
15	113.63	115.70	112.25	111.59
16	114.47	117.84	114.58	113.92
17	117.51	119.66	116.82	115.78
18	118.86	121.44	118.74	117.47

TABLE XVII  
RADIAL HEAT FLUX FOR INSIDE SURFACE FOR RUN 108

Thermocouple Station Number	Radial Heat Flux for Inside Surface, Btu/hr-ft <sup>2</sup> Peripheral Location			
	1	2	3	4
1	557.1	555.6	636.0	643.7
2	623.1	463.7	684.2	624.0
3	664.3	440.2	648.7	638.8
4	635.6	487.6	641.6	635.2
5	624.0	471.2	668.5	645.8
6	653.2	471.7	665.8	622.0
7	617.1	492.8	690.0	624.4
8	634.1	449.8	704.0	636.1
9	644.4	464.4	708.1	615.9
10	665.4	472.4	674.9	625.3
11	585.7	536.8	642.5	672.5
12	655.4	529.9	640.9	630.6
13	665.3	500.8	674.6	631.6
14	649.2	525.6	690.1	622.7
15	625.5	509.7	727.6	635.8
16	731.6	468.9	723.7	585.9
17	646.2	537.0	697.7	643.2
18	678.6	526.5	686.7	641.8

temperatures, the computed inside temperatures and the inside wall radial heat fluxes for every thermocouple located on the helical coil. The values given are for data run 108.

### Calculation of the Local Heat Transfer

#### Coefficient

For thermocouple 14-3 (thermocouple station 14, peripheral position 3):

$$\left\{ \begin{array}{l} \text{Local heat transfer} \\ \text{coefficient} \end{array} \right\} = h = \frac{(Q/A)_i}{[(t_w)_i - (t_b)_{14}]}$$

$$(t_b)_{14} = (t_b)_{in} + [(t_b)_{out} - (t_b)_{in}] \left( \frac{L_{14}}{L_{total}} \right)$$

$$= 88.40 + (105.20 - 88.40) \frac{(421.64)}{(7581)}$$

$$= 97.74^{\circ}\text{F}$$

$$\left\{ \begin{array}{l} \text{local heat transfer} \\ \text{coefficient} \end{array} \right\} = h = \frac{690.1}{(110.59 - 97.74)}$$

$$= 53.7 \text{ Btu/hr-ft}^2\text{-}^{\circ}\text{F}$$

$$= 304.9 \text{ Joules/sec-m}^2\text{-K}$$

### Calculation of the Dimensionless Axial Distance and the Dimensionless Inside Wall Temperature

By definition:

$$\left\{ \begin{array}{l} \text{Dimensionless} \\ \text{axial distance} \end{array} \right\} = z = \frac{\text{Axial distance along helical coil from inlet electrode, cm}}{\text{Tube inside radius, cm}}$$

and

$$\left\{ \begin{array}{c} \text{Dimensionless} \\ \text{wall temperature} \end{array} \right\} = T_w = \frac{[t_w - (t_b)_{\text{inlet}}]}{dt_b/dz}$$

$$dt_b/dz = \frac{[(t_b)_{\text{exit}} - (t_b)_{\text{inlet}}]}{\frac{\text{Total heated length, cm}}{\text{Tube inside radius, cm}}}$$

For thermocouple 14-3

$$z = \frac{421.64}{1.257/2} = 670.7$$

$$\frac{dt_b}{dz} = \frac{105.20-88.40}{\frac{298.5 \times 2.54}{1.257/2}} = \frac{16.8}{1.206 \times 10^3} = 0.01393$$

$$\therefore T_w = \frac{(110.59-88.40)}{0.01393} = 1592.9$$

Similar calculations were performed for the other thermocouples.

Table XVIII gives the results for run number 108.

#### Calculations of the Relevant

##### Dimensionless Numbers

Table II in Chapter V gives the definition of the dimensionless numbers evaluated.

For data run 108 and thermocouple station 14, the following dimensionless numbers were evaluated:

1. Reynolds Number:  $Re$

$$Re = (d_1)(G)/(\mu)$$

$$\text{where } G = W/(\pi d_1^2/4)$$

From page 102 in Appendix D

TABLE XVIII  
 DIMENSIONLESS AXIAL DISTANCE AND INSIDE WALL  
 TEMPERATURES FOR RUN 108

Dimensionless Axial Distance	Dimensionless Inside Wall Temperatures, $T_w$ Peripheral Location			
	1	2	3	4
8.1	472.2	565.8	394.7	299.6
20.2	528.6	717.5	469.7	387.8
32.3	487.4	734.2	502.2	368.0
56.6	570.7	765.4	564.9	445.4
80.8	719.3	912.5	675.9	567.2
105.1	714.1	922.8	702.1	602.9
129.3	879.3	1041.5	808.4	739.0
161.6	904.6	1108.3	837.2	754.8
202.0	979.6	1175.1	918.3	855.1
242.4	1029.1	1244.3	1019.9	922.8
288.9	1069.1	1201.9	1014.2	890.7
416.2	1229.1	1406.2	1242.6	1132.6
541.4	1452.7	1649.1	1443.8	1348.7
670.7	1633.0	1794.2	1592.9	1525.5
800.0	1811.1	1959.8	1712.1	1663.8
929.3	1871.7	2113.2	1879.1	1831.8
1050.5	2089.7	2243.9	2040.2	1965.8
1179.8	2185.3	2372.0	2177.8	2086.8



$$\begin{aligned}\mu = & \exp \left[ 3.8066 - 1.79809 \left( \frac{T-40}{60} \right) \right. \\ & + 0.38590 \left( \frac{T-40}{60} \right)^2 - 0.05878 \left( \frac{T-40}{60} \right)^3 \\ & \left. + 0.004173 \left( \frac{T-40}{60} \right)^4 \right] \quad (E.1)\end{aligned}$$

where T is measured in  $^{\circ}\text{F}$  and  $\mu$  in centipoise

at  $(t_b)_{14} = 97.74^{\circ}\text{F}$

$$\begin{aligned}\mu = & \exp \left[ 3.8066 - 1.79809 \left( \frac{97.74-40}{60} \right) + 0.38590 \left( \frac{97.74-40}{60} \right)^2 \right. \\ & \left. - 0.05878 \left( \frac{97.74-40}{60} \right)^3 + 0.004173 \left( \frac{97.74-40}{60} \right)^4 \right]\end{aligned}$$

$$\mu = 10.857 \text{ centipoise} = 0.10857 \text{ gm/(cm-sec)} \quad (E.2)$$

$$\therefore \text{Re} = (1.2573) \left[ \frac{28.49}{(3.1416/4)(1.257)^2} \right] \left[ \frac{1}{0.10857} \right]$$

$$= 265.7$$

2. Dean Number:  $De$

$$De = (\text{Re}) \left( \sqrt{d_1/D_c} \right)$$

$$De = 265.7 \left( \sqrt{1.257/25.4} \right)$$

$$= 59.1$$

3. Prandtl Number:  $Pr$

$$Pr = (C_p)(\mu)/(k)$$

From page 102 in Appendix D,

$$C_p = 0.553 + 0.04150 \left( \frac{T-60}{80} \right) + 0.0035 \left( \frac{T-60}{80} \right)^2$$

where T is measured in  $^{\circ}\text{F}$ , and  $C_p$  is in Btu/lbm- $^{\circ}\text{F}$

at  $(t_b)_{14} = 97.74^{\circ}\text{F}$

$$C_p = 0.553 + 0.04150 \left( \frac{97.74-60}{80} \right) + 0.0035 \left( \frac{97.74-60}{80} \right)^2$$

$$C_p = 0.573 \text{ Btu/lbm-}^{\circ}\text{F}$$

$$C_p = 2.398 \text{ Joules/gm-K}$$

From page 102 in Appendix D,

$$k = 0.1825 - 2.3 \times 10^{-4} (T)$$

where T is measured in  $^{\circ}\text{F}$  and k is in Btu/hr-ft- $^{\circ}\text{F}$

$$\text{at } (t_b)_{14} = 97.74^{\circ}\text{F}$$

$$k = 0.1825 - 2.3 \times 10^{-4} (97.74)$$

$$= 0.1600 \text{ Btu/hr-ft-}^{\circ}\text{F}$$

$$= 2.767 \times 10^{-3} \text{ Joules/sec-cm-}^{\circ}\text{C}$$

$$\mu = 0.10857 \text{ gm/(cm-sec) From Equation (E.2)}$$

$$\therefore \text{Pr} = \frac{(2.398)(0.10857)}{(2.767 \times 10^{-3})} = 94.1$$

4. Nusselt Number: Nu

$$\text{Nu} = (h) (d_i) / k$$

$$\text{Nu} = \frac{304.9 \times 1.257}{(100)^2 (2.767 \times 10^{-3})}$$

$$\text{Nu} = 13.85$$

5. Graetz Number: Gz

$$\begin{aligned} \text{Gz} &= \frac{(W) (C_p)}{(k) (L)} \\ &= \frac{(28.49)(2.398)}{(2.767 \times 10^{-3})(421.64)} \\ &= 58.56 \end{aligned}$$

6. Grashof Number: Gr

$$\text{Gr} = (d_i^3) (\rho^2) (g) (\beta) (\Delta t) / (\mu^2)$$

From page 102 in Appendix D:

$$\rho = 1/[0.924848 + 6.2796 \times 10^{-4} (T-65) + 9.2444 \times 10^{-7} (T-65)^2 + 3.057 \times 10^{-9} (T-65)^3]$$

where T is measured in  $^{\circ}\text{C}$  and  $\rho$  is in  $\text{gm/cm}^3$

$$\text{at } (t_b)_{14} = 97.74^{\circ}\text{F} = 36.71^{\circ}\text{C}$$

$$\rho = 1/[0.924848 + 6.2796 \times 10^{-4} (36.71-65) + 9.2444 \times 10^{-7} (36.71-65)^2 + 3.057 \times 10^{-9} (36.71-65)^3]$$

$$\rho = 1.102 \text{ gm/cm}^3$$

From page 103 in Appendix D,

$$\beta = \rho[6.2796 \times 10^{-4} + 1.84888 \times 10^{-6} (T-65) + 9.171 \times 10^{-9} (T-65)^2]$$

$\beta$  is calculated at  $t_{(\text{avg})}$

$$t_{(\text{avg})} = \frac{(t_w)_{\text{avg}} + (t_b)_{14}}{2}$$

$$(t_w)_{\text{avg}} = \frac{(111.5 + 113.39 + 110.59 + 109.65)}{4}$$

$$(t_w)_{\text{avg}} = 111.2^{\circ}\text{F} = 44.18^{\circ}\text{C}$$

$$t_{(\text{avg})} = \frac{(44.18 + 36.71)}{2} = 40.45^{\circ}\text{C}$$

$$\begin{aligned} \beta &= (\rho_{t_{(\text{avg})}})[6.2796 \times 10^{-4} + 1.84888 \times 10^{-6} (40.45-65) + 9.171 \times 10^{-9} (40.45-65)^2] \\ &= (\rho_{t_{(\text{avg})}})[5.881 \times 10^{-4}] \end{aligned}$$

$$\begin{aligned} \rho_{t_{(\text{avg})}} &= 1/[0.924848 + 6.2796 \times 10^{-4} (40.45-65) + 9.2444 \times 10^{-7} (40.45-65)^2 + 3.057 \times 10^{-9} (40.45-65)^3] \end{aligned}$$

$$\rho_{t_{(\text{avg})}} = 1.10$$

$$\begin{aligned} \beta &= (1.10)(5.881 \times 10^{-4}) \\ &= 6.469 \times 10^{-4}/^{\circ}\text{C} \end{aligned}$$

$$g = 980.66 \text{ cm/sec}^2$$

$$\mu = 0.10857 \text{ gm/(cm-sec)} \quad \text{From Equation (E.2)}$$

$$Gr = (1.257)^3 (1.102)^2 (980.66) (6.469 \times 10^{-4})$$

$$(44.18 - 36.71) \times \left[ \frac{1}{0.10857} \right]^2$$

$$= 970.4$$

7. Rayleigh Number: Ra

$$Ra = (Gr) (Pr)$$

$$= (970.4) (94.1)$$

$$= 9.13 \times 10^4$$

**APPENDIX F**

**CALCULATED RESULTS**

The calculated results for those experimental runs which were presented in Appendix C are presented here. The rest of the calculated results are available at:

School of Chemical Engineering  
Oklahoma State University  
Stillwater, Oklahoma 74074 U.S.A  
Attn: Dr. Kenneth J. Bell

THERMOCOUPLE STATION : 1

AT THE AVERAGE BULK FLUID TEMPERATURE AT THE THERMOCOUPLE STATION				AVERAGE VALUES FOR THE STATION			
RUN NUMBER	REYNOLDS NUMBER	DEAN NUMBER	PRANDTL NUMBER	HEAT FLUX J/SEC-SQ.M.	HEAT TRANSFER COEFFICIENT		NUSSELT NUMBER
	RE	DE	PR	Q/A	H1	H2	NU
102	408	90	111.344	1938	768.16	677.94	34.42
104	342	76	110.916	1962	764.87	697.75	34.28
108	219	48	111.458	1887	616.56	573.72	27.62
110	131	29	110.908	1931	477.63	460.26	21.41
112	30	6	112.877	1831	264.66	263.72	11.85
120	625	139	110.477	3644	989.89	850.85	44.38
202	1232	274	5.236	3356	1141.74	961.93	23.32
204	2374	528	5.248	3239	1508.14	1309.96	30.81
206	726	161	5.241	3355	915.96	785.07	18.71
208	1978	440	5.272	3192	1515.25	1274.81	30.97
210	2964	659	5.250	3245	1645.17	1474.77	33.61
214	4735	1053	5.213	3366	2229.14	2027.34	45.51
302	1857	413	35.901	2984	600.23	533.70	50.24
304	1488	331	35.887	3092	538.05	479.96	45.03
308	786	174	35.910	3108	396.94	358.29	33.22
312	366	81	35.952	1494	270.72	252.93	22.66
314	812	180	36.088	1489	402.74	362.93	33.70
320	601	133	36.021	881	339.65	306.41	28.42

THERMOCOUPLE STATION : 2

AT THE AVERAGE BULK FLUID TEMPERATURE AT THE THERMOCOUPLE STATION				AVERAGE VALUES FOR THE STATION			
RUN NUMBER	REYNOLDS NUMBER	DEAN NUMBER	PRANDTL NUMBER	HEAT FLUX J/SEC-SQ.M. Q/A	HEAT TRANSFER COEFFICIENT J/SEC-SQ.M.-K		NUSSELT NUMBER NU
	RE	DE	PR		H1	H2	
102	409	91	111.133	1941	644.96	591.24	28.90
104	343	76	110.697	1964	664.87	603.77	29.80
108	220	40	111.102	1889	520.79	482.66	23.34
110	132	29	110.362	1932	413.13	388.01	18.52
112	31	6	110.817	1849	207.44	203.55	9.30
120	627	139	110.227	3652	794.35	716.02	35.62
202	1240	276	5.199	3365	961.71	838.01	19.63
204	2381	529	5.229	3243	1314.32	1146.06	26.84
206	733	163	5.180	3368	763.55	691.22	15.58
208	1986	441	5.250	3195	1239.13	1051.97	25.32
210	2972	661	5.235	3246	1529.21	1348.43	31.23
214	4743	1055	5.203	3365	2130.67	1902.03	43.49
302	1862	414	35.824	2994	479.88	433.72	40.17
304	1493	332	35.789	3103	436.83	396.85	36.57
308	791	176	35.734	3128	319.03	298.28	26.71
312	368	82	35.781	1506	226.15	215.55	18.93
314	814	181	36.006	1497	317.54	295.81	26.57
320	603	134	35.953	887	269.60	252.26	22.56



THERMOCOUPLE STATION : 3

AT THE AVERAGE BULK FLUID TEMPERATURE AT THE THERMOCOUPLE STATION				AVERAGE VALUES FOR THE STATION			
RUN NUMBER	REYNOLDS NUMBER	DEAN NUMBER	PRANDTL NUMBER	HEAT FLUX J/SEC-SQ.M. Q/A	HEAT TRANSFER COEFFICIENT J/SEC-SQ.M.-K		NUSSELT NUMBER NU
	RE	DE	PR		H1	H2	
102	410	91	110.922	1938	718.76	635.55	32.21
104	343	76	110.478	1963	678.53	613.83	30.42
108	221	49	110.748	1886	547.32	496.87	24.53
110	133	29	109.820	1930	431.96	397.64	19.37
112	31	7	108.809	1856	203.43	199.17	9.13
120	628	139	109.977	3647	896.95	777.46	40.23
202	1248	277	5.163	3360	1162.70	968.94	23.71
204	2389	531	5.210	3239	1601.08	1254.19	32.69
206	741	164	5.121	3363	906.83	789.89	18.48
208	1993	443	5.227	3191	1586.15	1216.33	32.39
210	2979	662	5.220	3242	1793.29	1433.14	36.62
214	4751	1057	5.194	3361	2663.12	2122.27	54.35
302	1867	415	35.748	2987	524.48	458.10	43.91
304	1498	333	35.692	3099	470.97	418.39	39.43
308	796	177	35.559	3123	342.43	314.83	28.68
312	371	82	35.611	1505	232.18	220.40	19.44
314	817	181	35.924	1494	339.73	309.84	28.43
320	604	134	35.885	885	283.28	260.91	23.71

THERMOCOUPLE STATION : 4

AT THE AVERAGE BULK FLUID TEMPERATURE AT THE THERMOCOUPLE STATION				AVERAGE VALUES FOR THE STATION			
RUN NUMBER	REYNOLDS NUMBER	DEAN NUMBER	PRANDTL NUMBER	HEAT FLUX J/SEC-SQ.M. Q/A	HEAT TRANSFER COEFFICIENT		NUSSELT NUMBER NU
	RE	DE	PR		J/SEC-SQ.M.-K H1	H2	
102	411	91	110.503	1943	658.37	599.47	29.52
104	345	76	110.041	1965	654.40	595.85	29.35
108	222	49	110.044	1893	491.16	461.42	22.03
110	134	29	108.748	1939	381.85	363.50	17.14
112	33	7	104.945	1873	196.42	189.18	8.84
120	632	140	109.481	3651	829.53	739.45	37.22
202	1264	281	5.091	3366	1190.79	959.42	24.25
204	2474	535	5.173	3243	1480.00	1208.67	30.19
206	756	168	5.006	3376	884.87	752.95	17.99
208	2009	446	5.183	3196	1502.95	1186.43	30.67
210	2994	666	5.191	3244	1686.62	1359.15	34.42
214	4766	1060	5.175	3364	2256.95	1803.03	46.04
302	1877	417	35.596	2996	485.34	436.16	40.64
304	1509	335	35.498	3105	445.81	399.99	37.34
308	806	179	35.213	3131	331.89	306.65	27.81
312	375	83	35.275	1512	220.65	208.98	18.49
314	821	182	35.760	1497	330.50	302.39	27.67
320	607	135	35.749	887	286.30	264.37	23.97

THERMOCOUPLE STATION : 5

AT THE AVERAGE BULK FLUID TEMPERATURE AT THE THERMOCOUPLE STATION				AVERAGE VALUES FOR THE STATION			
RUN NUMBER	REYNOLDS NUMBER	DEAN NUMBER	PRANDTL NUMBER	HEAT FLUX J/SEC-SQ.M. Q/A	HEAT TRANSFER COEFFICIENT J/SEC-SQ.M.-K		NUSSELT NUMBER NU
	RE	DE	PR		H1	H2	
102	413	92	110.085	1952	498.43	474.65	22.35
104	346	77	109.608	1975	493.42	467.06	22.13
108	224	49	109.346	1900	407.12	384.92	18.27
110	136	30	107.691	1947	330.91	315.73	14.86
112	34	7	101.273	1879	204.13	192.52	9.21
120	635	141	108.989	3662	718.06	666.87	32.23
202	1279	284	5.021	3375	1070.29	918.16	21.77
204	2420	538	5.136	3243	1694.29	1282.69	34.54
206	771	171	4.895	3391	779.51	686.85	15.81
208	2024	450	5.139	3197	1729.12	1271.89	35.25
210	3010	669	5.161	3245	1835.45	1404.19	37.43
214	4781	1063	5.156	3362	2461.87	1816.27	50.20
302	1888	420	35.445	2994	511.02	449.05	42.81
304	1520	338	35.306	3106	462.58	411.04	38.76
308	816	181	34.871	3152	289.50	274.81	24.27
312	380	84	34.942	1524	195.41	186.57	16.38
314	826	183	35.597	1506	286.56	270.66	24.00
320	610	135	35.614	896	222.66	213.32	18.65

THERMOCOUPLE STATION : 6

AT THE AVERAGE BULK FLUID TEMPERATURE AT THE THERMOCOUPLE STATION				AVERAGE VALUES FOR THE STATION			
RUN NUMBER	REYNOLDS	DEAN	PRANDTL	HEAT FLUX J/SEC-SQ.M. Q/A	HEAT TRANSFER COEFFICIENT J/SEC-SQ.M.-K		NUSSELT NUMBER NU
	NUMBER RE	NUMBER DE	NUMBER PR		H1	H2	
102	415	92	109.670	1954	483.39	459.17	21.68
104	348	77	109.176	1975	493.45	468.80	22.14
108	225	50	108.655	1903	409.05	390.03	18.36
110	137	30	106.848	1951	322.11	308.40	14.48
112	35	7	97.782	1887	210.26	196.90	9.52
120	638	142	108.499	3673	603.70	571.71	27.10
202	1295	288	4.953	3392	831.34	760.52	16.88
204	2435	541	5.099	3250	1453.13	1204.76	29.60
206	787	175	4.768	3393	913.14	733.67	18.48
208	2039	453	5.096	3209	1222.72	1063.34	24.90
210	3025	673	5.132	3248	1843.23	1415.36	37.57
214	4797	1067	5.138	3364	2524.58	1858.22	51.46
302	1898	422	35.294	3003	462.55	420.15	38.75
304	1531	340	35.116	3124	375.60	349.00	31.48
308	827	184	34.533	3170	255.14	243.84	21.41
312	385	85	34.614	1530	189.33	180.55	15.88
314	831	185	35.435	1514	248.44	236.83	20.81
320	613	136	35.487	898	213.39	203.59	17.87

THERMOCOUPLE STATION : 7

AT THE AVERAGE BULK FLUID TEMPERATURE AT THE THERMOCOUPLE STATION				AVERAGE VALUES FOR THE STATION			
RUN NUMBER	REYNOLDS	DEAN	PRANDTL	HEAT FLUX J/SEC-SQ.M. Q/A	HEAT TRANSFER COEFFICIENT		NUSSELT NUMBER NU
	NUMBER RE	NUMBER DE	NUMBER PR		J/SEC-SQ.M.-K H1	H2	
102	417	92	109.258	1957	452.67	430.37	20.31
104	349	77	108.747	1980	446.54	426.85	20.04
108	227	50	107.970	1912	346.83	334.89	15.58
110	139	30	105.619	1961	288.34	277.99	12.97
112	37	8	94.460	1903	207.38	193.64	9.41
120	641	142	108.012	3676	570.50	537.96	25.62
202	1311	291	4.886	3398	804.81	728.60	16.32
204	2451	545	5.063	3262	1047.94	946.15	21.33
206	802	178	4.685	3414	798.82	694.69	16.13
208	2055	457	5.054	3221	920.12	839.34	18.72
210	3040	676	5.103	3256	1388.31	1173.24	28.28
214	4812	1070	5.119	3368	1998.99	1593.73	40.73
302	1909	424	35.145	3028	349.63	331.14	29.30
304	1541	343	34.926	3145	311.78	296.17	26.14
308	837	186	34.199	3177	255.74	243.10	21.47
312	389	80	34.290	1541	181.12	172.98	15.20
314	836	186	35.274	1518	244.83	233.49	20.51
320	616	137	32.346	902	202.36	194.24	16.95

THERMOCOUPLE STATION : 8

AT THE AVERAGE BULK FLUID TEMPERATURE AT THE THERMOCOUPLE STATION				AVERAGE VALUES FOR THE STATION			
RUN NUMBER	REYNOLDS NUMBER	DEAN NUMBER	PRANDTL NUMBER	HEAT FLUX J/SEC-SQ.M. Q/A	HEAT TRANSFER COEFFICIENT J/SEC-SQ.M.-K		NUSSELT NUMBER NU
	RE	DE	PR		H1	H2	
102	419	93	108.711	1960	422.02	401.49	18.94
104	352	78	108.179	1982	430.40	409.87	19.33
108	229	51	107.066	1912	350.87	334.00	15.77
110	141	31	104.269	1961	291.55	279.03	13.13
112	39	8	90.277	1905	218.08	201.56	9.93
120	646	143	107.368	3682	545.08	518.44	24.49
202	1332	290	4.798	3401	882.11	785.45	17.85
204	2471	549	5.016	3262	1163.68	1009.08	23.66
206	823	183	4.552	3421	885.76	744.53	17.83
208	2075	461	4.998	3221	1066.22	942.00	21.67
210	3060	681	5.065	3261	1283.72	1109.07	26.13
214	4833	1075	5.095	3367	2303.51	1668.33	46.92
302	1923	427	34.947	3026	361.01	338.01	30.27
304	1556	346	34.676	3141	334.81	313.77	28.08
308	851	189	33.762	3178	258.08	243.16	21.68
312	396	88	33.864	1539	192.05	180.79	16.13
314	843	187	35.061	1521	239.99	229.50	20.12
320	621	138	35.169	905	193.66	185.67	16.23

THERMOCOUPLE STATION : 9

AT THE AVERAGE BULK FLUID TEMPERATURE AT THE THERMOCOUPLE STATION				AVERAGE VALUES FOR THE STATION			
RUN NUMBER	REYNOLDS NUMBER	DEAN NUMBER	PRANDTL NUMBER	HEAT FLUX J/SEC-SQ.M.	HEAT TRANSFER COEFFICIENT		NUSSELT NUMBER
	RE	DE	PR	Q/A	H1	H2	NU
102	422	94	108.033	1962	420.76	402.97	18.90
104	354	76	107.474	1989	400.76	386.99	18.01
108	232	51	105.951	1919	329.94	317.85	14.84
110	143	31	102.616	1970	278.79	269.94	12.57
112	41	9	85.416	1933	214.93	201.62	9.84
120	651	144	106.571	3687	537.18	509.28	24.15
202	1359	302	4.693	3414	902.97	823.59	18.23
204	2498	555	4.957	3269	1213.57	1077.47	24.65
206	849	189	4.395	3444	817.85	734.36	16.40
208	2101	467	4.929	3230	1044.01	951.87	21.19
210	3086	686	5.018	3265	1350.81	1180.11	27.47
214	4859	1081	5.064	3371	2397.52	1781.31	48.80
302	1941	431	34.701	3029	370.38	347.35	31.07
304	1574	350	34.366	3150	321.75	306.16	27.00
308	869	193	33.225	3185	283.77	274.89	23.86
312	404	89	33.341	1542	215.53	205.94	18.12
314	851	189	34.798	1529	228.76	219.94	19.18
320	626	139	34.949	909	190.20	184.03	15.95

THERMOCOUPLE STATION : 10

AT THE AVERAGE BULK FLUID TEMPERATURE AT THE THERMOCOUPLE STATION				AVERAGE VALUES FOR THE STATION			
RUN NUMBER	REYNOLDS NUMBER	DEAN NUMBER	PRANDTL NUMBER	HEAT FLUX J/SEC-SQ.M.	HEAT TRANSFER COEFFICIENT		NUSSELT NUMBER
	RE	DE	PR	Q/A	H1	H2	NU
102	425	94	107.360	1967	391.35	376.83	17.58
104	357	79	106.776	1991	382.17	369.55	17.18
108	235	52	104.852	1923	316.37	306.13	14.24
110	146	32	101.000	1976	265.37	256.77	11.98
112	44	9	80.925	1939	211.41	198.94	9.72
120	657	146	105.782	3692	493.71	471.85	22.21
202	1386	308	4.591	3419	961.72	845.08	19.38
204	2524	561	4.900	3274	1117.26	988.98	22.66
206	876	195	4.246	3451	921.86	767.33	18.42
208	2127	473	4.852	3232	1085.62	959.43	22.00
210	3112	692	4.972	3270	1271.32	1111.19	25.83
214	4885	1086	5.034	3374	2135.02	1648.72	43.43
302	1959	435	34.458	3030	366.04	338.61	30.71
304	1593	354	34.060	3156	313.21	296.22	26.30
308	888	197	32.699	3178	301.60	281.40	25.39
312	412	91	32.829	1541	230.33	218.71	19.38
314	867	191	34.557	1527	237.12	223.48	19.89
320	631	140	34.751	913	178.30	171.22	14.95



THERMOCOUPLE STATION : 11

AT THE AVERAGE BULK FLUID TEMPERATURE AT THE THERMOCOUPLE STATION				AVERAGE VALUES FOR THE STATION			
RUN NUMBER	REYNOLDS	DEAN	PRANDTL	HEAT FLUX J/SEC-SQ.M. Q/A	HEAT TRANSFER COEFFICIENT		NUSSELT NUMBER NU
	NUMBER RE	NUMBER DE	NUMBER PR		J/SEC-SQ.M.-K H1	H2	
102	429	95	106.594	1969	395.97	385.51	17.80
104	360	80	105.982	1992	400.36	389.64	18.01
108	238	53	103.608	1923	340.60	329.00	15.35
110	149	33	99.186	1980	281.51	273.29	12.73
112	47	10	76.176	1955	213.39	205.35	9.87
120	663	147	104.885	3691	536.62	515.75	24.15
202	1417	315	4.478	3427	1182.47	1070.32	23.76
204	2554	568	4.835	3280	1260.23	1174.41	25.53
206	907	201	4.084	3475	865.20	827.13	17.22
208	2157	479	4.787	3241	1126.15	1062.03	22.79
210	3141	698	4.920	3275	1430.96	1313.03	29.04
214	4915	1093	5.000	3377	3186.27	2295.19	64.77
302	1979	440	34.182	3034	406.93	393.37	34.16
304	1614	359	33.713	3153	368.56	355.37	30.97
308	909	202	32.109	3200	296.00	290.15	24.94
312	422	93	32.254	1555	220.49	217.66	18.58
314	869	193	34.239	1531	263.08	257.49	22.08
320	637	141	34.483	915	195.48	191.79	16.40

THERMOCOUPLE STATION : 12

AT THE AVERAGE BULK FLUID TEMPERATURE AT THE THERMOCOUPLE STATION				AVERAGE VALUES FOR THE STATION			
RUN NUMBER	REYNOLDS NUMBER	DEAN NUMBER	PRANDTL NUMBER	HEAT FLUX J/SEC-SQ.M.	HEAT TRANSFER COEFFICIENT		NUSSELT NUMBER
	RE	DE	PR	Q/A	H1	H2	NU
102	438	97	104.536	1974	394.65	383.58	17.77
104	368	82	103.847	2000	380.11	371.47	17.12
108	247	54	100.307	1938	305.43	299.32	13.80
110	158	35	94.449	1998	254.62	248.98	11.56
112	57	12	65.096	1998	212.21	198.31	9.96
120	681	151	102.482	3704	494.24	477.94	22.29
202	1504	334	4.190	3459	991.49	873.44	19.79
204	2637	586	4.665	3293	1225.49	1100.36	24.73
206	994	221	3.689	3520	908.14	759.66	17.89
208	2239	498	4.589	3259	1063.44	964.38	21.42
210	3223	717	4.781	3282	1624.19	1380.27	32.86
214	4997	1111	4.908	3387	2148.77	1758.74	43.59
302	2037	453	33.438	3046	377.78	357.40	31.76
304	1674	372	32.786	3172	333.75	317.18	28.09
308	969	215	30.563	3237	259.86	251.06	21.96
312	449	100	30.745	1576	207.51	197.82	17.53
314	896	199	33.443	1542	240.25	232.24	20.20
320	653	145	33.814	918	210.60	202.74	17.69

THERMOCOUPLE STATION : 13

AT THE AVERAGE BULK FLUID TEMPERATURE AT THE THERMOCOUPLE STATION				AVERAGE VALUES FOR THE STATION			
RUN NUMBER	REYNOLDS	DEAN	PRANDTL	HEAT FLUX J/SEC-SQ.M. Q/A	HEAT TRANSFER COEFFICIENT		NUSSELT NUMBER NU
	NUMBER RE	NUMBER DE	NUMBER PR		J/SEC-SQ.M.-K H1	H2	
102	448	99	102.565	1985	341.38	332.66	15.39
104	377	83	101.805	2012	331.91	324.38	14.97
108	256	56	97.203	1950	276.38	270.28	12.51
110	166	37	90.099	2014	239.02	233.45	10.89
112	67	15	56.398	2051	210.45	199.73	10.03
120	698	155	100.193	3725	423.14	412.15	19.11
202	1592	354	3.935	3491	980.81	866.75	19.45
204	2720	605	4.506	3313	1059.48	966.32	21.30
206	1082	240	3.358	3574	919.58	793.18	17.94
208	2322	516	4.407	3276	1063.54	965.00	21.34
210	3304	735	4.650	3301	1196.92	1080.76	24.15
214	5079	1130	4.820	3395	1910.21	1551.96	38.68
302	2095	466	32.728	3074	313.31	301.05	26.37
304	1734	385	31.906	3195	303.82	289.96	25.61
308	1032	229	29.137	3250	283.44	269.82	24.02
312	477	106	29.351	1603	199.22	195.62	16.88
314	924	205	32.683	1553	228.42	219.67	19.23
320	670	149	33.173	931	186.15	181.35	15.66

THERMOCOUPLE STATION : 14

AT THE AVERAGE BULK FLUID TEMPERATURE AT THE THERMOCOUPLE STATION				AVERAGE VALUES FOR THE STATION			
RUN NUMBER	REYNOLDS NUMBER	DEAN NUMBER	PRANDTL NUMBER	HEAT FLUX J/SEC-SQ.M.	HEAT TRANSFER COEFFICIENT		NUSSELT NUMBER
	RE	DE	PR	Q/A	H1	H2	NU
102	458	101	100.585	1995	317.21	312.04	14.32
104	385	85	99.758	2021	308.94	304.58	13.96
108	265	59	94.141	1962	266.93	262.52	12.12
110	176	39	85.905	2031	233.02	228.27	10.66
112	79	17	49.159	2096	209.87	197.84	10.16
120	717	159	97.906	3735	409.36	401.35	18.53
202	1684	374	3.697	3516	1125.37	895.44	22.17
204	2807	624	4.351	3326	1143.08	1031.95	22.90
206	1176	261	3.064	3616	1105.47	806.02	21.37
208	2408	535	4.231	3291	1177.74	1017.62	23.53
210	3388	753	4.521	3313	1198.47	1098.22	24.11
214	5163	1148	4.731	3404	2022.32	1652.01	40.87
302	2155	479	32.016	3085	317.02	306.17	26.72
304	1798	400	31.031	3200	326.98	308.57	27.61
308	1099	244	27.759	3280	274.84	259.84	23.36
312	507	112	28.001	1620	201.08	193.06	17.08
314	952	212	31.923	1554	266.45	248.25	22.46
320	687	152	32.528	935	194.59	186.84	16.38

THERMOCOUPLE STATION : 15

AT THE AVERAGE BULK FLUID TEMPERATURE AT THE THERMOCOUPLE STATION				AVERAGE VALUES FOR THE STATION			
RUN NUMBER	REYNOLDS NUMBER	DEAN NUMBER	PRANDTL NUMBER	HEAT FLUX J/SEC-SQ.M.	HEAT TRANSFER COEFFICIENT		NUSSELT NUMBER
	RE	DE	PR	Q/A	H1	H2	NU
102	468	104	98.660	2000	311.72	304.12	14.10
104	394	87	97.768	2028	299.01	292.68	13.53
108	275	61	91.216	1971	264.15	258.08	12.02
110	185	41	81.989	2043	234.20	228.47	10.76
112	92	20	43.275	2146	217.06	206.13	10.68
120	736	163	95.693	3747	389.61	380.13	17.66
202	1777	395	3.482	3551	1025.70	881.22	20.08
204	2894	644	4.205	3342	1119.90	993.06	22.36
206	1272	283	2.811	3674	953.45	802.63	18.27
208	2496	555	4.067	3310	1109.35	960.44	22.07
210	3473	772	4.398	3324	1191.97	1046.94	23.91
214	5249	1167	4.646	3408	2247.35	1625.38	45.33
302	2218	493	31.324	3085	338.53	314.27	28.57
304	1864	414	30.188	3215	319.86	296.75	27.05
308	1169	260	26.468	3302	281.94	266.81	24.03
312	539	119	26.733	1641	205.21	199.93	17.48
314	982	218	31.186	1568	253.34	240.86	21.39
320	705	156	31.900	943	195.43	188.17	16.47

THERMOCOUPLE STATION : 16

AT THE AVERAGE BULK FLUID TEMPERATURE AT THE THERMOCOUPLE STATION				AVERAGE VALUES FOR THE STATION			
RUN NUMBER	REYNOLDS NUMBER	DEAN NUMBER	PRANDTL NUMBER	HEAT FLUX J/SEC-SQ.M. Q/A	HEAT TRANSFER COEFFICIENT J/SEC-SQ.M.-K		NUSSELT NUMBER NU
	RE	DE	PK		H1	H2	
102	478	106	96.786	2007	305.64	297.98	13.84
104	403	89	95.855	2034	294.10	287.52	13.33
108	285	63	88.420	1980	263.27	257.17	12.01
110	195	43	78.328	2053	240.78	234.56	11.10
112	107	23	38.439	2195	218.96	210.40	10.94
120	755	168	93.550	3760	376.29	366.35	17.09
202	1873	416	3.286	3588	1202.68	1080.88	23.41
204	2983	663	4.066	3363	1271.83	1204.54	25.30
206	1371	305	2.591	3738	957.11	879.38	18.20
208	2584	575	3.912	3337	1161.42	1124.42	23.01
210	3559	791	4.279	3344	1272.52	1224.02	25.45
214	5334	1186	4.562	3422	2233.20	2021.04	44.96
302	2281	507	30.652	3071	452.83	386.98	38.27
304	1931	429	29.375	3221	363.99	338.15	30.84
308	1243	276	25.257	3339	280.23	273.80	23.95
312	572	127	25.543	1661	230.40	225.60	19.68
314	1012	225	30.472	1585	249.21	246.42	21.07
320	723	160	31.288	946	233.20	224.38	19.68

THERMOCOUPLE STATION : 17

AT THE AVERAGE BULK FLUID TEMPERATURE AT THE THERMOCOUPLE STATION				AVERAGE VALUES FOR THE STATION			
RUN NUMBER	REYNOLDS NUMBER	DEAN NUMBER	PRANDTL NUMBER	HEAT FLUX J/SEC-SQ.M.	HEAT TRANSFER COEFFICIENT		NUSSELT NUMBER
	RE	DE	PR	Q/A	H1	H2	NU
102	488	108	95.076	2014	293.27	288.70	13.30
104	412	91	94.072	2041	279.59	275.48	12.69
108	294	65	85.910	1991	252.68	248.68	11.56
110	205	45	75.110	2057	271.88	263.32	12.59
112	122	27	34.654	2239	220.49	211.37	11.19
120	773	172	91.604	3771	359.11	352.82	16.34
202	1964	437	3.119	3614	1060.78	932.67	20.54
204	3066	682	3.943	3375	1111.65	1007.99	22.04
206	1465	326	2.411	3798	806.49	605.48	15.24
208	2669	593	3.775	3349	1120.98	996.84	22.13
210	3640	809	4.173	3351	1215.16	1093.41	24.24
214	5415	1204	4.486	3426	2125.85	1679.91	42.73
302	2342	521	30.040	3117	312.37	298.63	26.43
304	1996	444	28.640	3235	361.68	331.45	30.69
308	1315	292	24.190	3363	270.23	261.09	23.15
312	604	134	24.492	1687	206.31	189.84	17.66
314	1041	231	29.823	1589	249.72	239.82	21.14
320	740	164	30.729	950	244.82	231.87	20.68

THERMOCOUPLE STATION : 18

AT THE AVERAGE BULK FLUID TEMPERATURE AT THE THERMOCOUPLE STATION				AVERAGE VALUES FOR THE STATION			
RUN NUMBER	REYNOLDS NUMBER	DEAN NUMBER	PRANDTL NUMBER	HEAT FLUX J/SEC-SQ.M.	HEAT TRANSFER COEFFICIENT		NUSSELT NUMBER
	RE	DE	PR	Q/A	H1	H2	NU
102	498	111	93.299	2018	296.97	290.07	13.49
104	421	93	92.242	2046	283.27	278.06	12.88
108	305	67	83.345	1998	256.01	251.73	11.74
110	216	48	71.888	2052	384.54	364.39	17.88
112	139	30	31.252	2286	240.55	230.13	12.42
120	793	176	89.592	3773	368.46	357.89	16.80
202	2062	458	2.955	3646	1060.06	928.61	20.42
204	3157	702	3.817	3390	1182.83	1070.33	23.38
206	1568	349	2.241	3912	737.12	351.69	13.84
208	2759	613	3.638	3367	1134.66	1017.64	22.32
210	3727	829	4.064	3363	1284.59	1158.53	25.56
214	5502	1224	4.408	3435	2097.19	1756.11	42.07
302	2408	535	29.405	3126	325.13	308.14	27.54
304	2067	459	27.884	3261	328.61	312.26	27.92
308	1395	310	23.119	3389	274.61	264.53	23.59
312	640	142	23.435	1727	202.48	160.06	17.38
314	1072	238	29.150	1602	242.13	234.59	20.52
320	759	168	30.147	964	215.66	208.70	18.24



## APPENDIX G

### COMPUTER PROGRAM LISTINGS



```

      DELQ(J) = QIN(J)-QLOSS(J)-QOUT(J)
      PDELQ(J) = 2.00*DELQ(J)/(QIN(J)-QLOSS(J)+QOUT(J))*100.0
      APDELQ=APDELQ+PDELQ(J)
      ABSDQ=ABSDQ+ABS(DELQ(J))
      ABSPDQ=ABSPDQ+ABS(PDELQ(J))
1    CONTINUE
      RUNNO=NRUNS
      APDELQ=APDELQ/RUNNO
      ABSDQ=ABSDQ/RUNNO
      ABSPDQ=ABSPDQ/RUNNO
      CALL REYNO(NRUNS)
      WRITE (6,200) FLUID
      WRITE(6,204)
      WRITE(6,205)
      DO 2 K=1,NRUNS
        WRITE(6,206) NOORUN(K),TFLIN(K),CTFIN(K),TFLOUT(K),CTFOUT(K),TFAVG
1(K),TCAVG(K),FLVIS(K)
2    CONTINUE
      WRITE (6,200) FLUID
      WRITE(6,207)
      WRITE(6,208)
      WRITE(6,209)
      WRITE(6,210)
      DO 3 L=1,NRUNS
        WRITE(6,211) NOORUN(L),CURENT(L),VOLTS(L),WATTS(L),FLRT(L),FLRTMA
1(L),DELT(L),QIN(L),QLOSS(L),QOUT(L),DELQ(L),PDELQ(L),NRE(L)
3    CONTINUE
      WRITE(6,212) APDELQ
      WRITE(6,213) ABSDQ
      WRITE(6,214) ABSPDQ
100  FORMAT(12,2F10.5,5A4)
101  FORMAT(13,F7.1,6F10.2)
200  FORMAT(1H1,///,5X,48HHEAT BALANCE CALCULATIONS FOR EXPERIMENTAL RU
1NS.,15X,'MOHAMMAD A. ABUL-HAMAYEL',///,5X,'FLUID : ',5A4,///)
204  FORMAT(15X,6H RUN ,5X,27HINLET FLUID TEMPERATURE, F ,5X,27HEXIT FL
1UID TEMPERATURE, F ,5X,23H AVG. FLUID TEMPERATURE,5X,15HFLUID VIS
2CUSITY)
205  FORMAT(5X,6HNUMBER,5X,12HEXPERIMENTAL,5X,10HCORRECTED ,5X,12HEXPER
1IMENTAL,5X,10HCORRECTED ,9X,1HF,13X,1HC,16X,2HCP,/)
206  FORMAT(7X,13,4(9X,F7.2),6X,F7.2,7X,F7.2,11X,F7.4)
207  FORMAT (50X,'DELTA T',34X,'DELTA Q =',10X,'RE AT')
208  FORMAT (50X,'TOUT-TIN',5X,'QIN',16X,'QUOT',5X,'QIN-QLOSS',11X,'AVG
1. ')
209  FORMAT (3X,'RUN',4X,'I',8X,'V',7X,'W',3X,'FLOW RATE OF FLUID',3X,'
1DELT',4X,'W*3.4128',3X,'QLOSS',3X,'MCPDELTA T',4X,'-QOUT',3X,'ERRO
2R',4X,'FLUID')
210  FORMAT (3X,'NO.',3X,'AMPS',4X,'VOLTS',3X,'WATTS',2X,'%READING LB/
1HR',6X,'F',7X,'BTU/HR',4X,'BTU/HR',4X,'BTU/HR',5X,'BTU/HR',5X,'% ',
26X,'TEMP.',/)
211  FORMAT (3X,13,2X,F6.1,2X,F6.1,2X,F6.1,2X,F6.1,3X,F6.2,3X,F6.2,3X,F
23.2,1X,F8.2,2X,F8.2,3X,F8.2,3X,F6.2,2X,16)
212  FORMAT(//,5X,29HAVERAGE PERCENT DIFFERENCE = ,F6.2,3H %.)
213  FORMAT(/,5X,28HAVERAGE ABSOLUTE DEVIATION =,F10.3,8H BTU/HR.)
214  FORMAT(/,5X,36HAVERAGE ABSOLUTE PERCENT DEVIATION =,F6.2,3H %.)

```

STOP  
END

SUBROUTINE REYN0(NRUNS)

```

COMMON/FLDPRP/TFAVG(30),TCAVG(30),FLRTMA(30),NRE(30),FLVIS(30),NOO
LRUN(30)
DO 1 J=1,NRUNS
  IF (NOORUN(J).GT.300) GO TO 4
  IF (NOORUN(J).GT.200) GO TO 2
  FLVIS(J) = EXP(3.80666-1.79809*((TFAVG(J)-40.)/60.))+0.38590*((TFA
  LVG(J)-40.)/60.)**2)-0.05878*((TFAVG(J)-40.)/60.)**3)+0.004173*((
  2TFAVG(J)-40.)/60.)**4))
  GO TO 3
2 CONTINUE
  RHSVR=((1.3272*(20.0-TCAVG(J)))-(0.001053*(TCAVG(J)-20.0)*(TCAVG(J
  )-20.0)))/(TCAVG(J)+105.0)
  RHSLN=2.303*RHSVR
  FLVIS(J)=1.002*EXP(RHSLN)
  GO TO 3
4 CONTINUE
  FLVIS(J) = EXP(-6.92545+(2.3839E+03/(TCAVG(J)+273.15))-(1.08564E+0
  14/((TCAVG(J)+273.15)**2)))
3 CONTINUE
  FVFPS=2.42*FLVIS(J)
  DMLSRE=((0.495/12.0)*FLRTMA(J))/((3.1416/4.0)*(0.495*0.495/144.0)*
  1FVFPS)
  NRE(J)=DMLSRE
1 CONTINUE
RETURN
END

```

```

C
C *****
C
C COMPUTER PROGRAM: MAH#02
C
C PROGRAM TO COMPUTE THE INSIDE WALL TEMPERATURE FROM THE EXPERIMENTALLY
C MEASURED OUTSIDE WALL TEMPERATURES FOR HEAT TRANSFER STUDIES IN
C HELICALLY COILED TUBES WITH LAMINAR FLOW.
C BY MUHAMMAD A. ABUL-HAMAYEL
C
C *****
C
C DIMENSION T(18,4),TOS(4),TIS(4),CON(18,4),RESTI(18,4),RESTA(18,4),
C LAMPS(18,4),DEPTH(18,4),CPDIS(18,4),CRDIS(18,4),PARFA(18,4),RAREA(1
C 8,4),A(4),XAREA(18,4),QFLUX(4),TCASP(18,4),UNCT(1,4),TEMPER(18,4),
C JUNCORT(18,4)
C COMMON/CORDAT/UNCT,TCASP,T
C DO 2 I = 1,18
C READ(5,101)(TCASP(I,J),J=1,4)
C CONTINUE
10 READ(5,100)NRUN,NMO,NDAY,NYEAR,NSLI,TAMPS,VOLTS,TROOM
C IF(NRUN.EQ.0) GO TO 7
C WRITE(7,300)NRUN,NMO,NDAY,NYEAR,NSLI,TAMPS,VOLTS
C CPOWER=0.0
C DO 27 K=1,18
C NSTA=K
C TCK1=0.0
C CALL GEOM(DEPTH,CPDIS,CRDIS,PARFA,RAREA,A,XAREA,NRUN,NSTA,NSLI)
C READ(5,103)(UNCT(1,J),J=1,4)
C CALL TEMCOR(K,NRUN,TRCOM)
C DO 3 J = 1,4
C JUNCORT(K,J)=UNCT(1,J)
C CONTINUE
C DO 15 J = 1,4
C DO 14 I=1,NSLI
C T(I,J)=T(1,J)
14 CONTINUE
C TOS(J)=T(1,J)
C TEMPER(K,J)=TOS(J)
15 CONTINUE
16 CALL KCON(T,CON,NSLI)
C CALL ERESTI(T,RESTI,NSLI)
C SRINV=0.0
C DO 17 I=1,NSLI
C DO 17 J = 1,4
C RESTA(I,J)=RESTI(I,J)*DEPTH(I,J)/XAREA(I,J)
C SRINV=SRINV+1.0/RESTA(I,J)
17 CONTINUE
C TOTR=1.0/SRINV
C DO 18 I=1,NSLI
C DO 18 J = 1,4
C AMPS(I,J)=TAMPS*TOTR/RESTA(I,J)
18 CONTINUE

```

```

NSLI L=NSLI-1
DO 21 I=1,NSLI L
DO 21 J=1,4
INEG=I-1
IPUS=I+1
JNEG=J-1
JPOS=J+1
IF(JNEG.EQ.0)JNEG=4
IF(JPOS.EQ.5)JPOS=1
TERM1=(PAREA(I,J)/RAREA(IPOS,J))*(CRDIS(IPOS,J)/CPDIS(I,J))*((CON(
I,J)+CON(I,JNEG))/(CON(I,J)+CON(IPOS,J)))*(T(I,J)-T(I,JNEG))
TERM2=(PAREA(I,JPOS)/RAREA(IPOS,J))*(CRDIS(IPOS,J)/CPDIS(I,JPOS))*
((CON(I,J)+CON(I,JPOS))/(CON(I,J)+CON(IPOS,J)))*(T(I,J)-T(I,JPOS))
TERM4=T(I,J)
TERM5=2.0*CRDIS(IPOS,J)*(DEPTH(I,J)/(XAREA(I,J)*RAREA(IPOS,J)))*3.
+128*RESTI(I,J)*AMPS(I,J)*AMPS(I,J)/(CON(I,J)+CON(IPOS,J))
IF(INEG.GT.0)GO TO 19
TERM3=-525.76*RAREA(I,J)*CRDIS(IPOS,J)*(TOS(J)-TROOM)/(298.50*RAR
EA(IPOS,J)*(CON(I,J)+CON(IPOS,J)))
GO TO 20
19 TERM3=(PAREA(I,J)/RAREA(IPOS,J))*(CRDIS(IPOS,J)/CRDIS(I,J))*((CON(
I,J)+CON(INEG,J))/(CON(I,J)+CON(IPOS,J)))*(T(I,J)-T(INEG,J))
20 T(IPOS,J)=TERM1+TERM2+TERM3+TERM4-TERM5
21 CONTINUE
TCK2=T(10,3)
IF(ABS(TCK1-TCK2).LT.0.01) GO TO 23
TCK1=TCK2
DO 22 J=1,4
T(1,J)=(2.0/3.0)*(TOS(J)+0.5*T(2,J))
22 CONTINUE
GO TO 16
23 DO 24 J=1,4
TIS(J)=T(10,J)-0.5*(T(9,J)-T(10,J))
24 CONTINUE
TPOWER=0.0
DO 25 I=1,NSLI
DO 25 J=1,4
TPOWER=TPOWER+RESTA(I,J)*AMPS(I,J)*AMPS(I,J)
25 CONTINUE
CPOWER=CPOWER+TPOWER
WRITE(6,200)
WRITE(6,201)NRUN,NMO,NDAY,NYEAR
WRITE(6,202)INSTA
WRITE(6,203)TAMPS
WRITE(6,204)TPOWER
WRITE(6,205)
I=0
WRITE(6,206)I,(TOS(J),J=1,4)
WRITE(6,207)
DO 26 I=1,NSLI
WRITE(6,206)I,(T(I,J),J=1,4)
26 CONTINUE
WRITE(6,207)
I=11

```

```

WRITE(6,206)I,(TIS(J),J=1,4)
WRITE(7,301)(TIS(J),J=1,4)
CALL FLUXIT,CON,RESTA,AMPS,CPDIS,CRDIS,PAREA,RAREA,A,QFLUX)
WRITE(6,207)
WRITE(6,208)(J,QFLUX(J),J=1,4)
WRITE(7,301)(QFLUX(J),J=1,4)

C
C IF A PLOT OF T(INSIDE) & T(OUTSIDE) ARE NEEDED, ALL WHAT SHOULD
C BE DONE IS TO TAKE THE C OUT FROM THE NEXT CARD.
C CALL PLOT(TOS,TIS,NRUN,NMO,NDAY,NYEAR,NSTA)
27 CONTINUE
POWER=TAMPS*VOLTS
WRITE(6,209)NRUN,CPOWER
WRITE(6,210)NRUN,POWER
WRITE(6,211)
DO 6 I=1,18
WRITE(6,212)(UNCORT(I,J),J=1,4)
6 CONTINUE
WRITE(6,214)
DO 8 I=1,18
WRITE(6,212)(TEMPER(I,J),J=1,4)
8 CONTINUE
GO TO 10
100 FORMAT(5I5,3F10.2)
101 FORMAT(4F10.5)
103 FORMAT(4F10.1)
200 FORMAT(1H1,'CALCULATION OF INSIDE TEMPERATURES',4X,'M.ABUL-HAMAYEL
1')
201 FORMAT(1X,12HRUN NUMBER =,I4,I10,1H/,I3,1H/,I3)
202 FORMAT(1X,16HSTATION NUMBER =,I3)
203 FORMAT(1X,17HCURRENT IN COIL =,F6.1,5H AMPS)
204 FORMAT(1X,39HTOTAL POWER GENERATED IN THIS SEGMENT =,F8.2,6H WATTS
1/)
205 FORMAT(3X,1H1,5X,1H0,8X,2H90,7X,3H180,6X,3H270,/)
206 FORMAT(1X,I3,4F9.2)
207 FORMAT(1H )
208 FORMAT(1X,6HQFLUX(I,I1,3H) =,E14.7,27H BTU PER SQUARE FOOT PER HR)
209 FORMAT(1H1,35HCALCULATED POWER GENERATION FOR RUN,I4,2H =,F9.2,6H
1WATTS/)
210 FORMAT(1X,31HACTUAL POWER GENERATION FOR RUN,I4,2H =,F9.2,6H WATTS
1)
300 FORMAT(5I5,2E20.7)
301 FORMAT(4E20.7)
211 FORMAT(/////,5X,57HTEMPERATURE RECORDED BY THE THERMOCOUPLES ON TH
1E COIL, F.,//)
212 FORMAT(5X,4(F10.2,14X))
214 FORMAT(/////,5X,87HCORRECTED OUTSIDE SURFACE TEMPERATURES AS RECORD
1ED BY THE THERMOCOUPLES ON THE COIL, F.,//)
7 STOP
END

```

```

SUBROUTINE GEOM(DEPTH,CPDIS,CRDIS,PAREA,RAREA,A,XAREA,NRUN,NSTA,NS
  L1)
C
  DIMENSION DEPTH(18,4),CPDIS(18,4),CRDIS(18,4),PAREA(18,4),RAREA(18
  L,4),A(4),XAREA(18,4),S(91)
  SLIN=NSLI
  DELM=0.0054167
  RM=0.023333
  DELPHI=2.0*3.1416/360.0
  S(1)=1.0
  S(91)=1.0
  DO 10 K=1,45
    S(2*K)=4.0
  10 CONTINUE
  DO 11 K=2,45
    S(2*K-1)=2.0
  11 CONTINUE
  K=0.416667
  IF (NSTA.EQ.01) THETA = 0.7
  IF (NSTA.EQ.02) THETA = 0.6
  IF (NSTA.EQ.03) THETA = 0.9
  IF (NSTA.EQ.04) THETA = 1.2
  IF (NSTA.EQ.05) THETA = 1.2
  IF (NSTA.EQ.06) THETA = 1.2
  IF (NSTA.EQ.07) THETA = 1.4
  IF (NSTA.EQ.08) THETA = 1.8
  IF (NSTA.EQ.09) THETA = 2.0
  IF (NSTA.EQ.10) THETA = 2.15
  IF (NSTA.EQ.11) THETA = 4.3
  IF (NSTA.EQ.12) THETA = 6.25
  IF (NSTA.EQ.13) THETA = 6.3
  IF (NSTA.EQ.14) THETA = 6.4
  IF (NSTA.EQ.15) THETA = 6.4
  IF (NSTA.EQ.16) THETA = 6.2
  IF (NSTA.EQ.17) THETA = 6.2
  IF (NSTA.EQ.18) THETA = 4.5
  C1=DELM*R/SLIN
  DO 15 I=1,NSLI
    DO 15 J=1,4
      XI=I
      XJ=J
      C2=(SLIN-2.0*XI+1.0)/2.0
      PHIL=(2.0*XJ-3.0)*3.1416/4.0
      CSIN1=SIN((XJ-1.0)*3.1416/2.0)
      CSIN2=SIN(PHIL)
C    CALCULATION OF D SUB Z
      DEPTH(I,J)=(R-RM*CSIN1-(DELM/2.0)*((SLIN-2.0*XI+1.0)/SLIN)*(R*CSIN
      L1/(R-RM*CSIN1)))*THETA
C    CALCULATION OF D SUB PHI
      CPDIS(I,J)=(3.1416/2.0)*(RM+(DELM/2.0)*((SLIN-2.0*XI+1.0)/SLIN)*(R
      L1/(R-RM*CSIN2)))
C    CALCULATION OF D SUB R
      CRDIS(I,J)=(DELM/SLIN)*(R/(R-RM*CSIN1))

```



```

C      CALCULATION OF A SUB PHI
C      NOTE THAT THE FOLLOWING STATEMENT IS DIFFERENT FROM WHAT SINGH OR
C      GRAIN HAVE IN THEIR PROGRAMS.
C      PAREA(I,J)=(DELM*THETA/SLIN)*(R/(R-RM*CSIN2))*(R-RM*CSIN2-(DELM/2.
1J)*((SLIN-2.0*XI)/SLIN)*(R*CSIN2/(R-RM*CSIN2)))
C      CALCULATION OF A SUB R
C      MAKEA(I,J)=(3.1416*THETA/2.0)*(R-RM*CSIN1-(DELM/2.0)*((SLIN-2.0*XI
1+2.0)/SLIN)*(R*CSIN1/(R-RM*CSIN1)))*(RM+(DELM/2.0)*((SLIN-2.0*XI+2
2.0)/SLIN)*(R/(R-RM*CSIN1)))
C      A(I,J)=(3.1416*THETA/2.0)*(R-RM*CSIN1-(DELM/2.0)*((SLIN-2.0)/SLIN)*
1(R*CSIN1/(R-RM*CSIN1)))*(RM+(DELM/2.0)*((SLIN-2.0)/SLIN)*(R/(R-RM
2*CSIN1)))
C      CALCULATION OF A SUB Z
C      AM1=0.0
C      AM2=0.0
C      DO 14 K=1,91
C      XK=X
C      PHI=PHI+(XK-1.0)*DELPHI
C      Y=R-RM*SIN(PHI)
C      AM1=AM1+S(K)*1.0/Y
C      AM2=AM2+S(K)*1.0/(Y*Y)
14  CONTINUE
C      AM1=(DELPHI/3.0)*AM1
C      AM2=(DELPHI/3.0)*AM2
C      XAREA(I,J)=RM*C1*AM1+C2*C1*C1*AM2
15  CONTINUE
C      RETURN
C      END

SUBROUTINE TEMCOR(K,NRUN,TROOM)
C      DIMENSION UNCT(1,4),TCASP(18,4),T(18,4),TCOR(1,4)
C      COMMON/CORDAT/UNCT,TCASP,T
C      STEAMT=211.4
C      ROOMT=81.2
C      DO 3 J=1,4
C      TCOR(1,J)=TCASP(K,J)*((UNCT(1,J)-TROOM)/(STEAMT-ROOMT))
C      T(1,J)=UNCT(1,J)+TCOR(1,J)
3  CONTINUE
C      RETURN
C      END

```

```

C      SUBROUTINE KCON(T,CON,NSLI)
      DIMENSION T(18,4),CON(18,4)
      DO 10 I=1,NSLI
      DO 10 J=1,4
      CON(I,J)=7.8034+0.51691E-02*T(I,J)-0.88501E-06*T(I,J)*T(I,J)
10    CONTINUE
      RETURN
      END

C      SUBROUTINE ERESTI(T,RESTI,NSLI)
      DIMENSION T(18,4),RESTI(18,4)
      DO 10 I=1,NSLI
      DO 10 J=1,4
      RESTI(I,J)=0.21675E-05+0.11492E-08*T(I,J)+0.70965E-12*T(I,J)*T(I,J)
      -0.84327E-17*T(I,J)*T(I,J)*T(I,J)
10    CONTINUE
      RETURN
      END

C      SUBROUTINE FLUX(T,CON,RESTA,AMPS,CPDIS,CRDIS,PAREA,RAREA,A,QFLUX)
      DIMENSION T(18,4),CON(18,4),RESTA(18,4),AMPS(18,4),CPDIS(18,4),CRD
      LIS(18,4),PAREA(18,4),RAREA(18,4),A(4),QFLUX(4),QT(4),QL(4),QR(4),Q
      ZB(4)
      DO 10 J=1,4
      JNEG=J-1
      JPOS=J+1
      IF(JPOS.EQ.5)JPOS=1
      IF(JNEG.EQ.0)JNEG=4
      QT(J)=((CON(10,J)+CON(9,J))/2.0)*(RAREA(10,J)/CRDIS(10,J))*T(9,J)
      -T(10,J)
      QL(J)=((CON(10,J)+CON(10,JNEG))/2.0)*(PAREA(10,J)/CPDIS(10,J))*T(
      10,JNEG)-T(10,J)
      QR(J)=((CON(10,J)+CON(10,JPOS))/2.0)*(PAREA(10,JPOS)/CPDIS(10,JPOS
      ))*T(10,JPOS)-T(10,J)
      QB(J)=-QT(J)-QL(J)-QR(J)-3.4128*RESTA(10,J)*AMPS(10,J)*AMPS(10,J)
      QFLUX(J)=-QB(J)/A(J)
10    CONTINUE
      RETURN
      END

```

```

SUBROUTINE PLOT(TOS,TIS,NRUN,NMO,NDAY,NYEAR,NSTA)
C
  DIMENSION TOS(4),TIS(4),TPLOT(2,4),GRAPH(4,51),SYMBOL(3),ORD(51)
  DATA SYMBOL/1H0,1H1,1H /
  DATA ASTER/1H*/
  DO 10 J=1,4
    TPLOT(1,J)=TOS(J)
    TPLOT(2,J)=TIS(J)
10  CONTINUE
  DO 11 I=1,4
    DO 11 J=1,51
      GRAPH(I,J)=SYMBOL(3)
11  CONTINUE
  TMAX=TPLOT(1,1)
  TMIN=TPLOT(1,1)
  DO 12 I=1,2
    DO 12 J=1,4
      IF(TMAX.LT.TPLOT(I,J))TMAX=TPLOT(I,J)
      IF(TMIN.GT.TPLOT(I,J))TMIN=TPLOT(I,J)
12  CONTINUE
  ITEMP=TMIN/5.0
  TMIN=5*ITEMP
  DIFF=TMAX-TMIN
  DEL=0.01
  IF(DIFF.GT.0.5)DEL=0.05
  IF(DIFF.GT.2.5)DEL=0.1
  IF(DIFF.GT.5.0)DEL=0.2
  IF(DIFF.GT.10.0)DEL=0.4
  IF(DIFF.GT.20.0)DEL=0.6
  IF(DIFF.GT.30.0)DEL=0.8
  IF(DIFF.GT.40.0)DEL=1.0
  IF(DIFF.GT.50.0)DEL=2.0
  IF(DIFF.GT.100.0)DEL=3.0
  IF(DIFF.GT.150.0)DEL=4.0
  IF(DIFF.GT.200.0)DEL=5.0
  IF(DIFF.GT.250.0)DEL=6.0
  IF(DIFF.GT.300.0)DEL=7.0
  IF(DIFF.GT.350.0)DEL=8.0
  IF(DIFF.GT.400.0)DEL=9.0
  IF(DIFF.GT.450.0)DEL=10.0
  IF(DIFF.GT.500.0)DEL=20.0
  IF(DIFF.GT.1000.0)DEL=40.0
  DO 13 I=1,2
    DO 13 J=1,4
      L=(TPLOT(I,J)-TMIN)/DEL+0.5
      L=51-L
13  GRAPH(J,L)=SYMBOL(1)
  DO 14 I=1,51
    OKD(I)=SYMBOL(3)
14  CONTINUE
  DO 15 I=1,51,5
    ORD(I)=ASTER
15  CONTINUE

```

```

WRITE(6,200)NRUN,NMO,NDAY,NYEAR,NSTA
DO 16 I=1,51
WRITE(6,201)ORD(I),(GRAPH(J,I),J=1,4)
16 CONTINUE
WRITE(6,201)SYMBOL(3),(ASTER,I=1,8)
WRITE(6,202)TMIN
WRITE(6,203)TMAX
WRITE(6,204)DEL
200 FORMAT(1H1,12HRUN NUMBER =,I4,110,1H/,I3,1H/,I3,5X,16HSTATION NUMB
IER =,I3//)
201 FORMAT(17(4X,1A1))
202 FORMAT(//1X,23HBASE LINE TEMPERATURE =,F7.2)
203 FORMAT(1X,21HMAXIMUM TEMPERATURE =,F7.2)
204 FORMAT(1X,23HTEMPERATURE INCREMENT =,F6.2)
RETURN
END

```

```

C
C *****
C
C COMPUTER PROGRAM: MAH#03
C
C PROGRAM TO COMPUTE:
C 1. HEAT TRANSFER COEFFICIENTS
C 2. PERTINENT FLUID FLOW AND HEAT TRANSFER DIMENSIONLESS NUMBERS, AND
C 3. DIMENSIONLESS WALL TEMPERATURES AND AXIAL DISTANCES ALONG THE
C HELICAL COIL FOR HEAT TRANSFER STUDIES IN HELICALLY COILED TUBES
C WITH LAMINAR FLOW. BY MOHAMMAD A. ABUL-HAMAYEL
C
C *****
C
C *** NOTE:1. FLUID PROPERTIES ARE EVALUATED AT THE AVERAGE LOCAL FILM
C TEMPERATURE(=T(F,L)) AT EACH THERMOCOUPLE STATION.
C 2. T(F,L)=(T(WALL)+T(BULK FLUID))/2.0.
C 3. LOCAL H(AVG.)=(1/N)E((Q/A)/(T(WALL)-T(BULK FLUID))).
C
C DIMENSION QFLUX(8),TIS(8),TFLOC(8),HTC(8),AVTEMP(8);DAXDIS(18),DWT
C LEMP(18,8),QFLSI(4),TISSI(4),TFLSI(4),AVTESI(4),HTCSI(4)
C COMMON/DLSNOS/NRE,ABYR,NDE,PRANTL,PRFLNU(8),NRUN
C 1 READ(5,100) NRUN,NMO,NDAY,NYEAR,NSLI,TAMPS,VOLTS
C IF (NRUN.EQ.0) GO TO 15
C READ(5,101) FLRTHA,TFLIN,TFLOUT
C NOTE THAT TFLIN AND TFLOUT ARE ALREADY CORRECTED, AND ARE TAKEN
C FROM THE OUTPUT OF MAH#01 PROGRAM.
C TUBERA=0.495/(2.0*12.0)
C COILRA=10.0/(2.0*12.0)
C ABYR=TUBERA/COILRA
C HTL = 298.5/12.
C TINC1=(TFLOUT-TFLIN)/HTL
C CALCULATION OF DT SUB B/DZ
C TINC2=TINC1*TUBERA
C DO 7 I=1,18
C NSTA=I
C IF (I.EQ.01) TCDIS = 2./12.
C IF (I.EQ.02) TCDIS = 5./12.
C IF (I.EQ.03) TCDIS = 8./12.
C IF (I.EQ.04) TCDIS = 14./12.
C IF (I.EQ.05) TCDIS = 20./12.
C IF (I.EQ.06) TCDIS = 26./12.
C IF (I.EQ.07) TCDIS = 32./12.
C IF (I.EQ.08) TCDIS = 40./12.
C IF (I.EQ.09) TCDIS = 50./12.
C IF (I.EQ.10) TCDIS = 60./12.
C IF (I.EQ.11) TCDIS = 71.5/12.
C IF (I.EQ.12) TCDIS = 103./12.
C IF (I.EQ.13) TCDIS = 134./12.
C IF (I.EQ.14) TCDIS = 166./12.
C IF (I.EQ.15) TCDIS = 198./12.
C IF (I.EQ.16) TCDIS = 230./12.
C IF (I.EQ.17) TCDIS = 260./12.

```

```

IF (I.EQ.18) TCOIS = 292./12.
TAXOIS(1)=TCOIS/TURERA
TEFLU=TFLIN+(TINC1*TCOIS)
READ(5,102)(TIS(J),J=1,4)
READ(5,102)(QFLUX(J),J=1,4)
AVHTC=0.0
CAWT=0.0
DO 6 J=1,4
  TFLJC(J)=TEFLU
  HTC(J)=QFLUX(J)/(TIS(J)-TEFLU)
C   CALCULATION OF T-SUB-W
  UWTEMP(I,J)=(TIS(J)-TFLIN)/TINC2
  AVTEMP(J)=(TIS(J)+TFLOC(J))/2.0
  AVGTEM=AVTEMP(J)
  HTCDEF=HTC(J)
  CALL NUSELECT(AVGTEM,HTCOEF,PNSELT)
  PFLNU(J)=PNSELT
  AVHTC=AVHTC+HTC(J)
  CAWT=CAWT+TIS(J)
6  CONTINUE
  AVHTC=AVHTC/4.0
  CAWT=CAWT/4.0
  FILMT=(CAWT+TEFLU)/2.0
  CALL REPRDE(FLRTMA,FILMT)
  CALL NUSELECT(FILMT,AVHTC,PNSELT)
  CANUNO=PNSELT
C   THE FOLLOWING STATEMENTS ARE MAINLY FOR
C   CONVERTING TO THE SI UNITS.
  FILSI = (FILMT-32.)*5./9.+273.15
  CFBJ = 1055.056/(3600.*9.290304E-02)
  AVHTSI = AVHTC*CFBJ*1.8
  DO 500 J=1,4
    QFLSI(J) = CFBJ*QFLUX(J)
    HTC(SI(J) = HTC(J)*CFBJ*1.8
    TISSI(J) = (TIS(J)-32.)*5./9.+273.15
    TFLSI(J) = (TFLOC(J)-32.)*5./9.+273.15
    AVTESI(J) = (AVTEMP(J)-32.)*5./9.+273.15
500 CONTINUE
C   END OF CONVERTING THE UNITS
  WRITE(6,200)
  WRITE(6,201)NRUN,NMO,NDAY,NYEAR
  WRITE(6,202)INSTA
  WRITE(6,203)TAMPS,VOLTS
  WRITE(6,204)
  WRITE(6,205)(QFLUX(J),J=1,4)
  WRITE (6,502)(QFLSI(J),J=1,4)
  WRITE(6,206)(TIS(J),J=1,4)
  WRITE (6,506)(TISSI(J),J=1,4)
  WRITE(6,207)
  WRITE(6,208)(TFLOC(J),J=1,4)
  WRITE (6,508)(TFLSI(J),J=1,4)
  WRITE(6,209)(HTC(J),J=1,4)
  WRITE (6,509)(HTCSI(J),J=1,4)
  WRITE(6,216)(AVTEMP(J),J=1,4)

```

```

WRITE(6,516)(AVTEST(J),J=1,4)
WRITE(6,217)(PRFLNU(J),J=1,4)
WRITE(6,218) FILMT,FILSI
WRITE(6,219) NRE
WRITE(6,220) PRANTL
WRITE(6,221) NOE
WRITE(6,222) CANUND
WRITE(6,223) AVHTC,AVHTSI

C
C IF A PLOT OF HT IS NEEDED, ALL WHAT HAS TO BE
C DONE IS TO REMOVE THE C OUT OF THE NEXT CARD.
C CALL PLOT(NMO,NDAY,NYEAR,NSTAI)
7 CONTINUE
WRITE(6,213)
WRITE(6,214)
DO 8 K=1,18
WRITE(6,215)(DAXDIS(K),(DWTEMP(K,J),J=1,4)
8 CONTINUE
TEFLU=(TFLIN+TFLOUT)/2.0
CALL RFPKDE(FLRTMA,TEFLU)
CALL SKETCH(DWTEMP,NMO,NDAY,NYEAR)
DO 10 1
100 FORMAT(5I5,2E20.7)
101 FORMAT(3F17.2)
102 FORMAT(4F20.7)
200 FORMAT(1H1,2X,63H CALCULATION OF HEAT TRANSFER COEFFECIENTS IN A HE
      LICAL COIL BY , 'MOHAMMAD A. ABUL-HAMAYEL')
201 FORMAT(2X,12H RUN NUMBER =,I4,110,1H-,I2,1H-,I2)
202 FORMAT(2X,16H STATION NUMBER =,I3)
203 FORMAT(2X,17H CURRENT IN COIL =,F6.1,5H AMPS,10X,26H VOLTAGE DROP AC
      CROSS COIL =,F7.2,6H VOLTS)
204 FORMAT(//,2X,20H PERIPHERAL LOCATION ,14X,10H 1 ,2X,10H 2
      1 ,2X,10H 3 ,2X,10H 4 ,/2X,30H DEGREES CLOCKWISE F
      ROM NORTH ,4X,10H 0 ,2X,10H 90 ,2X,10H 180 ,2X,
      10H 270 ,//)
205 FORMAT(2X,30H HEAT FLUX, Q , BTU/HR-SQ.FT. =,2X,4(F10.3,2X))
206 FORMAT(//,2X,30H INSIDE WALL TEMPERATURE,TW, F=,2X,4(F10.3,2X))
207 FORMAT(//,2X,52H FOR FLUID TEMPERATURES MEASURED BY THE THERMOCOUP
      LES)
208 FORMAT(//,2X,30H LOCAL FLUID TEMPERATURE,TF, F=,2X,4(F10.3,2X))
209 FORMAT(//,2X,30H H(LOCAL), BTU/HR-SQ.FT.-F =,2X,4(F10.3,2X))
214 FORMAT(2X,14H DIMENSIONLESS ,07X,58H DIMENSIONLESS WALL TEMPERATURE,
      11/(WALL)-T(INLET))/(DTB/DZ),/2X,14H AXIAL DISTANCE,5X,10H 1
      2,2X,10H 2 ,2X,10H 3 ,2X,10H 4 ,/8X,1HZ,12X,10
      H 0 ,2X,10H 90 ,2X,10H 180 ,2X,10H 270 ,//)
215 FORMAT(2X,F10.3,7X,4(F10.3,2X))
216 FORMAT(//,2X,30H AVG. LOCAL TEMP.,(TF+TW)/2, F=,2X,4(F10.3,2X))
217 FORMAT(//,2X,30H PERIPHERAL NUSSELT NUMBER, NU=,2X,4(F10.3,2X))
218 FORMAT(//,2X,61H AT THE LOCAL (CIRCUMFERENTIALLY AVERAGED) FILM TEM
      PERATURE OF,F10.3,8H F , OR ,F10.3,4H K :)
219 FORMAT(//,2X,23H REYNOLDS NUMBER = RE = ,I7)
220 FORMAT(//,2X,23H PRANDTL NUMBER = PR = ,F7.2)
221 FORMAT(//,2X,23H DEAN NUMBER = DE = ,I7)
222 FORMAT(//,2X,23H NUSSELT NUMBER = NU = ,F10.3)

```

```

223 FORMAT(/,2X,35HAVERAGE HILOCAL) FOR THIS STATION =,F10.3,16H BTU/
    1HK-SQ.FT.-F,/,36X,1H=,F10.3,14H J/SEC-SQ.M.-K)
215 FORMAT(1H1,2X,90HDIMENSIONLESS AXIAL DISTANCE AND WALL TEMPERATURE
    1 VALUES FOR VARIOUS PERIPHERAL LOCATIONS.,//)
502 FORMAT (/,2X,30HHEAT FLUX, Q , J/SEC-SQ.M. =,2X,4(F10.3,2X))
506 FORMAT(/,2X,30HINSIDE WALL TEMPERATURE,TW, K=,2X,4(F10.3,2X))
508 FORMAT(/,2X,30HLOCAL FLUID TEMPERATURE,TF, K=,2X,4(F10.3,2X))
509 FORMAT(/,2X,30HH(LOCAL), J/SEC-SQ.M.-K =,2X,4(F10.3,2X))
516 FORMAT(/,2X,30HAVG. LOCAL TEMP., (TF+TW)/2, K=,2X,4(F10.3,2X))
15 STOP
END

```

SUBROUTINE KCPROF(FLRTMA,TEFLU)

L

```

COMMON/DLSNUS/NRE,ABYR,NDE,PRANTL,PRFLNU(8),NRUN
TEMPC=((TEFLU-32.0)*5.0)/9.0
IF (NRUN.GT.300) GO TO 3
IF (NRUN.GT.200) GO TO 1
FLVIS = EXP(3.80666-1.79809*((TEFLU-40.)/60.))+0.38590*(((TEFLU-40.
1)/60.))**2)-0.05878*(((TEFLU-40.)/60.))**3)+0.004173*(((TEFLU-40.)/6
20.))**4))
CPFLU = 0.553+0.0415*((TEFLU-60.)/80.)+0.0035*(((TEFLU-60.)/80.))**
12)
TCFLU = 0.1825-(2.3E-04*TEFLU)
GO TO 2
1 CONTINUE
RHSVR=(((1.3272*(20.0-TEMPC))-(0.001053*(TEMPC-20.0)*(TEMPC-20.0)))
1/(TEMPC+105.0)
RHSLN=2.303*RHSVR
FLVIS=1.002*EXP(RHSLN)
CPFLU=1.01881-0.4802E-03*TEFLU+0.3274E-05*TEFLU*TEFLU-0.604E-08*TE
1FLU*TEFLU*TEFLU
TCFLU=0.30289+0.7029E-03*TEFLU-0.1178E-05*TEFLU*TEFLU-0.550E-09*TE
1FLU*TEFLU*TEFLU
GO TO 2
3 CONTINUE
FLVIS = EXP(-6.92545+(2.3839E+03/(TEMPC+273.15))-(1.08564E+04/((TF
1MPC+273.15)**2)))
CPFLU = 0.53+0.16101E-02*(TEFLU-50.)-0.167946E-05*(((TEFLU-50.))**2)
1+0.783422E-08*(((TEFLU-50.))**3)
TCFLU = 0.09307-0.846193E-04*TEFLU+0.158015E-06*TEFLU*TEFLU
2 CONTINUE
FVFPS=2.42*FLVIS
DENJ=(((0.495/12.0)*FLRTMA)/((3.1416/4.0)*(0.495*0.495/144.0)*FVFPS
1)
NRC=RENU
PRANTL=(CPFLU*FVFPS)/TCFLU
DENJ=RENU*(SQRT(ABYR))
NDE=DENJ
RETURN
END

```



```

C      SUBROUTINE NUSELT(AVGTEM,HTC,PNSELT)
COMMON/DLSNOS/NRE,ABYR,NDE,PRANTL,PRFLNU(8),NRUN
CAVST=((AVGTEM-32.0)*5.0)/9.0
IF (NRUN.GT.300) GO TO 3
IF (NRUN.GT.200) GO TO 1
TCFLU = 0.1825-(2.3E-04*AVGTEM)
GO TO 2
1 CONTINUE
TCFLU=0.30289+0.7029E-03*AVGTEM-0.1178E-05*AVGTEM*AVGTEM-0.550E-09
1*AVGTEM*AVGTEM*AVGTEM
GO TO 2
2 CONTINUE
TCFLU = 0.09307-0.846193E-04*AVGTEM+0.158015E-06*AVGTEM*AVGTEM
3 CONTINUE
PNSELT=(HTC*(0.495/12.0))/TCFLU
RETURN
END

```

```

C      SUBROUTINE SKETCH(DWTEMP,NMO,NDAY,NYEAR)
DIMENSION DWTEMP(18,8),DWTP(18,8),GRAPH(18,51),SYMBOL(9),ORD(51)
COMMON/DLSNOS/NRE,ABYR,NDE,PRANTL,PRFLNU(8),NRUN
DATA SYMBOL/1H1,1H2,1H3,1H4,1H5,1H6,1H7,1H8,1H /
DATA ASTER/1H*/
DO 1 J=1,4
DO 1 I=1,18
DWTP(I,J)=DWTEMP(I,J)
1 CONTINUE
DO 2 I=1,18
DO 2 J=1,51
GRAPH(I,J)=SYMBOL(9)
2 CONTINUE
DTMAX=DWTP(1,1)
DTMIN=0.0
DO 3 J=1,4
DO 3 I=1,18
IF(DTMAX.LT.DWTP(I,J))DTMAX=DWTP(I,J)
3 CONTINUE
DIFF=DTMAX-DTMIN
DEL=0.2
IF(DIFF.GT.10.0)DEL=0.5
IF(DIFF.GT.25.0)DEL=1.0
IF(DIFF.GT.50.0)DEL=2.0
IF(DIFF.GT.100.0)DEL=5.0
IF(DIFF.GT.250.0)DEL=10.0
IF(DIFF.GT.500.0)DEL=20.0
IF(DIFF.GT.1000.0)DEL=30.0
IF(DIFF.GT.1500.0)DEL=50.0
IF(DIFF.GT.2500.0)DEL=75.0

```

```

IF(J)IFF.GT.3500.0)DEL=100.0
IF(J)IFF.GT.5000.0)DEL=150.0
IF(J)IFF.GT.7500.0)DEL=200.0
IF(J)IFF.GT.10000.0)DEL=500.0
DO 4 J=1,4
DO 4 I=1,18
L=(JWTP(I,J)-DTMIN)/DEL+0.5
L=51-L
4 GRAPH(I,L)=SYMBOL(J)
DO 5 K=1,51
ORD(K)=SYMBOL(9)
5 CONTINUE
DO 6 K=1,51,5
JRU(K)=ASTER
6 CONTINUE
WRITE(6,200)NRUN,NMO,NDAY,NYEAR
DO 11 J=1,51
WRITE(6,201)ORD(J),(GRAPH(I,J),I=1,18)
11 CONTINUE
WRITE(6,211)SYMBOL(9),(ASTER,I=1,120,5)
WRITE(6,206)
WRITE(6,212)
WRITE(6,207)DTMIN,DTMAX
WRITE(6,208)DEL,NRE,ABYR,PRANTL,NDE
200 FURMAT(1H1,2X,12H RUN NUMBER =,I4,1I10,1H-,I2,1H-,I2,/)
201 FURMAT(2X,4(1A1),2X,1A1,1X,1A1,2X,1A1,1X,1A1,2X,1A1,3X,1A1,3X,1A1
1,4X,1A1,12X,1A1,11X,1A1,12X,1A1,12X,1A1,12X,1A1,11X,1A1,12X,1A1)
211 FURMAT(2X,25(1A1,4X))
206 FURMAT(6X,2H50,3X,3H100,2X,3H150,2X,3H200,2X,3H250,2X,3H300,7X,3H
1400,7X,3H500,7X,3H600,7X,3H700,7X,3H800,7X,3H900,6X,4H1000,6X,4H11
200,6X,4H1200)
212 FURMAT(30X,'DIMENSIONLESS AXIAL DISTANCE',/)
207 FURMAT(2X,42HBASE LINE DIMENSIONLESS WALL TEMPERATURE=,F5.0,10X,39
1HMAXIMUM DIMENSIONLESS WALL TEMPERATURE=,F10.3,/)
208 FURMAT(2X,10HDELTA DWT=,F10.2,2X,1H,,2X,'RE = ',I7,2X,1H,,2X,'A/R
L = ',F7.4,2X,1H,,2X,'PR = ',F7.2,2X,1H,,2X,'DE = ',I7)
RETURN
END

```

```

C
SUBROUTINE PLOT(NMO,NDAY,NYEAR,NSTA)
DIMENSION HTPLOT(2,8),GRAPH(8,51),SYMBOL(3),ORD(51)
COMMON/DLSNOS/NRE,ABYR,NDE,PRANTL,PRFLNU(8),NRUN
DATA SYMBOL/1HC,1HA,1H /
DATA ASTER/1H*/
DO 1 J=1,4
HTPLOT(1,J)=PRFLNU(J)
1 CONTINUE
DO 2 I=1,4
DO 2 J=1,51

```

```

      GRAPH(I,J)=SYMBOL(3)
2  CONTINUE
      HTMAX=HTPLOT(1,1)
      HTMIN=0.0
      I=1
      DO 3 J=1,4
      IF(HTMAX.LT.HTPLOT(I,J))HTMAX=HTPLOT(I,J)
3  CONTINUE
      DIFF=HTMAX-HTMIN
      DEL = 0.2
      IF(DIFF.GT.10.0)DEL=1.0
      IF(DIFF.GT.50.0)DEL=2.0
      IF(DIFF.GT.100.0)DEL=5.0
      IF(DIFF.GT.200.0)DEL=10.0
      IF(DIFF.GT.500.0)DEL=20.0
      IF(DIFF.GT.1000.0)DEL=50.0
      IF(DIFF.GT.2000.0)DEL=100.0
      IF(DIFF.GT.5000.0)DEL=200.0
      IF(DIFF.GT.10000.0)DEL=500.0
      DO 4 J=1,4
      L=(HTPLOT(I,J)-HTMIN)/DEL+0.5
      L=51-L
4  GRAPH(J,L)=SYMBOL(1)
      DO 5 I=1,51
      ORD(I)=SYMBOL(3)
5  CONTINUE
      DO 6 I=1,51,5
      ORD(I)=ASTER
6  CONTINUE
      WRITE(6,200)NRUN,NMO,NDAY,NYEAR,NSTA
      DO 11 I=1,51
      IF(I.EQ.20) GO TO 7
      IF(I.EQ.21) GO TO 8
      IF(I.EQ.22) GO TO 9
      IF(I.EQ.23) GO TO 10
      WRITE(6,201) ORD(I),(GRAPH(J,I),J=1,4)
      GO TO 11
      GO TO 11
8  WRITE(6,203) ABYR,ORD(I),(GRAPH(J,I),J=1,4)
      GO TO 11
9  WRITE(6,204) PRANTL,ORD(I),(GRAPH(J,I),J=1,4)
      GO TO 11
10 WRITE(6,205) NDE,ORD(I),(GRAPH(J,I),J=1,4)
11 CONTINUE
      WRITE(6,201) SYMBOL(3),(ASTER,I=1,4)
      WRITE(6,206)
      WRITE(6,207)HTMIN,HTMAX
      WRITE(6,208) DEL
7  WRITE(6,202) NRE,ORD(I),(GRAPH(J,I),J=1,4)
200 FORMAT(1H1,2X,12HRUN NUMBER =,I4,I10,1H-,I2,1H-,I2,5X,16HSTATION N
      UMBER =,I3,/)
201 FORMAT(50X,5(4X,1A1))
202 FORMAT(10X,23HREYNOLDS NUMBER = RE = ,I7,10X,5(4X,1A1))
203 FORMAT(10X,23HTUBE/COIL RADIUS= A/R= ,F7.4,10X,5(4X,1A1))

```

```
204 FORMAT(10X,23HPRANDTL  NUMBER = PR = ,F7.2,10X,5(4X,1A1))
205 FORMAT(10X,23HDEAN    NUMBER = DE = ,17,10X,5(4X,1A1))
206 FORMAT(59X,1H1,4X,1H2,4X,1H3,4X,1H4,4X,756X,40HPERIPHERAL LOCATION
1,CLKWISE. FROM NORTH ,/)
207 FORMAT(2X,27HBASE LINE NUSSELT NUMBER = ,F5.1,10X,25HMAXIMUM NUSSE
1LT NUMBER = ,F10.3)
208 FORMAT(2X,10HDELTA NU = ,F10.1)
      RETURN
      END
```

```
C
C ***
C COMPUTER PROGRAM: MAH#04
C
C PROGRAM TO COMPUTE:
C 1. HEAT TRANSFER COEFFICIENTS, AND
C 2. PERTINENT FLUID FLOW AND HEAT TRANSFER DIMENSIONLESS NUMBERS
C FOR HEAT TRANSFER STUDIES IN HELICALLY COILED TUBES WITH LAMINAR FLOW.
C BY MUHAMMAD A. ABUL-HAMAYEL
C
C *** NOTE: 1. FLUID PROPERTIES ARE EVALUATED AT THE LOCAL BULK
C            FLUID TEMPERATURE AT EACH THERMOCOUPLE STATION.
C            2. LOCAL H(AVG.) = (1/N) * ((Q/A)/(T(WALL)-T(BULK FLUID))).
C
C DIMENSION QFLUX(8),TIS(8),TFLOC(8),QFLSI(4),TISSI(4),TFLSI(4),HTCS
C 11(4)
C COMMON/DLSNOS/NRE,ABYR,NDE,PRANTL,CANUNO,GRAETZ
C COMMON/INVALU/HTC(8),PRFLNU(8),TCFLU,NRUN
C READ(5,100) NRUN,NMO,NDAY,NYEAR,NSLI,TAMPS,VOLTS
C IF (NRUN.EQ.00) GO TO 15
C READ(5,101) FLRTMA,TFLIN,TFLOUT
C TUBERA=0.495/(2.0*12.0)
C COILRA=10.0/(2.0*12.0)
C ABYR=TUBERA/COILRA
C HTL = 298.5/12.
C TINC1=(TFLOUT-TFLIN)/HTL
C DO 7 I=1,18
C NSTA=I
C IF (I.EQ.01) TCSDIS = 2./12.
C IF (I.EQ.02) TCSDIS = 5./12.
C IF (I.EQ.03) TCSDIS = 8./12.
C IF (I.EQ.04) TCSDIS = 14./12.
C IF (I.EQ.05) TCSDIS = 20./12.
C IF (I.EQ.06) TCSDIS = 26./12.
C IF (I.EQ.07) TCSDIS = 32./12.
C IF (I.EQ.08) TCSDIS = 40./12.
C IF (I.EQ.09) TCSDIS = 50./12.
C IF (I.EQ.10) TCSDIS = 60./12.
C IF (I.EQ.11) TCSDIS = 71.5/12.
C IF (I.EQ.12) TCSDIS = 103./12.
C IF (I.EQ.13) TCSDIS = 134./12.
C IF (I.EQ.14) TCSDIS = 166./12.
C IF (I.EQ.15) TCSDIS = 198./12.
C IF (I.EQ.16) TCSDIS = 230./12.
C IF (I.EQ.17) TCSDIS = 260./12.
C IF (I.EQ.18) TCSDIS = 292./12.
C TEFLU=TFLIN+(TINC1*TCSDIS)
C READ(5,102)(TIS(J),J=1,4)
C READ(5,102)(QFLUX(J),J=1,4)
C CALL DMSNO(FLRTMA,TEFLU,TCSDIS)
```

```

      AVHTC=0.0
      DO 6 J=1,4
      TFLJC(J)=TEFLU
      HTC(J)=QFLUX(J)/(TIS(J)-TEFLU)
      AVHTC=AVHTC+HTC(J)
6    CONTINUE
      CALL NUSELT
      AVHTC=AVHTC/4.0
      CANJNO=(AVHTC*(0.495/12.0))/TCFLU
C    THE FOLLOWING STATEMENTS ARE MAINLY FOR
C    CONVERTING TO THE SI UNITS.
      TEFSI = (TEFLU-32.)*5./9.+273.15
      CFBJ = 1055.056/(3600.*9.290304E-02)
      AVHTSI = AVHTC*CFBJ*1.8
      DO 500 J=1,4
      JFLSI(J) = CFBJ*QFLUX(J)
      HTCST(J) = HTC(J)*CFBJ*1.8
      TISSI(J) = (TIS(J)-32.)*5./9.+273.15
      TFLSI(J) = (TFLOC(J)-32.)*5./9.+273.15
500  CONTINUE
C    END OF CONVERTING THE UNITS
      WRITE(6,200)
      WRITE(6,201)NRUN,NMO,NDAY,NYEAR
      WRITE(6,202)NSTA
      WRITE(6,203)TAMPS,VOLTS
      WRITE(6,204)
      WRITE(6,205)(QFLUX(J),J=1,4)
      WRITE(6,502)(QFLSI(J),J=1,4)
      WRITE(6,206)(TIS(J),J=1,4)
      WRITE(6,506)(TISSI(J),J=1,4)
      WRITE(6,207)
      WRITE(6,208)(TFLOC(J),J=1,4)
      WRITE(6,508)(TFLSI(J),J=1,4)
      WRITE(6,209)(HTC(J),J=1,4)
      WRITE(6,509)(HTCST(J),J=1,4)
      WRITE(6,217)(PRFLNU(J),J=1,4)
      WRITE(6,218) TEFLU,TEFSI
      WRITE(6,219) NRE
      WRITE(6,220) PRANTL
      WRITE(6,221) NDE
      WRITE(6,222) GRAETZ
      WRITE(6,223) AVHTC,AVHTSI
      WRITE(6,224) CANUNO ;
C
C    IF A PLOT OF HT IS NEEDED, ALL WHAT HAS TO BE DONE IS TO REMOVE
C    THE C OUT OF THE NEXT CARD.
C    CALL PLOT(NMO,NDAY,NYEAR,NSTA)
      WRITE(7,600) NSTA,NRUN,NRE,NDE,PRANTL,AVHTSI,CANUNO
7    CONTINUE
      GO TO 1
100  FORMAT(5I5,2E20.7)
101  FORMAT(3F10.2)
102  FORMAT(4E20.7)
200  FORMAT(1H1,2X,63H)CALCULATION OF HEAT TRANSFER COEFFICIENTS IN A HE

```

```

      ILICAL COIL BY , 'MOHAMMAD A. ABUL-HAMAYEL')
201 FORMAT(2X,12HNRUN NUMBER =,I4,I10,1H-,I2,1H-,I2)
202 FORMAT(2X,16HSTATION NUMBER =,I3)
203 FORMAT(2X,17HCURRENT IN COIL =,F6.1,5H AMPS,10X,26HVOLTAGE DROP AC
      1KUSS COIL =,F7.2,6H VOLTS)
204 FORMAT(//,2X,20HPERIPHERAL LOCATION ,14X,10H      1      ,2X,10H      2
      1      ,2X,10H      3      ,2X,10H      4      ,/2X,30HDEGREES CLOCKWISE F
      2KUM NORTH ,4X,10H      0      ,2X,10H      90      ,2X,10H      180      ,2X,
      310H      270      ,//)
205 FORMAT(2X,30HHEAT FLUX, Q , BTU/HR-SQ.FT. =,2X,4(F10.3,2X))
206 FORMAT(//,2X,30HINSIDE WALL TEMPERATURE,TW, F=,2X,4(F10.3,2X))
207 FORMAT(//,2X,52HFOR FLUID TEMPERATURES MEASURED BY THE THERMOCOUP
      LES)
208 FORMAT(//,2X,30HLOCAL FLUID TEMPERATURE,TF, F=,2X,4(F10.3,2X))
209 FORMAT(//,2X,30HHLOCAL), BTU/HR-SQ.FT.-F =,2X,4(F10.3,2X))
217 FORMAT(//,2X,30HPERIPHERAL NUSSELT NUMBER, NU=,2X,4(F10.3,2X))
218 FORMAT(//,2X,33HAT THE LOCAL FLUID TEMPERATURE OF,F10.3,8H F , OR
      1,F10.3,4H K :)
219 FORMAT(//,2X,23HREYNOLDS NUMBER = RE = ,I10)
220 FORMAT(//,2X,23HPRANDTL NUMBER = PR = ,F10.3)
221 FORMAT(//,2X,23HDEAN NUMBER = DE = ,I10)
222 FORMAT(//,2X,23HGRAETZ NUMBER = GZ = ,F10.3)
223 FORMAT(//,2X,35HAVERAGE H(LOCAL) FOR THIS STATION =,F10.3,16H BTU/
      1HK-SQ.FT.-F,//36X,1H=,F10.3,14H J/SEC-SQ.M.-K)
224 FORMAT(//,2X,46HAVERAGE NUSSELT NUMBER(=NU) FOR THIS STATION =,F10.
      13)
502 FORMAT (//,2X,30HHEAT FLUX, Q , J/SEC-SQ.M. =,2X,4(F10.3,2X))
506 FORMAT(//,2X,30HINSIDE WALL TEMPERATURE,TW, K=,2X,4(F10.3,2X))
508 FORMAT(//,2X,30HLOCAL FLUID TEMPERATURE,TF, K=,2X,4(F10.3,2X))
509 FORMAT(//,2X,30HHLOCAL), J/SEC-SQ.M.-K =,2X,4(F10.3,2X))
600 FORMAT (I2,I4,2I6,F8.3,2F8.2)
15 STOP
END

```

```

C      SUBROUTINE DMLSNO(FLRTMA,TEFLU,TCSDIS)
      COMMON/DLSNOS/NRE,ABYR,NDE,PRANTL,CANUNO,GRAETZ
      COMMON/INVALU/HTC(8),PRFLNU(8),TCFLU,NRUN
      TEMPC = (TEFLU-32.)*.5/.9.
      IF (NRUN.GT.300) GO TO 3
      IF (NRUN.GT.200) GO TO 1
      FLVIS = EXP(3.80666-1.79809*((TEFLU-40.)/60.))+0.38590*((TEFLU-40.
      1)/60.)**2)-0.05878*((TEFLU-40.)/60.)**3)+0.004173*((TEFLU-40.)/6
      20.)**4)
      CPFLU = 0.553+0.0415*((TEFLU-60.)/80.))+0.0035*((TEFLU-60.)/80.)**
      12)
      TCFLU = 0.1825-(2.3E-04*TEFLU)
      GO TO 2
1 CONTINUE
      RHSV = ((1.3272*(20.0-TEMPC))-(0.001053*(TEMPC-20.0)*(TEMPC-20.0)))

```

```

1/(TEMPC+105.0)
RHSLN=2.303*RHSVR
FLVIS=1.002*EXP(RHSLN)
CPFLU=1.01881-0.4802E-03*TEFLU+0.3274E-05*TEFLU*TEFLU-0.604E-08*TE
IFLU*TEFLU*TEFLU
TCFLU=0.30289+0.7029E-03*TEFLU-0.1178E-05*TEFLU*TEFLU-0.550E-09*TE
IFLU*TEFLU*TEFLU
GO TO 2
3 CONTINUE
FLVIS = EXP(-6.92545+(2.3839E+03/(TEMPC+273.15))-(1.08564E+04/((TE
MPC+273.15)**2)))
CPFLU = 0.53+0.16101E-02*(TEFLU-50.)-0.167946E-05*((TEFLU-50.)**2)
1+0.783422E-08*((TEFLU-50.)**3)
TCFLU = 0.09307-0.846193E-04*TEFLU+0.158015E-06*TEFLU*TEFLU
2 CONTINUE
FVFPS=2.42*FLVIS
RENI=((0.495/12.0)*FLRTMA)/((3.1416/4.0)*(0.495*0.495/144.0)*FVFPS
1)
NKE=RENO
PRANTL=(CPFLU*FVFPS)/TCFLU
DENO=RENO*(SQRT(ABYR))
NUE=DENO
GRAETZ=(FLRTMA*CPFLU)/(TCFLU*TCSDIS)
RETURN
END

```

```

SUBROUTINE NUSELT
C
COMMON/INVALU/HTC(8),PRFLNU(8),TCFLU,NRUN
DO 1 J=1,4
PRFLNU(J)=(HTC(J)*(0.495/12.0))/TCFLU
1 CONTINUE
RETURN
END

```

```

SUBROUTINE PLOT(NMO,NDAY,NYEAR,NSTA)
C
DIMENSION HTPLOT(2,8),GRAPH(8,51),SYMBOL(3),ORD(51)
COMMON/DLSNDS/NRE,ABYR,NDE,PRANTL,CANUNO,GRAETZ
COMMON/INVALU/HTC(8),PRFLNU(8),TCFLU,NRUN
DATA SYMBOL/1HC,1HA,1H /
DATA ASTER/1H*/
DO 1 J=1,4
HTPLOT(1,J)=PRFLNU(J)
1 CONTINUE
DO 2 I=1,4

```



```

      DO 2 J=1,51
      GRAPH(I,J)=SYMBOL(3)
2  CONTINUE
      HTMAX=HTPLOT(1,1)
      HTMIN=0.0
      I=1
      DO 3 J=1,4
      IF(HTMAX.LT.HTPLOT(I,J))HTMAX=HTPLOT(I,J)
3  CONTINUE
      DIFF=HTMAX-HTMIN
      DEL=1.0
      IF(DIFF.GT.50.0)DEL=2.0
      IF(DIFF.GT.100.0)DEL=5.0
      IF(DIFF.GT.200.0)DEL=10.0
      IF(DIFF.GT.500.0)DEL=20.0
      IF(DIFF.GT.1000.0)DEL=50.0
      IF(DIFF.GT.2000.0)DEL=100.0
      IF(DIFF.GT.5000.0)DEL=200.0
      IF(DIFF.GT.10000.0)DEL=500.0
      DO 4 J=1,4
      L=(HTPLOT(I,J)-HTMIN)/DEL+0.5
      L=51-L
4  GRAPH(J,L)=SYMBOL(I)
      DO 5 I=1,51
      ORD(I)=SYMBOL(3)
5  CONTINUE
      DO 6 I=1,51,5
      ORD(I)=ASTER
6  CONTINUE
      WRITE(6,200)NRUN,NMO,NDAY,NYEAR,NSTA
      DO 11 I=1,51
      IF(I.EQ.20) GO TO 7
      IF(I.EQ.21) GO TO 8
      IF(I.EQ.22) GO TO 9
      IF(I.EQ.23) GO TO 10
      WRITE(6,201) ORD(I),(GRAPH(J,I),J=1,4)
      GO TO 11
7  WRITE(6,202) NRE,ORD(I),(GRAPH(J,I),J=1,4)
      GO TO 11
8  WRITE(6,203) ABYR,ORD(I),(GRAPH(J,I),J=1,4)
      GO TO 11
9  WRITE(6,204) PRANTL,ORD(I),(GRAPH(J,I),J=1,4)
      GO TO 11
10 WRITE(6,205) NDE,ORD(I),(GRAPH(J,I),J=1,4)
11 CONTINUE
      WRITE(6,201)SYMBOL(3),(ASTER,I=1,4)
      WRITE(6,206)
      WRITE(6,207)HTMIN,HTMAX
      WRITE(6,208) DEL
200 FORMAT(1H1,2X,12H RUN NUMBER =,I4,110,1H-,I2,1H-,12,5X,16HSTATION N
      UMBER =,I3,/)
201 FORMAT(50X,5(4X,1A1))
202 FORMAT(10X,23HREYNOLDS NUMBER = RE =,I7,10X,5(4X,1A1))
203 FORMAT(10X,23HTUBE/COIL RADIUS= A/R=,F7.4,10X,5(4X,1A1))

```

```

204 FORMAT(10X,23HPRANDTL  NUMBER = PR = ,F7.2,10X,5(4X,1A1))
205 FORMAT(10X,23HDEAN    NUMBER = DE = ,I7,10X,5(4X,1A1))
206 FORMAT(59X,1H1,4X,1H2,4X,1H3,4X,1H4,756X,40HPERIPHERAL LOCATION,CL
1XWISE. FROM NORTH ,/)
207 FORMAT(2X,27HBASE LINE NUSSELT NUMBER = ,F5.1,10X,25HMAXIMUM NUSSE
1LT NUMBER = ,F10.3)
208 FORMAT(2X,10HDELTA NU =,F10.1)
      RETURN
      END

```

```

C
C *****
C
C COMPUTER PROGRAM: MAHW05
C
C PROGRAM TO COMPUTE:
C 1. HEAT TRANSFER COEFFICIENTS, AND
C 2. PERTINENT FLUID FLOW AND HEAT TRANSFER DIMENSIONLESS NUMBERS
C FOR HEAT TRANSFER STUDIES IN HELICALLY COILED TUBES WITH LAMINAR FLOW.
C BY MUHAMMAD A. ABUL-FAMAYEL
C
C *****
C
C *** NOTE: 1. FLUID PROPERTIES ARE EVALUATED AT THE LOCAL BULK
C             FLUID TEMPERATURE AT EACH THERMOCOUPLE STATION.
C             2. LOCAL  $h(AVG.) = ((1/N)E(Q/A))/((1/N)E(T(WALL)) - T(BULK FLUID))$ .
C
C DIMENSION QFLUX(8),TIS(8),QFLSI(4),TISST(4)
C COMMON/INVALU/FLRTMA,TEFLU,TCSDIS,CAWALT,CAHTC,NRUN
C COMMON/DLSNOS/NRE,ABYR,NDE,PRANTL,GRAETZ,GRASOF,RAYLAY,CANUNO
1 READ(5,100) NRUN,NMO,NDAY,NYEAR,NSLI,TAMPS,VOLTS
IF (NRUN.EQ.00) GO TO 15
READ(5,101) FLRTMA,TFLIN,TFLOUT
TUBERA=0.495/(2.0*12.0)
COILRA=10.0/(2.0*12.0)
ABYR=TUBERA/COILRA
HTL = 298.5/12.
TINC1=(TFLOUT-TFLIN)/HTL
DO 7 I=1,18
NSTA=I
IF (I.EQ.01) TCSDIS = 2./12.
IF (I.EQ.02) TCSDIS = 5./12.
IF (I.EQ.03) TCSDIS = 8./12.
IF (I.EQ.04) TCSDIS = 14./12.
IF (I.EQ.05) TCSDIS = 20./12.
IF (I.EQ.06) TCSDIS = 26./12.
IF (I.EQ.07) TCSDIS = 32./12.
IF (I.EQ.08) TCSDIS = 40./12.
IF (I.EQ.09) TCSDIS = 50./12.
IF (I.EQ.10) TCSDIS = 60./12.
IF (I.EQ.11) TCSDIS = 71.5/12.
IF (I.EQ.12) TCSDIS = 103./12.
IF (I.EQ.13) TCSDIS = 134./12.
IF (I.EQ.14) TCSDIS = 166./12.
IF (I.EQ.15) TCSDIS = 198./12.
IF (I.EQ.16) TCSDIS = 230./12.
IF (I.EQ.17) TCSDIS = 260./12.
IF (I.EQ.18) TCSDIS = 292./12.
TEFLU=TFLIN+(TINC1*TCSDIS)
READ(5,102)(TIS(J),J=1,4)
READ(5,102)(QFLUX(J),J=1,4)
CAWFLX=0.0
CAWALT=0.0

```

```

      DO 5 J=1,4
      CAQFLX=CAQFLX+QFLUX(J)
      CAWALT=CAWALT+TIS(J)
6    CONTINUE
      CAQFLX=CAQFLX/4.0
      CAWALT=CAWALT/4.0
      CAHTC=CAQFLX/(CAWALT-TEFLU)
      CALL DMLSNO
C    THE FOLLOWING STATEMENTS ARE MAINLY FOR
L    CONVERTING TO THE SI UNITS.
      TEFSI = (TEFLU-32.)*5./9.+273.15
      CAWASI = (CAWALT-32.)*5./9.+273.15
      CFBJ = 1055.056/(3600.*9.290304E-02)
      CAQFSI = CAQFLX*CFBJ
      CAHSI = CAHTC*CFBJ*1.8
      DO 500 J=1,4
      QFLSI(J) = CFBJ*QFLUX(J)
      TISSI(J) = (TIS(J)-32.)*5./9.+273.15
500  CONTINUE
C    END OF CONVERTING THE UNITS
      WRITE(6,200)
      WRITE(6,201)NRUN,NMO,NDAY,NYEAR
      WRITE(6,202)NSTA
      WRITE(6,203)TAMPS,VOLTS
      WRITE(6,208) ABYR
      WRITE(6,204)
      WRITE(6,205)(QFLUX(J),J=1,4)
      WRITE(6,502)(QFLSI(J),J=1,4)
      WRITE(6,206)(TIS(J),J=1,4)
      WRITE(6,506)(TISSI(J),J=1,4)
      WRITE(6,207)
      WRITE(6,218) TEFLU,TEFSI
      WRITE(6,219) NRE
      WRITE(6,220) PRANTL
      WRITE(6,221) NDE
      WRITE(6,222) GRAETZ
      WRITE(6,223)
      WRITE(6,224) CAWALT,CAWASI
      WRITE(6,225) CAQFLX,CAQFSI
      WRITE(6,226) CAHTC,CAHSI
      WRITE(6,227) CANUND
      WRITE(6,228) GRASOF
      WRITE(6,229) RAYLAY
      WRITE(7,700) NSTA,NRUN,GRASOF,GRAETZ,CAQFSI,CAHSI,TEFLU,CAWALT
7    CONTINUE
      GO TO 1
100  FUKMAT(515,2E20.7)
101  FORMAT(3F10.2)
102  FORMAT(4E20.7)
200  FORMAT(1H1,2X,63H"CALCULATION OF HEAT TRANSFER COEFFECIENTS IN A HE
      LICAL COIL BY 'MOHAMMAD A. ABUL-HAMAYEL'")
201  FURMAT(2X,12H"RUN NUMBER =",I4,I10,1H-,I2,1H-,I2)
202  FUKMAT(2X,16H"STATION NUMBER =",I3)
203  FOKMAT(2X,17H"CURRENT IN COIL =",F6.1,5H AMPS,10X,26H"VOLTAGE DROP AC

```

```

      CROSS COIL =,F7.2,6H VCLTS)
204 FORMAT(//,2X,20HPERIPHERAL LOCATION ,14X,10H 1 ,2X,10H 2
1 ,2X,10H 3 ,2X,10H 4 ,/2X,30HDEGREES CLOCKWISE F
20H NORTH ,4X,10H 0 ,2X,10H 90 ,2X,10H 180 ,2X,
30H 270 ,//)
205 FORMAT(2X,30HHEAT FLUX, Q , BTU/HR-SQ.FT. =,2X,4(F10.3,2X))
206 FORMAT(//,2X,30HINSIDE WALL TEMPERATURE,TW, F=,2X,4(F10.3,2X))
207 FORMAT(//,2X,52HFOR FLUID TEMPERATURES MEASURED BY THE THERMOCOUP
LES)
208 FORMAT(2X,29HTUBE-TO-COIL DIAMETER RATIO =,F10.6)
213 FORMAT(//,2X,33HAT THE LOCAL FLUID TEMPERATURE OF,F10.3,8H F , OR
1,F10.3,4H K :)
219 FORMAT(//,2X,23HREYNOLDS NUMBER = RE = ,I10)
220 FORMAT(//,2X,23HPRANDTL NUMBER = PR = ,F10.3)
221 FORMAT(//,2X,23HDEAN NUMBER = DE = ,I10)
222 FORMAT(//,2X,23HGRAETZ NUMBER = GZ = ,F10.3)
223 FORMAT(///,2X,64HTHE FOLLOWING ARE PERIPHERALLY AVERAGED VALUES FO
R THIS STATION:,//)
224 FORMAT(2X,26HAVERAGE WALL TEMPERATURE =,F10.3,8H F , OR ,F10.3,2H
K)
225 FORMAT(//,2X,19HAVERAGE HEAT FLUX =,F10.3,14H BTU/HR-SQ.FT.,2X,2H =
1,F10.3,12H J/SEC-SQ.M.)
226 FORMAT(//,2X,35HAVERAGE HEAT TRANSFER COEFFICIENT =,F10.3,16H BTU/H
R-SQ.FT.-F,2X,2H =,F10.3,' J/SEC-SQ.M.-K')
227 FORMAT(//,2X,23HNUSSELT NUMBER = NU = ,F10.3)
228 FORMAT(//,2X,23HGRASHOF NUMBER = GR = ,E20.9)
229 FORMAT(//,2X,23HRAYLEIGH NUMBER = RA = ,E20.9)
502 FORMAT (//,2X,30HHEAT FLUX, Q , J/SEC-SQ.M. =,2X,4(F10.3,2X))
506 FORMAT(//,2X,30HINSIDE WALL TEMPERATURE,TW, K=,2X,4(F10.3,2X))
700 FORMAT (I2,I4,E14.7,5F9.3)
15 STOP
      END

```

# SUBROUTINE DMLSNO

C

```

COMMON/INVALU/FLRTMA,TEFLU,TCSDIS,CAWALT,CAHTC,NRUN
COMMON/DLSNOS/NRE,ABYR,NDE,PRANTL,GRAETZ,GRASOF,RAYLAY,CANUNO
TUBEID=0.495/12.0
TEMPC=((TEFLU-32.0)*5.0)/9.0
CAWTC=((CAWALT-32.0)*5.0)/9.0
AVWBC = (CAWTC+TEMPC)/2.
IF (NRUN.GT.300) GO TO 3
IF (NRUN.GT.200) GO TO 1
FLVIS = EXP(3.80666-1.79809*((TEFLU-40.)/60.))+0.38590*((TEFLU-40.
1)/60.)**2)-0.05878*((TEFLU-40.)/60.)**3)+0.004173*((TEFLU-40.)/6
20.)**4))
CPFLU = 0.553+0.0415*((TEFLU-60.)/80.))+0.0035*((TEFLU-60.)/80.))**
12)
TCFLU = 0.1825-(2.3E-04*TEFLU)
SPVJLB = 0.924848+6.2796E-04*(TEMPC-65.))+9.2444E-07*((TEMPC-65.))**

```

```

12)*3.057E-09*((TEMPC-65.))**3)
RUEFBT = 1./SPVOLA
DVDTAV = 6.2796E-04+1.84988E-06*(AVWBC-65.)+9.171E-09*((AVWBC-65.))
**2)
SPVOLA = 0.924848+6.2796E-04*(AVWBC-65.)+9.244E-07*((AVWBC-65.))**
12)*3.057E-09*((AVWBC-65.))**3)
BETA = DVDTAV/(1.8*SPVOLA)
GU TO 2
1 CONTINUE
RHSLN=((1.3272*(20.0-TEMPC))-(0.001053*(TEMPC-20.0)*(TEMPC-20.0)))
1/(TEMPC+105.0)
RHSLN=2.303*RHSLN
FLVIS=1.002*EXP(RHSLN)
CPFLU=1.01881-0.4802E-03*TEFLU+0.3274E-05*TEFLU*TEFLU-0.604E-08*TE
1FLU*TEFLU*TEFLU
TCFLU=0.30289+0.7029E-03*TEFLU-0.1178E-05*TEFLU*TEFLU-0.550E-09*TE
1FLU*TEFLU*TEFLU
RUEFBT=0.999986+0.1890E-04*TEMPC-0.5886E-05*TEMPC*TEMPC+0.1548E-07
1*TEMPC*TEMPC*TEMPC
RUEFAV = 0.999986+0.1890E-04*AVWBC-0.5886E-05*(AVWBC**2)+0.1548E-0
17*(AVWBC**3)
DRDTAV = 0.189E-04-1.1772E-05*AVWBC+0.4644E-07*AVWBC*AVWBC
BETA = -DRDTAV/(1.8*RUEFAV)
GU TO 2
3 CONTINUE
FLVIS = EXP(-6.92545+(2.3839E+03/(TEMPC+273.15))-(1.08564E+04/((TE
1MPC+273.15)**2)))
CPFLU = 0.53+0.16101E-02*(TEFLU-50.)-0.167946E-05*((TEFLU-50.))**2)
1+0.783422E-08*((TEFLU-50.))**3)
TCFLU = 0.09307-0.846193E-04*TEFLU+0.158015E-06*TEFLU*TEFLU
RUEFBT = 0.824605-0.700505E-03*TEMPC-0.101516E-05*(TEMPC**2)
1+0.296294E-08*(TEMPC**3)
RUEFAV = 0.824605-0.700505E-03*AVWBC-0.101516E-05*(AVWBC**2)
1+0.296294E-08*(AVWBC**3)
DRDTAV = -0.700505E-03-0.203032E-05*AVWBC+0.888882E-08*(AVWBC**2)
BETA = -DRDTAV/(1.8*RUEFAV)
2 CONTINUE
DENFBT=62.43*RUEFBT
FVFPS=2.42*FLVIS
RENJ=((0.495/12.0)*FLRTMA)/((3.1416/4.0)*(0.495*0.495/144.0)*FVFPS
1)
NKE=RENO
PRAYTL=(CPFLU*FVFPS)/TCFLU
DENJ=RENO*(SQRT(ABYR))
NDE=DENO
GRAETZ=(FLRTMA*CPFLU)/(TCFLU*TCSDIS)
CANUNO=(CAHTC*TUBEID)/TCFLU
DELTAT=CAWALT-TEFLU
GRAVITY=4.175E+08
GRASOF=(TUBEID*TUBEID*TUBEID*GRAVITY*DENFBT*DENFBT*BETA*DELTAT)/(FV
1FPS*FVFPS)
KAYLAY=GRASOF*PRANTL
RETURN
END

```

## APPENDIX H

### ERROR ANALYSIS

The error in the calculated heat transfer coefficient was determined. An error analysis [suggested by Singh (37)] was performed. The analysis is as follows:

From Chapter V

$$h = \frac{Q/A}{[t_w - t_b]} = f(Q/A, t_w, t_b) \quad (H.1)$$

or

$$dh = \frac{\partial f}{\partial (Q/A)} \cdot d(Q/A) + \frac{\partial f}{\partial t_w} \cdot dt_w + \frac{\partial f}{\partial t_b} \cdot dt_b \quad (H.2)$$

From Equation (H.1)

$$\frac{\partial f}{\partial (Q/A)} = \frac{1}{(t_w - t_b)} ; \frac{\partial f}{\partial t_w} = - \frac{Q/A}{(t_w - t_b)^2} ; \frac{\partial f}{\partial t_b} = \frac{Q/A}{(t_w - t_b)^2}$$

Substituting in Equation (H.2)

$$dh = \frac{1}{(t_w - t_b)} \cdot d(Q/A) - \frac{Q/A}{(t_w - t_b)^2} \cdot dt_w + \frac{Q/A}{(t_w - t_b)^2} \cdot dt_b$$

or

$$\frac{dh}{h} = \frac{d(Q/A)}{Q/A} - \frac{dt_w}{(t_w - t_b)} + \frac{dt_b}{(t_w - t_b)} \quad (H.3)$$

To estimate the error in  $h$ , the error in the measurement of  $(Q/A)$ ,  $t_w$  and  $t_b$  will be estimated.

The error in the heat flux,  $Q/A$ , depends upon the error associated with the primary measurements used to determine the heat flux. These measurements together with an estimate of their error are:

- |                            |             |
|----------------------------|-------------|
| 1. Coil current            | $\pm 1.0\%$ |
| 2. Coil voltage            | $\pm 1.0\%$ |
| 3. Coil dimensions         | $+ 0.1\%$   |
| 4. Inside wall temperature | $\pm 1.0\%$ |
| 5. Room temperature        | $\pm 0.5\%$ |



If all of the above mentioned measurements were in error to the extent indicated and in the same direction, the maximum error in the heat flux is 9.21%.

From Appendix B, the calibration data on the bulk fluid and the wall thermocouples indicate that at an average temperature of 210°F:

1. The bulk fluid thermocouples had an average correction of +0.61°F or 0.34°C.
2. The surface thermocouples on the coil had an average correction of + 1.0°F or 0.57°C.

The calibrations were performed using the Doric Digital Thermocouple Indicator to measure the thermocouple outputs. The Digital Thermocouple Indicator had a stated accuracy of  $\pm 0.3^\circ\text{F}$  for the above  $0^\circ\text{F}$  range. Since the calibrations were made in-situ, the above mentioned corrections reflect the inaccuracies of the Digital Thermocouple Indicator and the associated thermocouple wires.

Based on the above data, the average error in the bulk fluid temperature and the surface of the helical coil was estimated to be  $0.3^\circ\text{F}$ .

Now, since the inside wall temperature was determined by a numerical solution, the average error in the wall temperature would be affected by the errors in the coil dimensions, the room temperature, the flow rate and any computational errors. Taking all the errors into account, the combined total error in the inside wall temperature is taken to be  $0.5^\circ\text{F}$ .

Rewriting Equation (H.3),

$$\frac{dh}{h} = \frac{d(Q/A)}{Q/A} - \frac{(dt_w/t_w)}{[1-(t_b/t_w)]} + \frac{(dt_b/t_b)}{[(t_w/t_b)-1]} \quad (\text{H.4})$$

The average bulk fluid and inside wall temperature were estimated to be 103°F and 117°F, respectively.

The maximum error in the heat transfer coefficient would occur when the error in the independent variables are all additive.

Therefore,

$$\frac{dh}{h} = 0.0921 + \frac{\left(\frac{0.5}{577}\right)}{[1-(563/577)]} + \frac{\left(\frac{0.3}{563}\right)}{[(577/563)-1]}$$

$$= 0.149 = 14.9\%.$$

VITA

Mohammad A. Abul-Hamayel

Candidate for the Degree of

Doctor of Philosophy

Thesis: HEAT TRANSFER IN HELICALLY COILED TUBES WITH LAMINAR FLOW

Major Field: Chemical Engineering

Biographical:

Personal Data: Born in Jeddah, Saudi Arabia, February 2, 1947,  
the son of Mr. and Mrs. Abdul-Kadir A. Abul-Hamayel.

Education: Graduated from Al-Falah High School, Jeddah, Saudi Arabia in 1964; received Bachelor of Science in Engineering (Chemical Engineering) degree from Arizona State University in August 1970; received Master of Science in Chemical Engineering from University of California at Santa Barbara in June, 1973; completed the requirements for the Doctor of Philosophy degree in Chemical Engineering at Oklahoma State University in May, 1979.

Professional Experience: Graduate Assistant, Chemical Engineering Department, University of Petroleum and Minerals, Dhahran, Saudi Arabia, 1970-1971 and 1973-1974.